JAERI-Review
97-013

ANNUAL REPORT OF NAKA FUSION RESEARCH ESTABLISHMENT

from April 1, 1996 to March 31, 1997

October 1997

Naka Fusion Research Establishment

日本原子力研究所
Japan Atomic Energy Research Institute

本レポートは，日本原子力研究所が不定期に公刊している研究報告書です。
入手の問合わせは，日本原子力研究所研究情報部研究情報課（〒319-11 茨城県那珂郡東海村）あて，お申し越しください。なお，このほかに財団法人原子力弘済会資料センター（〒319-11 茨城県那珂郡東海村日本原子力研究所内）で複写による実費領布をおこなっております。

This report is issued irregularly.
Inquiries about availability of the reports should be addressed to Research Information Division, Department of Intellectual Resources, Japan Atomic Energy Research Institute, Tokai-mura, Naka-gun, Ibarakiken 319-11, Japan.

編集兼発行　日本原子力研究所
印　　刷　ニッセイエブロ株式会社

JAERI-Review 97-013

Annual Report of Naka Fusion Research Establishment from April 1, 1996 to March 31, 1997

Naka Fusion Research Establishment

Japan Atomic Energy Research Institute
Naka-machi, Naka-gun, Ibaraki-ken

(Received October 1, 1997)

This report provides an overview of research and development activities at Naka Fusion Research Establishment, JAERI, during the period from April 1, 1996 to march 31, 1997. The activities in Naka Fusion Research Establishment are highlighted by high temperature plasma research in JT-60 and JFT-2M, and progress in ITER-EDA, including technology development.

The objectives of the JT-60 project are to contribute to the ITER physics R&D and to establish the physics basis for a steady state tokamak fusion reactor like SSTR.

To achieve these objectives, improvements and regulation of the facilities and developments of the instruments were performed. The highlights are as follows. The construction for the divertor modification from the original open type to the W-shaped semi-closed type for improving the particle control was started on February 1997. In the power supply system, the thyristor converter was partially rearranged to increase the plasma current with the high triangularity. The world record of plasma input power 40 MW was achieved by NBI with the beam energy of 90 keV using positive ion source. Also in negative-ion based NBI, the beam output of 18.4 A/350 keV(6.4 MW) with hydrogen and 13.5 A/400 keV(5.4 MW) with deuterium were achieved as the world record. Furthermore, a plasma input power of 3.2 MW/350 keV to JT-60 was realized with the single ion source. In LHRF system, a protection system of the antenna from the arcing was developed by means of detection of the light caused breakdown.

The followings are the results concerning the plasma performance. By extending the operational region of the high β_p H-mode, the world record of the fusion triplet, $n_D\tau_E T_{i0}$ = 1.53×10^{21} keV s m^{-3}, was achieved. It was found that the fusion triplet became maximum in the same region of the safety factor as the ITER operation.

Optimization of the reversed shear mode in a higher current regime realized a high fusion

Editors: Shimizu M.(chief), Ide S., Matsukawa M., Kurihara R., Koizumi K., Takahashi I.

performance plasma with high temperature and density. The main achieved parameters of the plasma are as follows; the energy confinement time 0.97 s, the ion temperature 16.5 keV, the electron density 0.97×10^{20} m^{-3}, the fusion triplet 0.78×10^{21} keV s m^{-3}. The fusion power by D-D reaction was 53 kW, and assuming that the half of the fuel was tritium, the expected fusion output was 10.6 MW. The ratio of the output to the input power becomes 1.05, therefore it can be concluded that the plasma is in an equivalent break even condition. Moreover, in a reversed shear plasma, the highest values of the energy confinement time and the stored energy on JT-60 (1.08 s and 10.9 MJ) were recorded. Generation of radiative divertor, confinement of high energy ions, current profile control by RF current drive and impurity confinement in reversed shear plasmas were investigated systematically.

The poloidal coil system was modified so as to increase the triangularity. As the result an instability driven by the pressure gradient at the plasma edge was drastically suppressed, then a plasma with the confinement improvement factor of more than two and the fusion triple product of 0.27×10^{21} keV s m^{-3} was successfully maintained for 2.6 seconds. Furthermore, by raising the triangularity a full current drive plasma was successfully maintained with high confinement property and high fraction (60%) of the bootstrap current for three times longer than was formally achieved. A driven current of 270 kA was demonstrated by the negative ion based neutral beam injector (N-NBI) for the first time, and a profile of the current was estimated. The current drive efficiency by N-NBI was proved to be better by 1.6 times than that by standard energy (~90 keV) positive ion based NBI.

Objectives of the JFT-2M program are (1) advanced and basic researches for the development of high-performance plasmas for nuclear fusion and (2) contribution to the physics R&D for ITER, with a merit of flexibility of a medium-size device. The modified closed divertor was found to improve compatibility of the H-mode with the dense and cold divertor plasma. In an H-mode plasma, suppression of the density fluctuation was found to occur in a high shear region of the radial electric field. It was demonstrated that the m=2 tearing mode was suppressed by the O-mode ECH for the first time in an elongated plasma. Plasma coupling experiment of the combline antenna for FWCD was carried out in collaboration with General Atomics. Planning of the Advanced Material-Tokamak Experiments (AMTEX) was initiated.

The primary objective of theory and analysis is to improve the physical understanding of the magnetically confined tokamak plasma. Remarkable progress has been made on understanding of physics of the reverse shear plasma, stability properties of ideal MHD, TAE and kinetic ballooning modes. Progress was also made in understanding of VDE mechanism and nature of divertor asymmetry. New Implicit Monte Carlo method is also developed for the analysis of impurity ionization and recombination. Selective He ash exhaust is also demonstrated using OFMC code simulation.

The main focus of the NEXT (Numerical Experiment of Tokamak) project is to simulate

tokamak plasmas using particle and fluid models on the developing technology of massively parallel computers.

Major highlights of fusion reactor technology development in FY 1996 are as follows. In the blanket technology, R&D activities have led to the successful fabrication of a medium-scale shielding blanket mock-up. In the superconducting magnet development, superconducting cable composed of 13.6 tons of Nb_3Sn strand and 6.8 tons of copper strand for the CS Model Coil and CS Insert Coil was completed successfully. In the beam technology, a 139 hours operation of a Cs-seeded negative ion source was demonstrated at high current density. In the RF heating technology, the maximum efficiency of 40% was obtained with the depressed collector at 170 GHz for 50 msec for the gyrotron development for ITER. In the tritium technology, significant achievements such as the development of the high efficiency electrolytic reactor and the verification of the feasibility of the membrane technology to the large capacity detritiation system were obtained. In the development of plasma facing components, thermal cycling experiment was performed successfully to demonstrate durability of mock-ups at a transient heat load of 15 MW/m^2 for 15 sec for a repetition of 10^3 cycles. In the reactor structure development, fabrication and testing of the ITER vacuum vessel full-sector model completed 60% at the end of March 1997.

In the fusion reactor design, the DREAM concept of a fusion power reactor progressed regarding the gross reactor configuration, the reactor internal structures, the plant design, and the building. In the area of safety research, safety evaluation code development, basic experiments of LOVA and ICE, and the study of tokamak dust removal methods were also carried out.

The Detailed Design Report (DDR) of ITER was issued by the Director in November 1996, as the basis of the Final Design Report (FDR). After the formal review by the Technical Advisory Committee (TAC), the DDR was officially accepted by the ITER Council at its 11th Meeting held in December 1996. The DDR is composed of various technical documents on the detailed design of plasma parameters, tokamak components, plant system and tokamak building. The major results of safety analyses described in the Non-site Specific Safety Report (NSSR) -1 was also included in the DDR. The technical review of the DDR is being conducted by the four Parties. The Japanese Home Team contributes to the design progress in the various fields through the conduction of design tasks in close collaboration with the Joint Central Team (JCT). The JCT member built up to 155 including 45 Japanese members as of March 1997. The FDR will be prepared by the end of 1997 for presentation at the ITER Council.

Keywords: Fusion Research, JAERI, JT-60, JFT-2M, DIII-D, Plasma Physics, Fusion Engineering, ITER, ITER-EDA, Fusion Reactor Design, Annual Report

那珂研究所年報（平成８年度）

日本原子力研究所
那珂研究所

（1997年10月1日受理）

原研・那珂研究所における平成８年度（1996年４月～1997年３月）の研究開発活動について報告する。那珂研究所の主な活動は、ＪＴ－６０とＪＦＴ－２Ｍにおける高温プラズマの研究、及び工学技術開発を含むＩＴＥＲ工学設計活動（ITER-EDA）である。

ＪＴ－６０プロジェクトの目的は、ＩＴＥＲ物理Ｒ＆Ｄに貢献しＳＳＴＲのような定常トカマク核融合炉の概念構築のための物理基盤を固めることにある。これらを遂行するために装置の改造や調整及び機器開発を進めた。主なものを列挙する。まず、ＪＴ－６０をオープンダイバータから粒子制御をより積極的に行う W 型のセミクローズド化ダイバータの改造工事に着手した。電源システムにおいては、高三角度でのプラズマ電流増大のため、サイリスタ電源の一部組み替えを実施した。正イオンNBIでは、約90 keVのビームエネルギーで重水素ビームによるプラズマ加熱入力 40 MW の世界記録を達成した。負イオンNBIでは、水素負イオンビームで18.4 A/350 keV(6.4 MW)、重水素負イオンビームで13.5 A/400 keV(5.4 MW)の世界最高の負イオンビーム出力を達成している。またＪＴ－６０への入射パワーとしては、単一のイオン源で3.2 MW/350 keVを達成している。ＬＨＲＦでは、アンテナ先端部でのブレークダウン時に発生するアーク光を検出してＲＦ入力を抑制するシステムを開発した。

また、プラズマ性能に係わる成果を以下に示す。高ベータ・ポロイダルＨモードの放電領域を拡張することにより、核融合三重積 $n_D\tau_E T_{i0}$ の世界最高値 1.53×10^{21} keV s m^{-3} を達成した。また、ＩＴＥＲ運転と同じ安全係数の領域で核融合三重積が最大になることを見いだした。

高電流領域での負磁気シア放電の最適化により、高温／高密度の高性能プラズマを得た。主なパラメータはエネルギー閉じ込め時間0.97秒、イオン温度16.5 keV、電子密度 0.97×10^{20} m^{-3}、核融合三重積 0.78×10^{21} keV s m^{-3} である。ＤＤ核融合反応による出力は53 kWで、燃料の半分が三重水素であったと仮定すると出力は10.6 MWとなる。これと入力パワーとの比は1.05で、すなわちこのプラズマは等価臨界条件を達成しているので

那珂研究所：〒311-01　茨城県那珂郡那珂町向山801-1
編集者：清水　正亜（責任者）、井手　俊介、松川　誠、栗原　良一、小泉　興一、
高橋　一路

ある。また、負磁気シア放電によりＪＴ－６０におけるエネルギー閉じ込め時間と蓄積エネルギーの記録を塗り替えた（1.08 秒、10.9 MJ）。負磁気シアプラズマにおける、放射冷却ダイバータの生成、高エネルギーイオンの閉じ込め、ＲＦ電流駆動による電流分布制御や不純物閉じ込め等も系統的な研究が進んでいる。

ポロイダルコイル系の改造により、三角度をより大きくつけられるようになり、周辺の圧力勾配により駆動される不安定性が抑制され、閉じ込め改善度 2 以上で核融合三重積 0.27×10^{21} keV s m^{-3} を 2.6 秒間維持することができた。さらに、高閉じ込め／高ブートストラップ電流（60%）のプラズマを従来の三倍長く完全電流駆動することができた。

負イオン中性粒子入射装置（Ｎ－ＮＢＩ）実験では、Ｎ－ＮＢＩによる駆動電流 270kA が初めて示され、駆動電流分布を評価した。また、Ｎ－ＮＢＩによる電流駆動効率は従来の正イオン源（~90 keV）の 1.6 倍であることを示した。

ＪＦＴ－２Ｍプロジェクトの目的は、中型装置の機動性を生かした、核融合プラズマの先進的及び基礎的研究開発、及びＩＴＥＲ物理Ｒ＆Ｄへの貢献である。閉ダイバータ配位が、Ｈモードと高密度・低温ダイバータの両立により効果的であることを示した。また、Ｈモード中に密度揺動が抑制される領域は径電場のシアが強くなる領域と相関があることを示した。非円形トカマクで初めて、ＯモードＥＣＨによりｍ＝２テアリングモードを抑制した。ゼネラル・アトミクス社との協力の元楕形ＦＷＣＤアンテナの結合実験を進めている。先進材料トカマク実験計画が開始された。

理論／解析の目的は、トカマクプラズマ物理のより深い理解である。負磁気シアプラズマ、理想ＭＨＤの安定特性、ＴＡＥや運動論的バルーニングモードなどの物理理解が進んだ。また、ＶＤＥメカニズムやダイバータの非対象性の性質について理解も深まった。不純物のイオン化／再結合の解析のために、新しい陰解モンテカルロ法を開発した。ＯＦＭＣコードを用い、ヘリウム灰の選択的な排気を示した。

ＮＥＸＴ（数値トカマク計画）では、現在進展が著しい高並列コンピュータ技術により、粒子／流体モデルを用いてトカマクプラズマをシミュレートする。

核融合炉技術開発の主な進展は次の通りである。ブランケット工学に関しては 、R&D として遮蔽ブランケット中規模モックアップの製作に成功した。超電導磁石開発に関しては 、中心ソレノイド・モデル・コイルとインサート・コイル用の 13.6 トン Nb_3Sn 素線と 6.8 トン銅素線から成る超電導ケーブルが完成した。負イオン源開発に関しては 、セシウム添加型負イオン源を 139 時間運転した。ＲＦ加熱工学に関しては、ＩＴＥＲ用ジャイロトロンが 170 GHz、50 ミリ秒間の発振に成功して 40%の最大効率を得た。トリチウム技術に関しては 、高効率電解反応器の開発や大容量トリチウム除去システムへの膜技術の適用性の実証などの成果が得られた。プラズマ対向機器開発に関しては 、モックアップの熱サイクル試験を 15 MW/m^2、15 秒間の非定常熱負荷で 1000 サイクル行って耐熱性能を実証した。炉構造工学に関しては、遮蔽体を内蔵する薄肉二重壁構造の実規模真空容器のセクタモデルの製作を進め、全体の約 60%の製作を終了した。

核融合炉設計研究に関しては、核融合動力炉ＤＲＥＡＭについて、炉の全体形状、炉

心構造、プラント設計及び建屋の概念検討を進めた。また、安全性研究に関しては、安全評価コードの開発、ＬＯＶＡとＩＣＥの予備実験、及びトカマク炉内に生じるダストの除去方法の検討を行った。

平成8年11月にはＩＴＥＲ最終設計報告書の基盤となる詳細設計報告書が完成し、ＩＴＥＲ所長からＩＴＥＲ理事会に提出された。技術諮問委員会の公式レビューを経て詳細設計報告書は、同年12月の第11回ＩＴＥＲ理事会で承認された。詳細設計報告書は、プラズマパラメータ、トカマク機器、プラントシステムとトカマク建屋に関する技術設計書や図面から構成されており、「非サイト依存安全解析書-1」の主要な解析結果を含んだものである。これを受けて各極は、それぞれの極内で詳細設計報告書の技術内容のレビューを現在進めている。日本国内チームは、共同中央チーム (JCT) との堅密な協力のもと、タスクの推進を通じて様々の分野で設計の推進に貢献している。共同中央チームには、1997年3月現在、日本からのメンバー45名を含む155名が着任している。なお、最終設計報告書は、1997年12月までに取り纏められる予定である

Contents

目　次

Foreword

Naka Fusion Research Establishment (NAKA) of Japan Atomic Energy Research Institute (JAERI), has been conducting fusion experiments on JT-60, JFT-2M, and DIII-D (US-Japan collaboration). Engineering activities focus on the R&D for the International Thermonuclear Experimental Reactor (ITER) Engineering Design Activities (EDA). JAERI, as the Japanese implementing institute for ITER EDA, organized the Japanese Home Team, and is working for technology R&D and designs in cooperation with the Joint Central Team (JCT).

The programmatic objectives of the JT-60 project are to investigate the confinement improvement and the steady-state operation study, including disruption control, divertor study, and energetic particle physics. JFT-2M and DIII-D are exploring advanced tokamak concepts such as stability control and particle control. Theoretical and computational efforts have been carried out on the topics of confinement analysis, MHD stability and burning physics.

As for the ITER technology R&D, ongoing activities cover superconducting magnets, neutral beam heating, radio frequency heating, plasma facing components, reactor structure, remote maintenance, blanket and tritium technology. The ITER Detailed Design Report, issued by the ITER Director in November 1996, was reviewed by the Fusion Council and the suggestions and recommendations were submitted to IC-12.

Optimization of reversed shear operation in JT-60 culminated in achievement of the equivalent breakeven condition on an assumption of 50:50 DT mixture. Parameters achieved were the energy confinement time of 0.97s, the ion temperature of 16.5 keV, the electron density of 0.97×10^{20} m^{-3} and the fusion triple product of 0.78×10^{21} keV s m^{-3}. Experiments with a negative-ion-based neutral beam injection have been made with powers up to 3.2 MW/unit and beam energies of up to 400 keV. Progress in the ITER technology R&D has been made in establishment of heat treatment technique to avoid the SAGBO (Stress Accelerated Grain Boundary Oxidation) crack, completion of the 4 layers of CS model coil winding and development of the 1/2 scale blanket module integrated with first wall.

The JAERI fusion program has been conducted along the Third Phase Basic Program of Fusion Research and Development laid down by the Atomic Energy Commission of Japan in 1992. Present emphases of Naka fusion program are to contribute to ITER.

Hiroshi Kishimoto
Director General
Naka Fusion Research Establishment, JAERI

I. JT-60 PROGRAM

Objectives of the JT-60 project are to contribute the ITER physics R&D and to establish the physics basis for a steady state tokamak fusion reactor like SSTR. Significant progress in key physics for ITER and SSTR design has been made in recent JT-60 experiments.

By extending the operational region of the high β_p H-mode, the world record of the fusion triple product, $n_D\tau_E T_{i0} = 1.53\times10^{21}$ keV·s·m^{-3}, was achieved. It was found that the fusion triple product became maximum in the same region of the safety factor as the ITER operation.

Optimization of the reversed shear mode, which has been investigated experimentally since FY 1996, in a higher current regime realized a reproducible high fusion performance plasma with high temperature and density. The main achieved parameters of the plasma are as follow; the energy confinement time 0.97 s, the ion temperature 16.5 keV, the electron density 0.97×10^{20} m^{-3}, the fusion triple product 0.78×10^{21} keV·s·m^{-3}, and the fusion power by D-D reaction in the deuterium plasma was 53 kW. Assuming that the half of the fuel was tritium, expected fusion output was 10.6 MW, while the input power was 10.1 MW, then the ratio of the output to the input power becomes 1.05. Therefore it can be concluded that the plasma is in an equivalent break even condition. Moreover in a reversed shear plasma, the highest values of the energy confinement time and the stored energy on JT-60 (1.08 s and 10.9 MJ) were recorded. Generation of radiative divertor, confinement of high energy ions, current profile control by RF current drive and impurity confinement in reversed shear plasmas had been investigated systematically.

Based on the result in FY 1995 the poloidal coil system was modified so as to increase the triangularity for better plasma stability. As the result an instability driven by the pressure gradient at the plasma edge (giant ELM) was drastically suppressed, then a plasma with the confinement improvement factor of more than two and the fusion triple product of 0.27×10^{21} keV·s·m^{-3} was successfully maintained for 2.6 seconds. Furthermore, by raising the triangularity it was succeeded to maintain a full current drive plasma which had high confinement property and high fraction (60%) of the bootstrap current for three times longer than that formally achieved. These achievement are important to determine an operational mode and a plasma shape of a steady state fusion reactor.

Experiments of the negative ion based neutral beam injector (N-NBI) had progressed to reach the power of 3.2 MW/unit (80% of the full spec) and the beam energy of 400 keV (80% of the full spec). A driven current of 270 kA was demonstrated by N-NBI for the first time, and a profile of the current was estimated. The current drive efficiency by N-NBI was proved to be better by 1.6 times than that by standard energy (~90 keV) positive ion based NBI. It was also shown that behavior of beam ions was consistent with the classical theory.

Divertor Modification of JT-60

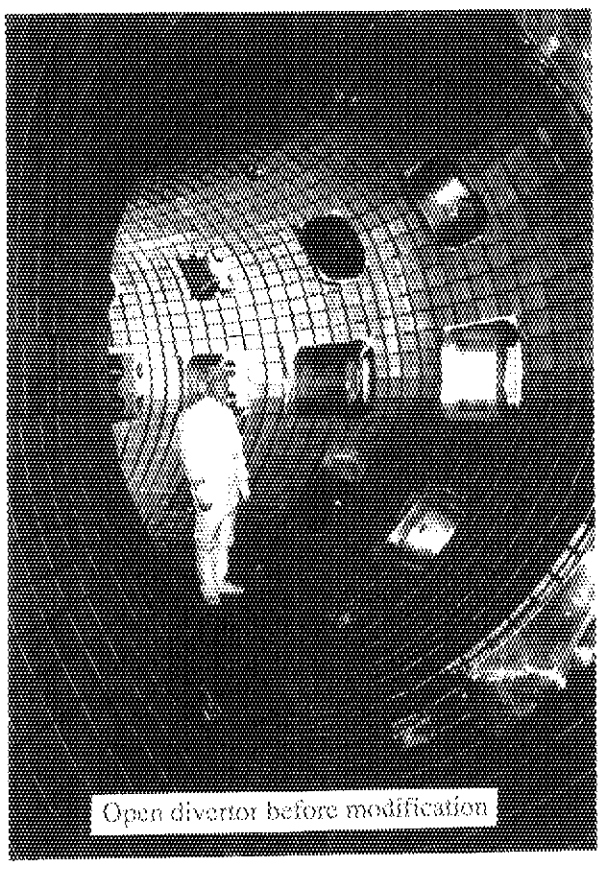

Open divertor before modification

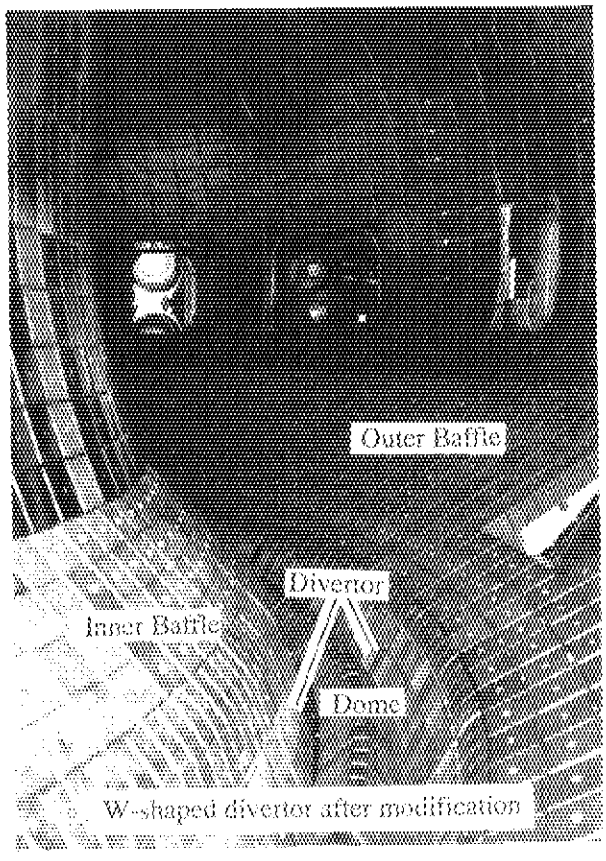

W-shaped divertor after modification

Development of N-NBI for JT-60

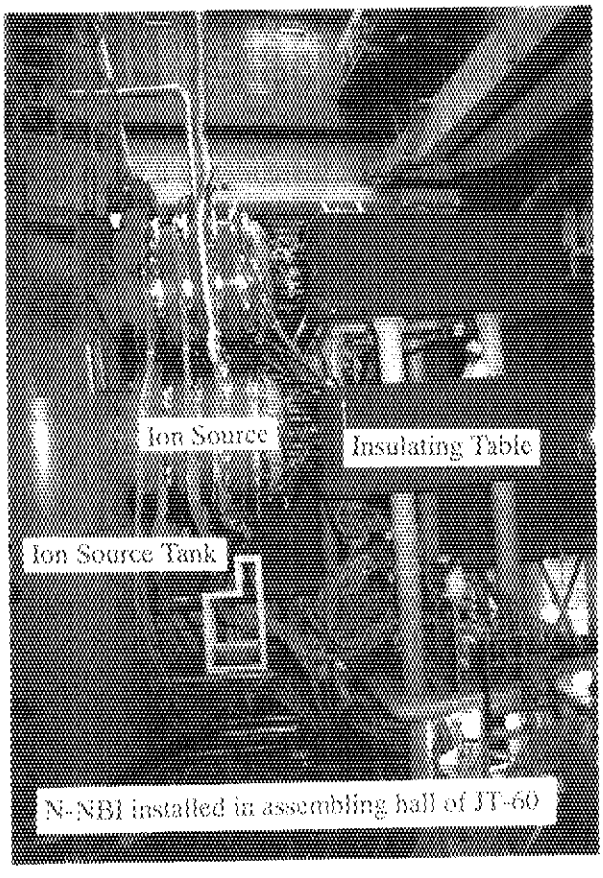

N-NBI installed in assembling hall of JT-60

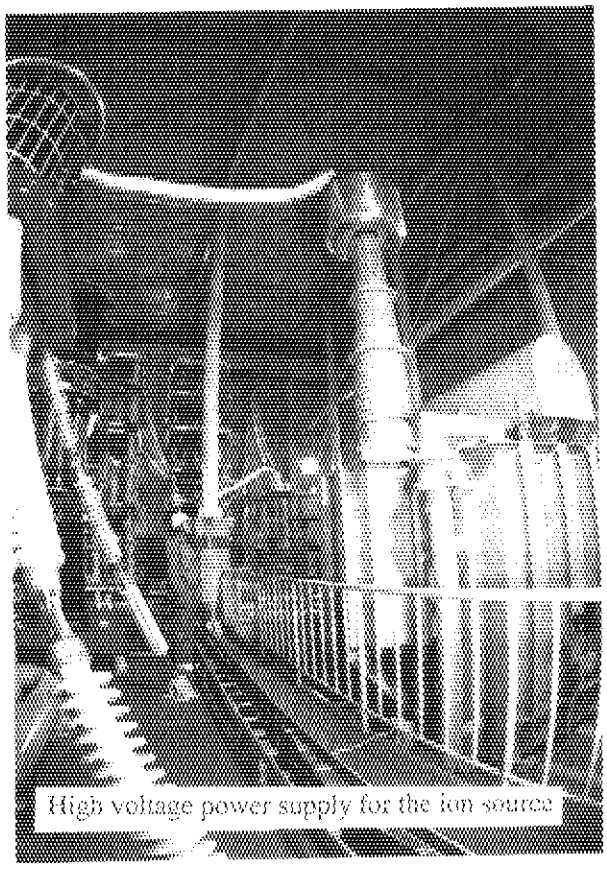

High voltage power supply for the ion source

1. Operation and Machine Improvements

In FY 1996, a total of 1,964 pulses were run during the period of 9-cycle operations and wall conditioning. The total number of shots carried out for the past twelve years amounts to 22,148 as shown in Fig.I.1-1.

In mid-April, a few carbon fiber composite (CFC) tiles broke away from the divertor in the experimental campaign aiming at high-Q_{DT} plasma performance. These divertor tiles were replaced by new ones in a shutdown period of May. In this shutdown, various maintenance works including inspection of high pressure gas facilities such as the pellet injector and the NBI cryopump system were performed in JT-60 facilities.

Following this short shutdown, wall conditionings by NBI-heated tokamak pulses and boronization were performed in June. Campaigns of high βp H-mode and negative shear experiments were started from July aiming at obtaining plasmas with high-Q_{DT} performance. In July, the negative-ion based NBI (N-NBI) system was inspected by the STA. Although a few CFC tiles were broken away from the first wall in experiments with high triangular configuration in mid-September, the repair work of the tiles was done at the succeeding maintenance week and no disturbance was made to the experiments started from late in September. After that, the campaign of negative shear experiments was conducted and break-even condition was achieved and the effective energy multiplication factor Q_{DT} = 1.05 was obtained on October 31.

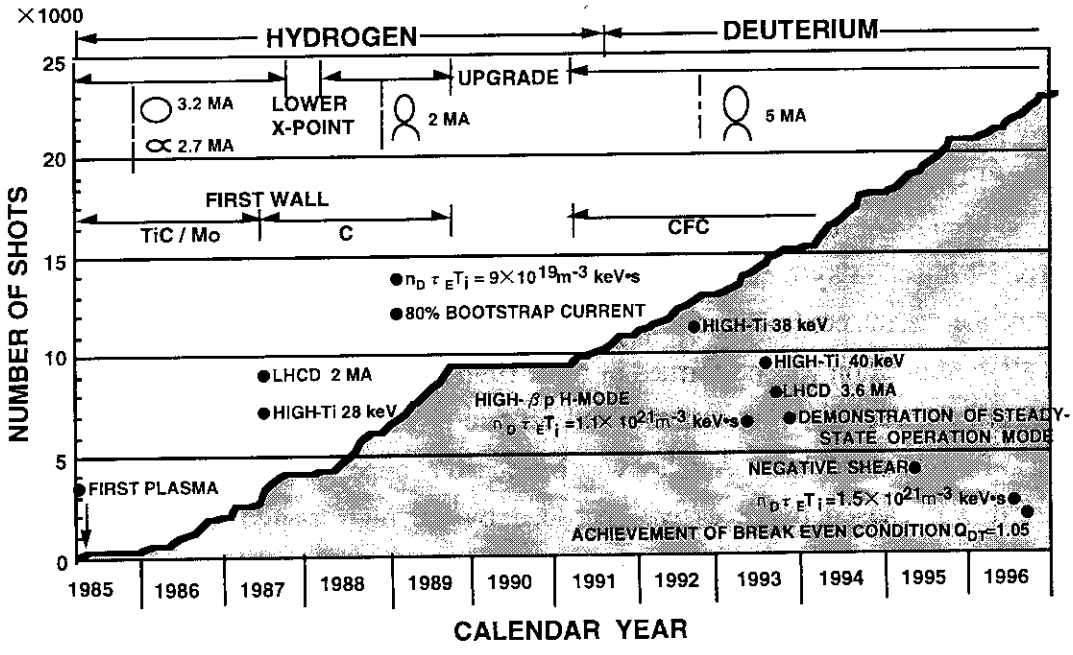

Fig.I.1-1 Progress in JT-60 operation

Annual maintenance of the JT-60 facilities were performed from November through December in 1996. In this shutdown, the cooling pipes in the toroidal field coils were inspected, and a detailed inspection of the motor generator for the toroidal field power supply was also carried out. The operation restarted in mid-January 1997 and experiments with hydrogen continued till

early in February. In this period, the N-NBI beam of 320 keV, 3.2 MW with hydrogen was successfully injected into JT-60. In mid-February, a shutdown started for the modification of the divertor from open-type to the W-shaped semi-closed pumped divertor. This modification is scheduled to finish in May 1997. In this period, a detailed inspection of the motor generator for the poloidal field power supply was also performed.

In spite of many troubles caused by aged deterioration of facility components and exploitation of new areas in core-plasma performance, JT-60 was satisfactorily operated throughout the year. The database obtained in the operation and maintenance was arranged and made useful for maintenance plan and measures for improving the aged deterioration of the facilities.

1.1 Tokamak

1.1.1 Operation and maintenance of the JT-60 machine

Operation and maintenance of the JT-60 machine have been carried out almost on schedule.

In relation to toroidal field coil (TFC), the inspection of TFC have been made two times, in May and in December, 1996 during the regular shutdown. Air tightness test was carried out for all cooling pipes, and inside of 16 cooling pipes selected were observed by fiber scope. Any deterioration of the cooling pipes were not found. Temperature measuring system, which can serve for safety operation of TFC-9 with a damaged coil turn, has been modified to strengthen the monitoring functions by installing the work station.

Three types of plasma configurations, namely, standard, high elongation, and high triangularity plasma configurations have been operated by changing the combination of the poloidal field coils (PFC). Feeder temperature has been measured for the high triangularity plasma configuration because of its excess temperature from the rating during operation.

The pellet injection system has been operated for studies for disruption with injection of Ne pellets and of the plasma confinement improvement with deuterium pellet injection.

The 8th boronization was performed in April 1996 by using boronization system.

As regard the troubles, first wall tiles fell off two times. One was prototypal tile due to lack of strength at P1 section in April. Another was happened at upper of inboard tiles at P14 section in September. It was caused by excessive heat load by the high triangularity operation. In both troubles, damaged tiles were replaced immediately and we could restart the operation of JT-60 in the next week. The vacuum leakage was occurred at P18 section due to damage of the diagnostic window. Electrical insulation was become to wrong due to damage of the honeycomb plate at NBI in P17 section. These troubles were rapidly repaired and there were not so much effect to operation schedule.

From February to June, modifications of the divertor, the vacuum exhaust facility, the gas injection facility and the pellet injection facility have been performed. In the vacuum exhaust facility,

turbo molecular pumps were replaced to advanced levitated type for being free from charging radioactivity and for reducing maintenance fee. In the gas injection facility, the injection port was increased from two to six. This relocation of gas injection port is expected to improve plasma confinement, progress in study of radiation loss and helium ash exhaust. The pellet injection facility will replace from air-gun pellet injector to centrifuge pellet injector. This modification realize continuative pellets injection and will be expected to maintain high density plasma. As the other modification, differential exhaust system for electromagnetic diagnostics and leak test stand for D_2 have been modified to remotely-controllable system and the check booth of JT-60 was also installed.

1.1.2 Modification of divertor

Modification from open divertor to W-shaped pumped divertor was completed almost on schedule. This construction started end of February in 1997, and was completed in May.

The W-shaped divertor consists of inclined targets, dome and inner, outer baffles. This W-shape configuration was adopted to realize radiative divertor plasma for reduction the heat load to the divertor targets and good H-mode confinement simultaneously. Designed maximum plasma current and toroidal magnetic field are 3MA and 4T, respectively. Maximum net heating power is 30MW. High radiative steady operation with 70% radiation loss of the net heating power and low radiative short-pulse operation with 30% loss are assumed. So, heat flux to the divertor targets is expected to be $5MW/m^2$ x 10s - $10MW/m^2$ x 4s.

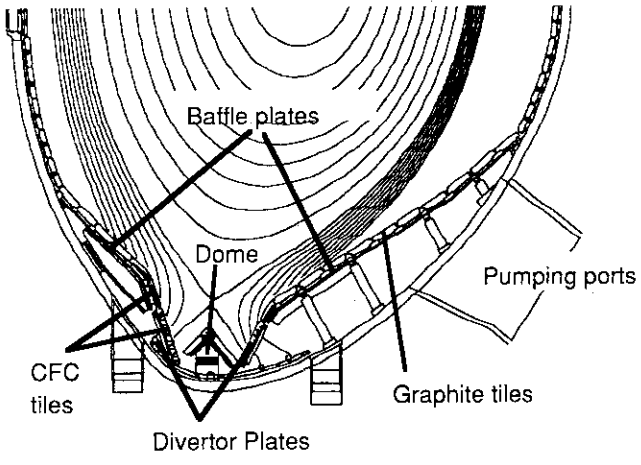

Fig.I.1.1-1 Structure of W-shaped divertor

The structure of this W-shaped divertor, which is shown in Fig.I.1.1-1, is segmented toroidally and poloidally. Divertor and dome are composed of 125 toroidal-segments. Inner and outer baffles consist of 72 blocks. Materials of these structure are mainly stainless steel (SUS-316) and Inconnel (Inconel-625) with low cobalt content. Inconel was used for the baffle plates to avoid thermal stress during baking of vacuum vessel, because vacuum vessel was made of Inconel. Stainless steel was used for the divertor base plate, since the divertor was fixed to the present cooling basement, which was made of stainless steel. Gaps between adjacent components are gas-sealed by insert-sliding mechanism. Sliding parts are electrically insulated by sprayed ceramic coating to avoid arcing. CFC tiles are used for the divertor targets, top of the dome and baffle tiles at the divertor throat. For other parts, isotropic graphite tiles are used. These tiles were designed in consideration of strength for halo current and

orientation of carbon fiber for heat load.

This W-shaped divertor has inertial cooling system. Even without water cooling, however, high power operation is possible with intervals of 20 minutes. Divertor tiles tapered with edge level difference of 0.5mm were fabricated to avoid heat concentration to the edge. These tiles were aligned with good accuracy of assembling. Cryo-pumps of three NBI heating units are used as a divertor pumping system. Effective pumping speed at the pumping entrance in the divertor region is estimated to be about 40 m^3/s. This pumping speed can be changed during a discharge by fast shutter valves of the NBI cryo-pumps for active control of particle exhaust. The leakage conductance of the baffles is estimated to be 1/10 - 1/20 of pumping speed.

1.2 Control System

1.2.1 Operation of the control system

The control system constantly works in the JT-60 experiments according to the required schedule. A function was newly developed in this fiscal year to increase shot availability (= shot numbers per day) under the condition that the temperature at the most narrow point of the toroidal field coil conductor with coolant leakage be kept below the limit of the electric insulator material. When the operator completes a next discharge condition set, this function calculates the waiting time for sequence start, so that the coil be cooled down low enough at the next excitation. In addition, in order that the coil safety be guaranteed, this function finally checks whether the temperature at 1 minute before discharge decreases below the allowable level. As the result from its installation to the working system, the availability of JT-60 experiment was increased by 20 %.

Corresponding to the modification of the first wall to a closed divertor type, part of the existing magnetic sensors were moved, and several pairs of magnetic probes were newly installed. Hence, new coefficients of the formulas for calculation of the macroscopic controlled parameter such as plasma major radius, were established using the JT-60 new equilibrium data files.

For the maintenance of the control system, annual inspections were made of the computer system, control boards, and the signal processing system for plasma control in the shut-down period of November and December. The general purpose computer system, containing all of the JT-60 discharge result data, was superseded to a UNIX workstation system, a new data base system, having been developed for two years, was come into operation. The software change for the data handling was smoothly conducted.

1.2.2 Development of a precise long-time digital integrator for magnetic measurements

Magnetic field measurements are indispensable for control and diagnostics of a tokamak plasma. The existing methods for the measurement are (i) integration of time-derivative of magnetic field, and (ii) direct measurements of absolute magnetic field using rotating coils, Hall-element sensors, etc. The latter seems to be incompatible with 14-MeV neutron field, while the former has

a problem of signal drift inevitable in an integrator, and thus it could not work for a long period of discharge (e.g. 1000 s for ITER). We chose the VF (voltage-to-frequency)-UDC (up-down counter) method for the development from the following view points: Its high accuracy is expected equivalent to analog integration. Wider dynamic range is allowed in a large digital accumulator, and drift can be compensated more precisely in a digital system.

The current results of the development are as follows [1.2-1]: (1) Technical causes of drift in the old VF-UDC system for JT-60 were analyzed. A new VF converters, then, have been developed with taking all measures identified in the analysis. (2) The first version of the new VF converter (VF#1) showed small amount of drift for 24 hours in a stand-alone integration test with input short. (3) Conversion linearity of the VF#1 is much improved from 0.027 % FS (the old VF) to 0.002 % FS (VF#1) in the ranges of ±10V and 1±0.5MHz. A dead band width at 0-V input is reduced from a few mV to several tens of micro volts. (4) A new method for drift compensation is being installed in the VF#2, which can suppress the amount of drift with constant speed to several counts for 1000-s integration.

The measurement with the VF-UDC in JT-60 experiments will be conducted in June 1997.

1.2.3 DSP application to fast parallel processing in JT-60U plasma shape reproduction

Recently the experimental observation has been recognized that the full shape reproduction and control is one of the important issues for improving plasma energy confinement performance. The requirements for more sophisticated plasma position and shape real-time control stimulates development of the parallel processing system.

In the methods of plasma shape reproduction, the core computational procedure is to determine the outermost magnetic surface using the flux function [1.2-2]. We adopted a TMS320C40 DSP as a main real-time processor, because this DSP has 6 ports to communicate separately with other DSP's for parallel processing. A newly designed system is composed of 8 nodes of the DSPs, four of which have 32-MB memories [1.2-3]. This system was succeeded to work in parallel, and reproduces plasma shape in real time. The shape identification calculation can

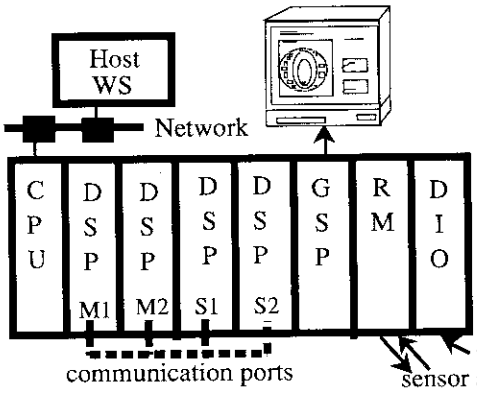

Symbol	Type	Function /Manufacturer
CPU	MVME147	MC68030, 25MHz / Motorola
DSP M1, M2	DSP8040	TMS320C40x 2, 40MHz, 2MB / MTT
DSP S1, S2	DSP8044	TMS320C40x 2, 40MHz, 32MB / MTT
GSP	UDC6000TI	Graphics Processor TMS34020, 33MHz / Univision
RM	DSP8230	Digital Input (32 ch) / MTT
DIO	VMIVME5576	Reflective Memory (256kB) / VMIC

Fig.I.1.2-1 Configuration of the improved JT-60U plasma shape reproduction system

be performed at every 25 ms, and the full shape can be drawn at every 50 ms at JT-60U. This system configuration is shown in Fig.I.1.2-1.

1.2.4 Development of JT-60U plasma equilibrium control model

In general, it is necessary to have a precise model for design and/or optimize a control system. We have developed a plasma equilibrium control model for JT-60, which shows that it can accurately reproduce the time evolution of plasma vertical and horizontal positions on the computer [1.2-4]. This model has been re-built for JT-60U in a workstation by using MATLAB (a system analysis code, made by the Math Works, Inc.). Simulations using this updated model has shown that the control method includes a cause to deteriorate control performance and to induce large voltage fluctuations in a plasma. Since this cause comes from the error in the analog-to-digital conversions and the quantization process in digital computing, a developed new method was predicted to be effective in the simulations to improve the control performance [1.2-5].

This new method was applied to the JT-60 plasma experiments, and we confirmed the plasma control performances are greatly improved as follows [1.2-6]: (1) Control accuracy improvement: The steady-state deviations from the nominal references are reduced to less than 5 mm for Rp with the half of the old control gain, 2 mm for Zp, and 2 mm for Xp with an improved gain. In the Rp-tracking test with the 10-Hz oscillation with 3-cm amplitude, Rp is well controlled by the new algorithm, while the overshooting is observed under the old control algorithm. In the step response, the error of control is less than 10 kA for Ip, and less than 1 cm for Rp, Zp, or Xp. (2) Fluctuation suppression: No irregular fluctuation of the position parameters is observed under the control of the new algorithm. Voltage fluctuation observed in the period under the old control is greatly suppressed by the new algorithm. The reduced amount of peak-to-peak voltage are : 1600 V->300 V (Vertical field coil), 32 V-> 16 V (Divertor coil). In addition, the fluctuation of one-turn voltage difference between inboard and outboard is completely suppressed to 1/10 (3V -> 0.3 V).

1.2.5 Development of the JT-60 new control systems

Since requirements of modification for advanced plasma control and efficient sequential control increase, two control systems began to be developed. Concerning a new plasma control system, we chose an Alpha-288 VME board (made by DEC. Ltd.) for a main processors, and built a VME-bus system together with the I/O boards and a reflective memory module as shown in Fig. I.1.2-2. This system is expected to execute the real-time program approximately 300 times faster than the old mini-computer (1 MIPS), and its performance test is being conducted aiming at installation to the actual system by the second quarter of 1998.

Concerning a new discharge sequential control system, we performed system design of the hardware configuration. This system is composed of three workstations (WS's) with network ports, and each of them has its particular role to supervise the JT-60 subsystems. The roles of the

workstations are as follows: SQ-WS is a master for the sequential control of all the subsystems. This WS sends the all command messages and receives the replies. DC-WS is a master for discharge condition files, and distributes the appropriate condition to the corresponding subsystem, after compiling procedures. RD-WS is a master for result data acquisition. This receives result data from all subsystems, and builds an intermediate file before transferring it to the JT-60 database production server. The new system will be expected to come into operation in 1998.

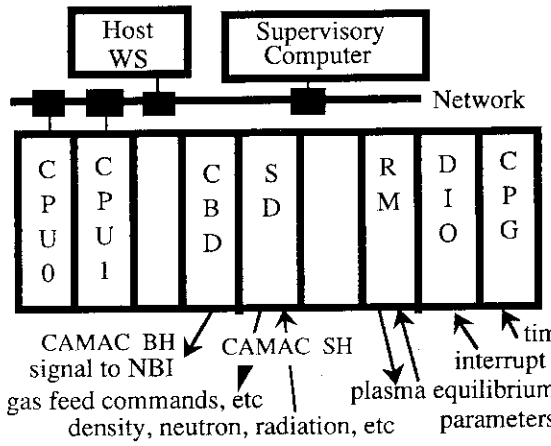

Symbol	Type	Function /Manufacturer
CPU0,1	AXPvme280	DEC 21066A, 288MHz, 64MB/ DEC
CBD	CBD8210	CAMAC Branch Driver / CES
SD	VSHD2992	CAMAC Serial Driver / HYTEC
RM	VMIVME5576	Reflective Memory (256kB) / VMIC
DIO	DSP8230	Digital Input (32 ch) / MTT
CPG	CPG241	Clock Pulse Generator / MTT
WS	Alpha WS 255	UNIX-WS alpha 255MHz / DEC

BH: Branch Highway SH: Serial Highway

Fig.I.1.2-2 Configuration of the plasma real-time control system.

References

[1.2-1] K. Kurihara and Y. Kawamata, "Development of a precise long-time digital integrator for magnetic measurements in a tokamak", in Proceedings of 19th Symposium on Fusion Technology, Lisbon (Portugal, 1996)

[1.2-2] K. Kurihara, Fusion Technol. 22 p.334 (1992).

[1.2-3] H. Adachi, Y. Kawamata, K. Kurihara, "DSP application to fast parallel processing in JT-60U plasma shape real-time visualization," in Proceedings of Symposium on Scientific Research Technologies, Tokyo (1996) (in Japanese).

[1.2-4] K. Kurihara, Fusion Engineering and Design. 19 (1992) 235-257.

[1.2-5] M. Yoshida and K. Kurihara, "The Influence of the Analog-to-Digital Conversion Error on the JT-60 Plasma Position/Shape Feedback Control System," JAERI-Tech 95-053 (1995) (in Japanese).

[1.2-6] K. Kurihara and JT-60 Control Group, JAERI-Review 97-047 (1997).

1.3 Power Supply

1.3.1 Operation and maintenance of the JT-60 power supplies

The JT-60 power supplies were operated on schedule without any serious problems throughout this fiscal year, though thirteen years have passed since they were completed. In November and December 1996 and March 1997, annual maintenance of the power supplies were performed according to the regulations for electric equipment in Naka Fusion Research Establishment. In particular, detailed inspections of two motor-generators for the toroidal field coil power supply (TFPS) and the poloidal field coil power supply (PFPS) were conducted without removing their rotors. The total operation time of the TFPS motor-generator amounts to 13,476 hrs and that of the PFPS motor-generator 13,793 hrs. In the TFPS motor-generator, two oil-pumps

for lifting the thrust bearings up were renewed. A half of guide bearings in the middle stage were replaced by new ones according to the results of liquid penetrant tests (PTs). On the other hand, some mechanical parts of the liquid rheostat (LRH) were renewed and all of the guide bearings in the lower stage were replaced by new ones in the PFPS motor-generator.

1.3.2 Modification of the PFPS for high triangularity operation

Since significant improvements of the plasma performance have been observed in the high triangularity divertor operation with plasma current up to 2 MA in JT-60 [1.3-1], combination of the poloidal field coils and the converters in the PFPS was rearranged for the high triangularity operation (d £ 0.4) with higher plasma current up to about 3 MA. A new connection bus bar switch for changing the operation modes of the "high triangularity", "standard/high elongation" was introduced. The high triangularity operation after the modification is scheduled in June 1997.

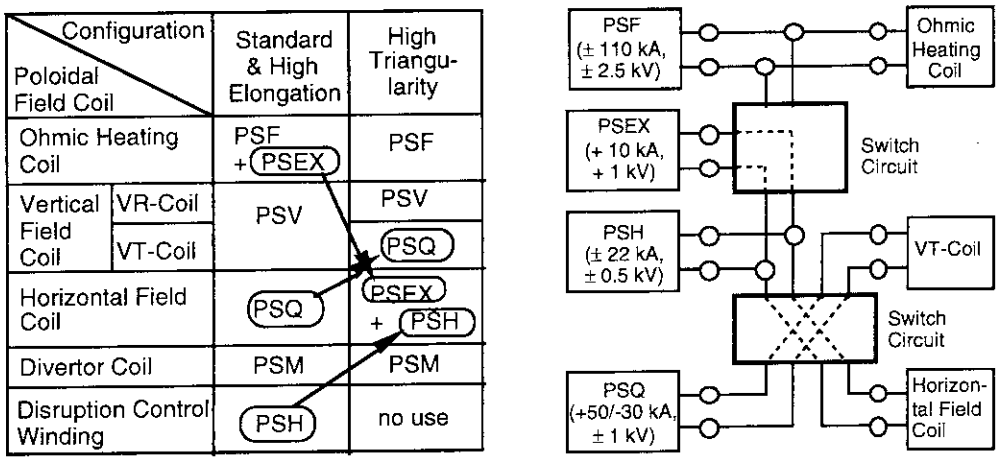

Fig.I.1.3-1 Combination of the poloidal field coils and the PFPS converters for the divertor configurations of "standard", "high elongation" and "high triangularity".

1.3.3 Development of a current-driven PWM converter with high power-factor

As a basic technology development, we have continued to develop a current-driven PWM converter for a superconducting coil power supply, because the semiconductor performance for power applications has been drastically increased up in recent years to be feasible for next generation tokamaks. Since the PWM converter is able to operate with a power factor of unity, the power distortion to commercial transmission lines caused by reactive power fluctuations can be decreased in comparison with conventional thyristor converters. Hence, a PWM converter using IBGTs was developed and tested to clarify its possible technical issues. The output ratings of the designed converter are about 250V and 500A, and the switching frequency is about 1KHz. Results from preliminary tests shows that the pulse modulation method has to be improved to produce zero voltage output with a large current for applying super conducting coils.

References

[1.3-1] Y. Kamada and et al., in Proc. of 16th Int. Conf. on Plasma Physics and Controoled Nuclear Fusion Research, IAEA-

CN-64/A1-6, Montréal, Canada(1196).

1.4 Neutral Beam Injection System

1.4.1 Positive-ion based NBI system

The beam of 40 MW at an energy of around 90 keV, that is the world highest deuterium neutral beam power, has been injected successfully by the simultaneous injection of 14 beamline units. This achievement has been produced through the pursuit of the optimum conditions for the beam acceleration based on the improvement of the accelerator for the ion source. As the result of this injection, the JT-60 has been able to expand the plasma experimental area with a higher power NBI heating.

1.4.2 Negative-ion based NBI system

The beam injection experiment for the negative-ion based NBI system (N-NBI) has been continued, augmenting the beam power gradually, ever since the beam into the plasma by the N-NBI had been injected successfully for the first time in the world in March 1996. The deuterium neutral beam of 2.5 MW at an energy of 350 keV has been injected with two ion sources in September 1996. As this result, it was confirmed that the characteristics of the NBI current drive and plasma heating with a high neutral energy beam have agreed with a theoretical estimation.

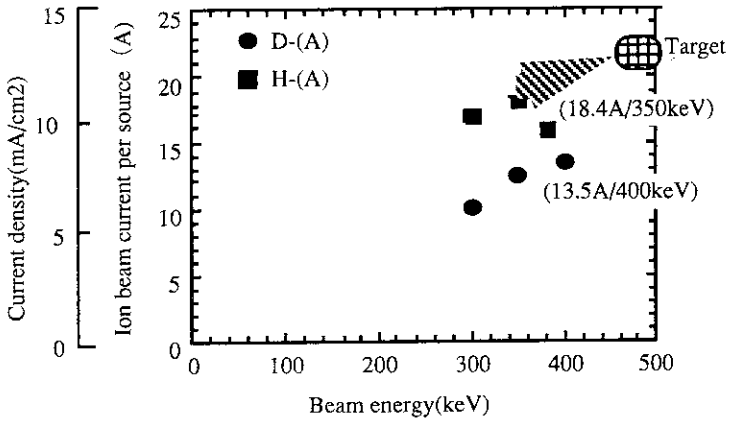

Fig. 3.1.3.9 Progress of negative ion beams in the N-NBI for JT-60

After the partial remodeling for the ion source and the power supply, the hydrogen neutral beam of 3.2 MW at 350 keV has been injected with one ion source in February 1997. And the negative-ion beam power per one ion source has reached 400 keV, 13.5 A with deuterium and 350 keV, 18.4 A with hydrogen, that is the world highest negative-ion beam. They are shown in Fig.I.1.4-1.

The current drive and plasma core heating experiments with the N-NBI will be progressed strongly in JT-60, aiming at a rated injection power of 10 MW, for the establishment of the technical and physical bases of the ITER construction.

1.5 Radio-frequency System

1.5.1 LHRF system

The lower hybrid range of frequencies (LHRF) system has contributed to successful experiments on the reversed magnetic shear mode [1.5-1] and assist for start up of plasma current [1.5-2] mainly in FY 1996. Total shot numbers of the discharge supported by LH injection for A,

B and C units are 369, 379 and 315, respectively. The maximum generated power of 8-klystrons for A, B and C units are 3.4, 3.0 and 2.6 MW, respectively . The main troubles in this FY were 1) degradation of klystrons due to reduced standoff capability around electron gun, and 2) malfunction in the crowbar circuit of C unit triggered by electric noises from the negative ion based NBI system.

An RF breakdown in the antenna mouth could cause serious damages of the antenna. In order to avoid heavy breakdown in the main vacuum part of the antenna, an additional arc detector was equipped in the antenna system as shown in Fig. I. 1. 5-1. When arc lights detected, RF injection is immediately shut down during 100 msec and then is restarted by the protection system. This arc detector works only during RF injection to distinguish the arc from relative strong stray lights at the plasma initiation of the discharge. The arc detector is a key device for efficient antenna-conditioning without terrible breakdown.

In addition, as an efficient conditioning technique of the antenna, RF injection pulse was modulated with intermittent short pulses, for example, pulse length of 20 msec and duty of 50 %. This pulse-modulated injection could lead to stable power up without hard breakdown, while with small breakdown necessary for progress of the conditioning. Therefore , the damage of the antenna is reduced, and plasma shot number required decreases. For the current drive

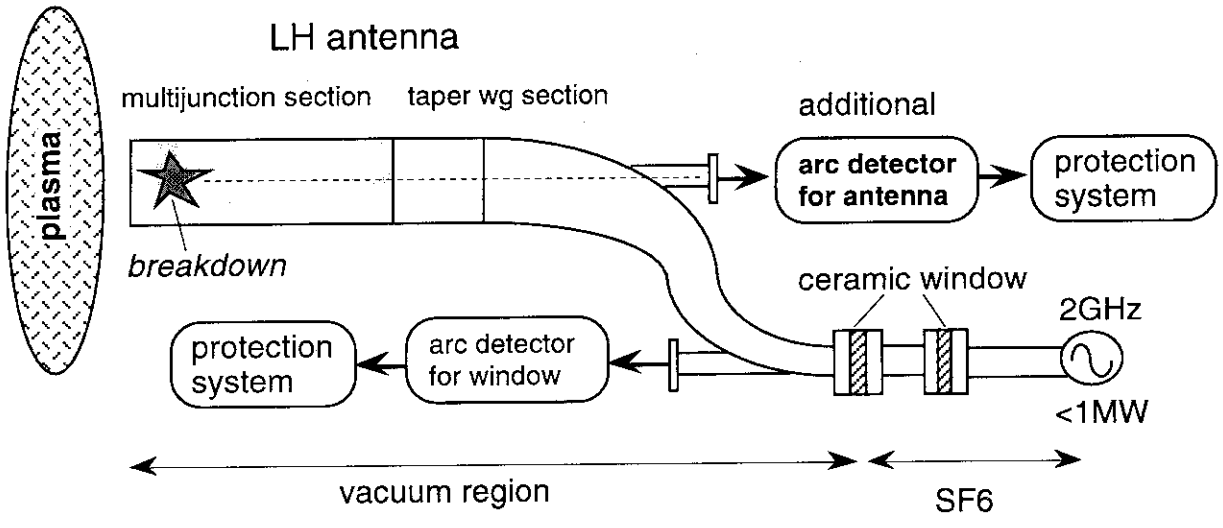

Fig. I.1.5-1 Arc detector system for antenna and RF window

experiments using pulse-modulated injection, the current drive efficiency did not degrade under the same averaged input power. The hard X-ray profile showed a little bit wider, namely broad current profile, in pulse-modulated injection compared with that of no modulation.

1.5.2 ICRF system

The ion cyclotron range of frequencies (ICRF) system was operated well at 102 MHz in FY 1996. The frequency of the system was changed to 102 MHz from 116 MHz in December 1995,

in order to keep up central plasma heating with the low toroidal magnetic field (B_T) operation. The resonant B_T of the second harmonics of hydrogen was reduced from 3.8 T to 3.34 T. From January 1996, RF power at 102 MHz had been injected to the plasma occasionally. Impedance matching between the antenna and the transmission line using the stub tuners and the high power phase shifters, adjustment of the phase control, and the antenna conditioning were taken place. About 80 shots were devoted to impedance matching and antenna aging after the frequency change. Following the antenna aging, the coupled power reached 4.3 MW (short pulse) in 80 shots and 4.6 MW for 1 sec at last in November 1996. The maximum stand-off voltage in the antenna was ~ 34 kV and is close to the maximum voltage achieved at 116 MHz. It means that low coupling resistance limited the coupled power.

At 102 MHz, the coupling resistance of the antenna, R_C, was 60 - 70% of that at 116 MHz [1.5-3]. Figure I.1.5-2 shows the R_C versus the gap between the separatrix and the first wall of the vacuum vessel on equatorial plane. The Faraday shield of the ICRF antenna is ~ 3 cm behind the first wall surface. The stand-off voltage in the antenna versus the coupled power P_{IC} at 102 MHz and 116 MHz is shown in Fig. I.1.5-3. It is clear that the P_{IC} at 102 MHz was limited by the antenna voltage stand-off.. In contrast with at 102 MHz, P_{IC} at 116 MHz was limited mainly by the generator capability [1.5-4]. Reduction of R_C results from RF characteristics of the antenna which was designed to obtain best coupling at ~ 120 MHz. For the closed divertor plasma expected in the operation in 1997, a little larger antenna-separatrix gap and lower SOL density due to the baffle plate are foreseen, and then lower R_C is expected. Improvement of antenna voltage stand-off of the coupling system is effective to couple higher power.

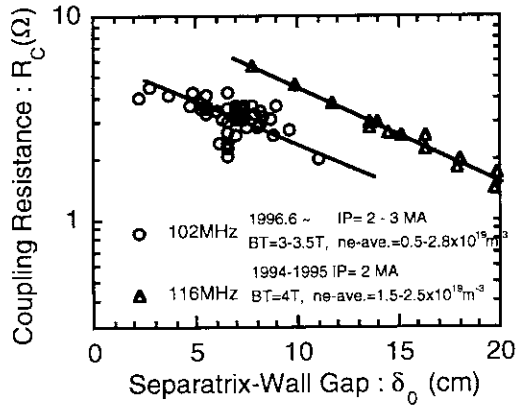

Fig. I.1.5-2 Coupling resistance at 116 and 102 MHz voltage

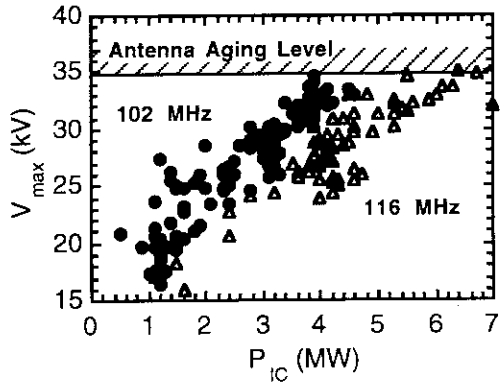

Fig. I.1.5-3 Coupled power limited by the antenna stand-off at 102 MHz.

To increase the stand-off voltage, short plunger and outer conductor of the stub tuner were newly designed and fabricated. The new plunger is a conservative mechanical contact type as a substitution of the former choke plunger, which acts as a equivalent short circuit without

mechanical contact. The choke plunger had an advantage in capability of quick movement during high power RF pulse. However the choke plunger requires precision in narrow gaps in its structure to keep high voltage stand-off capability. When the uniformity of the gap is lost after lots of operations for many years, the arcing tends to occur in high voltage operation and damages the structure. Importance of quick movement of the plunger during the discharge shot had become lower because frequency feedback control works well to keep good impedance matching.

For the new contact type plunger, "multilam band" is used as a contact element, as well as the high power phase shifter. Reliability of the contact element is confirmed in a 10 thousand strokes' endurance test of the high power phase shifter. The new short plunger will be installed in the stub tuner in April 1997.

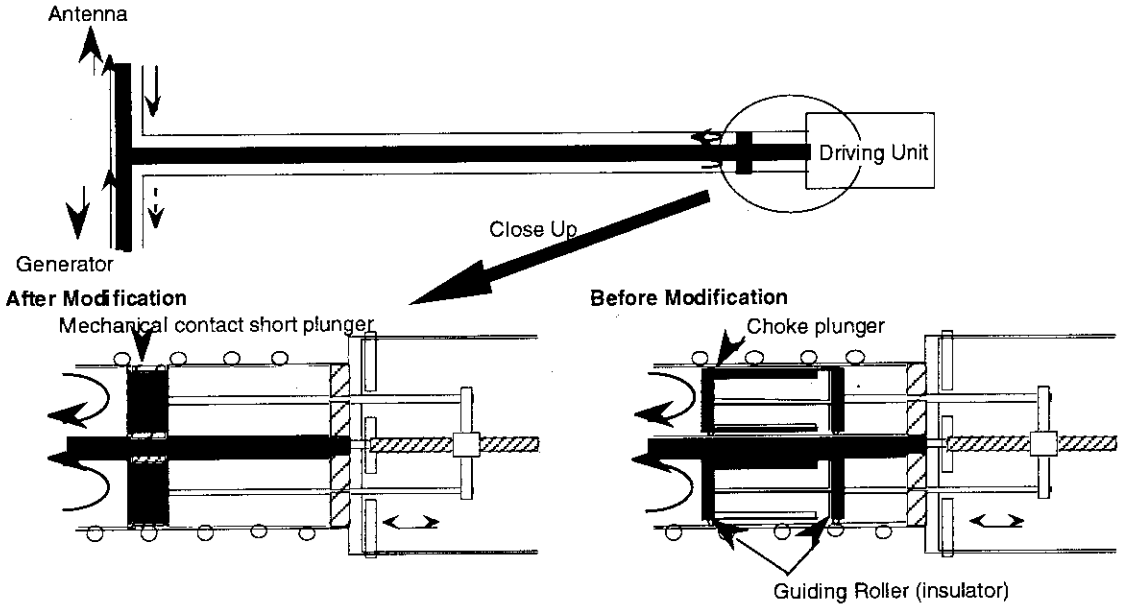

Fig. I.1.5-4 Modification of the Stub Tuner

Reference

[1.5-1] S. Ide, M. Seki, et al., "Sustainment and Modification of Reversed Magnetic Shear by LHCD on JT-60U", Plasma Physics and Controlled Fusion 38 (1996) 1645-1652.

[1.5-2] R. Yoshino, M. Seki, "Low electric field (0.08 Vm-1) plasma-current start-up in JT-60U", Plasma Physics and Controlled Fusion 39 (1997) 205-222.

[1.5-3] S. Moriyama, et al., "ICRF Coupling at 102 MHz", Review of JT-60U Experimental Results from January to November 1996, Section 5.4, JAERI-Research, 1997.

[1.5-4] S. Moriyama, et al., "ICRF Coupling Study and Technology Development for JT-60U", Proc. US-Japan workshop for RF technology, Florida, Dec. 1995.

1.6 Diagnostic System

During the reconstruction phase of the divertor, electrostatic probes, a reciprocating probe, mm-wave interferometers, multichannel borometers, a visible fiber array, ion gauges and Penning gauges were newly installed for the detailed study of the divertor plasmas. Significant progress was also made in the diagnostic system as described in the following sections.

1.6.1 Automatic analysis of sawtooth inversion radius with adaptive neural network [1.6-1]

A neural network algorithm was applied to the electron cyclotron emission (ECE) data of JT-60U plasma, and sawtooth inversion radii are automatically acquired to obtain information concerning current profiles. To detect the time of sawtooth collapse, a method of adaptive signal prediction by a three-layered perceptron is applied to the time series of ECE data which were obtained by a grating polychromator system. The collapse time is determined from the time when the prediction error is maximized in magnitude. This work was performed by a collaboration with Toyama Kenritsu University.

1.6.2 Elimination of non-thermal emission from FTS interferogram during ELM[1.6-2]

A Fourier-transform spectrometer system (FTS) is used for the measurement of time evolution of electron temperature profile. In the ELMy H-mode phase, however, electron temperature measurement by FTS becomes difficult because the interferogram suffers from intense non-thermal emission from plasma which relates to ELM. In order to remove and reconstruct the interferogram, a high-pass filter and smoothing method is applied. The electron temperature deduced by Fourier-transforming the reconstructed interferogram showed a good agreement with the result of a relatively calibrated grating polychromator system.

1.6.3 Determination of radial position in the measurement of electron temperature profiles from ECE [1.6-3]

The effects of relativistic frequency down-shift and optical thickness at the medium electron temperatures are important to determine the radial position of the electron temperature profile from the electron cyclotron emission. Exclusion of the effects in the determination results in a pseudo radial displacement (Δr) of the obtained electron temperature profile. The displacement depends on only three parameters (electron temperature, T_e, optical depth, τ, and major radius, R). In order to evaluate the radial position correctly for any tokamak, a scaling of the displacement is found as Δr (m)= 0.0009 R(m) T_e(keV) (1+ 40/(5τ)). This scaling is applicable for τ > 5 where the error is less than 0.5% of the major radius.

1.6.4 Upgrade of MSE diagnostics

A new polarimeter with nine viewing points for the motional Stark effect (MSE)

spectroscopy was installed in December, 1995 in addition to the old one [1.6-4]. By using old and new polarimeters, we can measure the region of R = 3.04-4.29 m with 14 chords, which almost covers from the axis to the surface for a standard configuration. To reduce the error by background light, multi-layer dielectric mirrors are used in the new spectrometer. The aluminum-coated mirrors in the old polarimeter have also been changed to multi-layer dielectric mirrors. The whole MSE system had been operated routinely in 1996 and safety-factor profiles were obtained in various types of discharges.

1.6.5 Optical fiber array viewing divertor region for 2-dimensional spectroscopic measurement

A 32-channel optical fiber array system viewing the divertor region from the side was installed to measure poloidal emission profiles of hydrogen isotopes and impurities. This array system guides the visible light emitted in the divertor region to a spectrometer composed of filter optics. The emission profiles of five different spectral lines are measured simultaneously by this spectrometer with a 32-ch photomultiplier array at a fast sampling rate of 160 μs and with photodiode arrays at a slow sampling rate of 2.8 ms. The poloidal contours of spectral emissions in the divertor region are constructed by analyzing both emission profiles from this system and from a existing 60-channel optical fiber array system viewing from the top.

1.6.6 Fast sampling charge exchange recombination spectroscopy [1.6-5]

A Charge exchange recombination spectroscopy (CXRS) system with a three interference filter assembly and photomultipliers has been developed for the faster measurements of ion temperatures (Ti) and toroidal rotation velocities (Vt). Each filter has a 0.2 - 1 nm bandwidth (FWHM), and the three filters have a slightly different peak wavelength to its selected CXR line, depending on the Ti and Vt at the measuring position. 12 assemblies viewing on and off the neutral beam line were installed for the space-resolved Ti, Vt and the background measurements. The maximum sampling rate of this system is 160 μs. This is faster than 16.7 ms of the existing CXRS system composed of spectrometers and CCD cameras.

1.6.7 Neutron fluctuation measurement system [1.6-6]

In JT-60U, neutron emission monitors with the time resolution of 1ms and 14 MeV - neutron detectors with the time resolution of 10 ms have been used from the beginning of the DD discharges. In this fiscal year, the neutron detector with a fast time resolution of 40 μs and a spatial resolution of 15 cm was installed in order to study the correlation between the MHD behaviors (such as sawtooth activities and fishbone instability) and the neutron emissions. The detector, which is composed of a plastic scintillator (NE102A) and a photomultiplier, is operated in the current mode to get a fast response. The detector is mounted approximately 2 m away from the surface of the vacuum vessel near the mid plane.

References

[1.6-1] Isei N., Ooi Y., Iwama N., et al., to be submitted to Jounal of Plasma and Fusion Research.
[1.6-2] Isayama A., Isei N., Ishida S., et al., JAERI-Research 97-047, 138 (1997).
[1.6-3] Sato M., Isei N., Isayama A., et al., (Proc. International Conference on Plasma Physics, Nagoya, Japan 1996) Vol. 2, p.1438.
[1.6-4] Fujita T., Kubo H. and Oikawa T., JAERI-Research 97-047, 143 (1997).
[1.6-5] Koog J.S., Sakasai A., JAERI-Research 97-047, 146 (1997).
[1.6-6] Morioka A., Nishitani T., Kondoh T., et al., JAERI-Research 97-047, 148 (1997).

1.7 Data Analysis System

1.7.1 FAME system

The FAME (Fast Analyzer for Magnetohydrodynamic(MHD) Equilibrium) system has been developed in 1993 to provide about 130 MHD equilibria in time series which are enough for the non-stationary analysis of the experimental data of JT-60U within a shot interval. The FAME system have stored all the equilibrium data in JT-60U from 1993. In FY1996, the efforts of utility development and update have been concentrated on more effective use of the FAME system. An equilibrium animating system has been developed on a workstation arranged in the central control room. The system can provide animations of MHD equilibrium analyzed by the FAME. In order to display typical equilibrium data such as an ellipticity, an internal inductance, and so on as functions of time with other experimental data, the DAISY (DAta Illustration SYstem) and the software of FAME system are improved.

The new system, FAME-II, with a high processing speed utilizing IBM RS/6000 SP is being introduced, succeeding the former FAME system. The FAME-II system is a MIMD type small scaled parallel computers with 7 microprocessors and the maximum theoretical speed is 3.42 GFLOPS. For the software system of FAME-II, MHD equilibrium analysis code SELENE and its input data production code FBI are tuned up taking the parallel processing into consideration as well as the former FAME system. Consequently, the computational performance of the FAME-II system for special use of JT-60U equilibrium analyses becomes more than 3 times faster than the existing FAME system. The new system also has the file server system with the large capacity of the mass data storage of 50 GB, which can afford to store all the equilibrium data in JT-60U for coming 3 years.

1.7.2 Data Link System and Video Conference System

The effectiveness of the remote participation in JT-60 experiments from PPPL was successfully demonstrated during QDT >1 campaign from the end of October to the beginning of November, by utilizing the Data Link System and the video conferencing systems. Participants from both JAERI and PPPL jointly analyzed and discussed the JT-60 data and recognized achievement of a high fusion performance in JT-60 reversed shear discharges. This success is

envisaged to be a new model of the international collaboration via computer and communication networks for the twenty-first century.

In July '96, a remote diagnostics operation and a remote data analysis were simultaneously tested. A neutron diagnostic system on the JT-60 has been successfully operated from Los Alamos National Laboratory (LANL) via the JAERI- DOE leased, overseas line. Remote analysis of JT-60 data from PPPL was done by using the Data Link System and the video conferencing systems for the discussion between JAERI and PPPL.

In October '96, the Data Link System was completed for exchanging experimental data of JT-60 through the Data Link. Selected data among approximately 2100 typical JT-60 shots were transferred to this system for the use under the regulation of remote access under the Three Large Tokamak Agreement. A new database of detailed experimental data with the amount of 6MB per diagnostic for each shot were also prepared.

The Data Link System provided data analysis tools; a first magnetic boundary identification code (FBI), a MHD equilibrium analysis code (SELENE), and a plasma profile monitoring tool (SLICE).

A multi-point bridge system was introduced for ISDN based video-conferencing capabilities to enable multi-point connections. The JT-60 control room is now connected to PPPL and LANL via the video conference systems using ISDN lines.

1.7.3 Computer System and Database

The main frame of computer system have been replaced from the MSP operating system on FACOM M-780 (FEP) to the UNIX operating system on workstations due to the plan organized by the Center for Promotion of Computational Science and Engineering. According to the plan, all plasma analysis codes, utility codes, and many databases have been transplanted to the new system. Especially, computer graphic programs and data handling programs have been almost newly developed for the UNIX system. The preparation of the transplantation had been started from FY1994 and carefully carried out. The new UNIX system have enabled to realize a distributed processing system and augment the data processing capacity by about 10 times.

The database related software was also largely changed. The database structure was redesigned to a more flexible one and database managing programs, NDBS, were converted from the original one on FEP. A network data transfer program, IFDB, was also ported from the original ISP-to-FEP version. After the completion of CO2 interferometer, YAG Thomson scattering system and scintillating fiber neutron detectors, their data were added to JT-60 experimental database. Plasma equilibrium data calculated by FAME system were also added.

Some subsystems and programs of JT-60 data processing system were improved during FY1996 to replace aged mini-computers and meet the demands of plasma diagnostic systems. Since January 1996 a workstation-based prototype CICU system had been tested in detail on

behalf of one of present CICU systems based on mini-computers. After the improvement of hardware and software components, the final design of new CICU systems was completed. New CICU systems consist of VME modules with CAMAC serial highway drivers. They have been under a practical test for the complete replacement of CICU systems.

A new mass data acquisition system, FDS, was developed. It uses a UNIX workstation and a VME-based opto-electric conversion module with memory. It would be used as a successor to a present minicomputer-based TMDS system. New programs to calculate physics data from TMDS raw data were developed for some diagnostic systems and the results were stored as a new database in the JT-60 file server or the newly introduced TMDS server.

Reference

[1.7-1] Hamamatsu K., Matsuda T., Nishitani T., et al.," Remote Laboratory in Fusion Experiments, Present Status and Progress", J. Plasma Fusion Res., **73**, 385 (1997) (in Japanese)

[1.7-2] Aoyagi T., " Data Processing System for JT-60", J. Plasma Fusion Res., **72**, 1370 (1996) (in Japanese)

2. Experimental Results and Analysis

2.1 Reversed Shear Experiments

2.1.1 Achievement of high fusion performance [2.1-1, 2]

Significant improvement in fusion performance has been achieved in thermonuclear fusion regime with 16 MW of deuterium-neutral beam injection into reversed shear discharges at 2.8 MA of plasma current. The core plasma energy is efficiently confined due to the internal transport barrier formed for both ions and electrons at ~70% of the plasma minor radius near the boundary of the negative shear region.

In the best shot the plasma stored energy increased up to the JT-60U record value of 10.9 MJ with a high DD neutron emission rate of 4.5×10^{16} /s. Plasmas that could have been produced in an assumed D-T (deuterium-tritium) fuel are simulated by using the TOPICS code and the TRANSP code simply considering the full D beams with the experimental beam energy into a plasma of 50:50 D-T mixture. Good agreements are obtained with confidence among these analyses for D-D analysis and D-T simulation. The projected fusion power is equivalent to 10.7 MW with 83% from thermonuclear reactions. This large fraction of thermonuclear reactions should be emphasized in contrast to the other high performance regimes such as TFTR supershot, JET hot ion H mode and JT-60U high β_p H mode, in which substantial fraction of fusion power came from beam-thermal reactions. A simple ratio of the fusion power to the actual beam absorption power, P_{DT}/P_{abs} would be 0.68. For transient plasmas, the fusion amplification factor can be defined from the effective heating power that can be estimated by subtracting the dW/dt term (the loss power from the plasma) from P_{abs} [2.1-3]. Following this definition, the equivalent fusion amplification factor Q_{DT}^{eq} reached 1.05 with a high fusion triple product of $n_D(0)\tau_E T_i(0) = 7.8 \times 10^{20}$ m^3•s•keV. The remarkable progress in fusion performance can be attributed to the stable increase in plasma current with a wide reversed shear region up to 70-80% of plasma minor radius (see Fig.I,2,1-1) and a well optimized control of the beam deposition profile during the current ramp-up. The high performance reversed shear plasmas, which had an L-mode edge, terminated into a disruptive beta collapse when q_{min} decreased to ~ 2. Pressure profile broadening with an H-mode edge would improve the stability and lead to a quasi-steady-state operation as observed in the high β_p H mode [2.1-4].

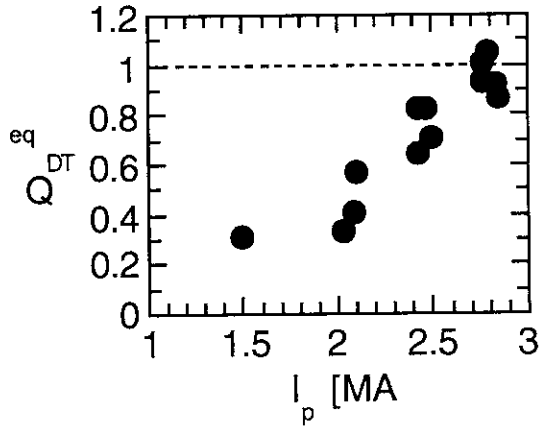

Fig. I.2.1-1. The calculated Q_{DT}^{eq} as a function of plasma current, Ip, for reversed shear discharges. The fusion performance has been improved with the incease in Ip.

2.1.2 Internal transport barrier and confinement [2.1-2, 5, 6, 7]

Steep gradients in profiles for electron density, electron temperature and ion temperature, which indicate the formation of Internal Transport Barrier (ITB), are observed in JT-60U reversed shear plasmas. Significant reduction of thermal transport are obtained both for ions and for electrons [2.1-8]. The steep gradient zones have a radial extent of ~20% of plasma minor radius and are located inside the radius of q_{min}. To obtain high performance plasmas, it was essential to form a q profile with a large radius of q_{min} (up to 80% of plasma minor radius) in a low q regime (q_{min} ~ 2). The formation of ITB in an early phase and the control of pressure and current profiles during the current ramp-up with keeping the ITB were key techniques to obtain a large radius of q_{min} in a low q_{min} regime [2.1-6]. The ITB was formed by on-axis beam heating into a low density target plasma with reversed shear that was formed by current ramp-up without beam heating. The foot (outer edge) of ITB was formed at ~0.45a at first and moved outward up to ~0.8a while the position of q_{min} also moved outward from ~0.65a to ~0.8a. The foot of ITB was located at or inside the radius of q_{min}, which was observed in many discharges with the radius of q_{min} ranged between 0.5a and 0.8a. The energy confinement time increased with the increase in the radius of ITB and with the decrease in q_{min} for a fixed toroidal field. High H factors, $\tau_E/\tau_E^{ITER89P}$, up to 3.3 were obtained with an L-mode edge. The effective one-fluid thermal diffusivity in the ITB was less than the value predicted by Chang-Hinton's neoclassical theory. The reversed shear plasmas are characterized by the achievement of high confinement with relatively low beam power (P_{abs} ~12.5 MW), while high confinement is obtained in high power regime (P_{abs} ~25 MW) for the high β_p H mode [2-1.5]. The values of H/q_{95} and β_t increased with the increase in the plasma current (or the decrease in q_{95}), and the highest performance was achieved at q_{95} = 3 (2.8 MA). The performance was limited by disruptive beta collapses with β_N ~ 2 at q_{min} ~ 2.

2.1.3 MHD activities and stability [2.1-7, 9, 10]

Various MHD fluctuations including resistive modes and ideal modes were observed in JT-60U reversed shear discharges.

Resistive modes, which were observed continuously, can be classified by their localization in the minor radius; near ρ_{ITB}, at distinctly inside or outside of ρ_{ITB}, and near the plasma surface. Here, ρ_{ITB} is the normalized radius at the steep pressure gradient generated by the ITB. Resistive modes localized near ρ_{ITB} were observed, when the pressure gradient and β were large enough and q_{min} was between integer values. Fluctuations with and without in-out asymmetry were observed in electron temperatures. Resistive modes without in-out asymmetry seem to be the double tearing mode while resistive modes localized near ρ_{ITB} with in-out asymmetry are not identified yet. Most of reversed shear discharges with an L-mode edge were terminated with a hard collapse which resulted in the disruption. The upper limit of the achieved β_N in reversed shear

discharges lies in the same region with that in high β_p discharges. On the other hand, hard collapses in reversed shear discharges often occurred even in the quite low β_N region. The hard collapses in the low β_N region sometimes occurred at $q_{min} \sim 4$ or $q_{min} \sim 3$ with the growth time of the ideal MHD instabilities. Some of low β_N collapses seemed to be associated with surface modes such as external kink modes, because β_N collapses sometimes occurred when the NB injection power was reduced and the surface q was close to integer values. We also observed a growth of the rotating mode near the plasma surface and the mode locking for hard collapses. Before hard collapses at $q_{min} \sim 2$, precursor oscillations in electron temperatures were observed to be localized in the ITB region. The amplitude of the precursor oscillations increased with the growth time longer than 1.5 ms, which is in the growth time range of resistive MHD instabilities. The collapse, which followed these resistive modes, explosively grew from the ITB region with a very fast growth time of the order of ~ 10 μs. Ideal MHD stability analysis showed that the experimental beta limit ($\beta_N \sim 2$) at $q_{min} \sim 2$ is close to the theoretical one for the ideal low n (n=1) kink modes [2.1-11].

2.1.4 Formation, control and sustainment of reversed shear by LHCD [2.1-12, 13]

By using lower hybrid wave (LHW) current drive (LHCD), it has been experimentally demonstrated that reversed magnetic shear can be maintained and controlled [2.1-13]. Formation of a reversed magnetic shear configuration by an LHW injection alone was successfully demonstrated [2.1-12]. Strongly reversed magnetic shear, which is even stronger than one formed by a normal scenario (NBI heating at current ramp-up), with large area of shear reversal was formed by an LHW injection alone. Furthermore, intense gradient was found in the electron temperature profile, which suggested the confinement improvement. Moreover, the attainable β_N in this discharge was comparable to that of normal reversed shear discharge.

References

[2.1-1] Ishida S., Fujita T., Asakura N., et al., submitted to Phys. Rev. Lett. (1997).
[2.1-2] Koide Y. and the JT-60 Team, Phys. Plasmas **4**, 1623 (1997).
[2.1-3] JET Team, Nucl. Fusion **32**, 187 (1992).
[2.1-4] Mori M., Ishida S., Ando T., et al., Nucl. Fusion **34**, 1045 (1994).
[2.1-5] Fujita T., Ide S., Kimura H., et al., to be published in Proc. 16th IAEA Fusion Energy Conf., Montréal, 1996, IAEA-CN-64/A1-4.
[2.1-6] Fujita T., Hatae T., Oikawa T., et al., submitted to Nucl. Fusion (1997).
[2.1-7] Neyatani Y. and the JT-60 Team, Plasma Phys. Controlled Fusion **38**, A181 (1996).
[2.1-8] Fujita T., Ide S., Shirai H., et al., Phys. Rev. Lett. **78**, 2377 (1997).
[2.1-9] Takeji S., Fujita T., Ozeki T., et al., JAERI-Research 97-047, 10 (1997).
[2.1-10] Ishida S., Takeji S., Isayama A., et al., to be published in Controlled Fusion and Plasma Physics (Proc. 24th Eur. Conf. Berchtesgaden, 1997).
[2.1-11] Ozeki T., Azumi M., Ishii Y., et al., Plasma Phys. Control. Fusion **39**, A371 (1997).
[2.1-12] Ide S., Naito O., Fujita T., et al., to be published in Proc. 16th IAEA Fusion Energy Conf., Montréal, 1996, IAEA-CN-64/E-3
[2.1-13] Ide S., Fujita T., Naito O., et al., Plasma Phys. Controlled Fusion, **38**, 1645 (1996).

2.2 High-β_p H-mode and High Triangularity Discharges

2.2.1 High β_p H-mode confinement at high current with high power neutral beam injection

The high-β_p H-mode discharges, which may bring out more higher fusion triple product, are configured to achieve a peaked beam deposition profile with a large aspect ratio A~4.3 and a low triangularity δ~0.05. It is essential for achieving the high-β_p H-mode confinement to create a sawtooth-free target plasma with a central q slightly above unity by injecting the main beams before the sawtooth onset, which would have produced a weak central magnetic shear configuration. The new technical advancements also contributed to high-β_p H-mode JT-60U experiments in 1996 are as follows:

1) fast current ramp-up operation allowing the main beams to be injected in the current flat top phase at high currents up to 2.7 MA

2) intense beam power of up to 41 MW at 90-95 keV.

The highest fusion triple product $n_D(0)\tau_E T_i(0)$ was transiently achieved with high additional heating power injection of 37 MW at the maximum and Z_{eff}~2.2 at q_{95}=2.9 during an ELM-free high-β_p H-mode, where $n_D(0)\tau_E T_i(0)$ reached ~1.5 x $10^{21}m^{-3}\cdot s\cdot keV$ with the central ion temperature T_i=45±5 keV, the stored energy W_{dia}=8.6 MJ, and the neutron yield S_n=5.2 x 10^{16} /s at the maximum. The high performance high-βp H-mode plasma was also sustained at q95=3.0 with successive ELMs.

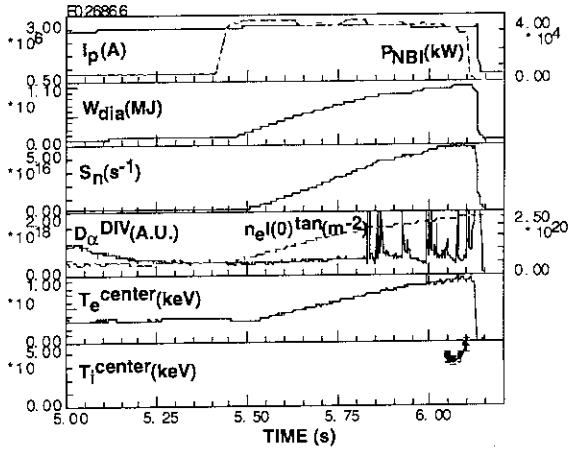

Fig.I.2.2-1 Discharge waveforms of a record shot to show the highest stored energy in high-β_p H-mode.

As shown in Fig.I.2.2-1, W_{dia} and S_n reaches 9.3 MJ and 4.9 x 10^{16} /s and $n_D(0)\tau_E T_i(0)$~5.1 x $10^{20}m^{-3}\cdot s\cdot keV$ was achieved at peak, respectively. It is found that both W_{dia} and S_n increase with increase of plasma current above 2.2 MA. These experimental evidences showing that the fusion performance is peaked around q95~3 independent of transient, stationary states (dW/dt~0) support the argument that the fusion performance can be maximized around q95~3 where ITER would have achieved self-ignition. In the high-βp mode phase just before the H- mode transition, the presence of internal transport barrier is clearly indicated in the electron density and ion temperature profile at r/a ~ 0.7 while the q profiles measured from motional Stark effect spectroscopy reveals the central q value of ~ 1.4 slightly above unity with a weak central shear [2.2-1].

References

[2.2-1] S.Ishida, Y. Neyatani, Y. Kamada, A. Isayama, T. Fujita et al., in Plasma Physics and Controlled Nuclear Fusion Research 1996 (Proc. 16th Int. Conf. Montreal, Canada 1996),.

2.3 H-mode Study

Impact of the neutral particles on the H-mode transition power threshold has been studied [2.3-1]. The fact that the compiled threshold database from various tokamaks has not yet been successful hitherto in providing a unique and reliable threshold power scaling is mainly ascribed to the ambiguities involved with the size and density dependencies. In particular, the density dependence is regarded as the most crucial but difficult to analyze issue, due to its sensitivities to the wall conditions. Based on the results of deliberate experimental investigations at JT-60U, we have first documented that (1) the edge neutral particle density literally determines the degree to which the threshold power depends on the density, and (2) the density boundary, below which the H-mode transition cannot occur, may also be governed by the edge neutrals. Therefore, information on the edge neutral particles can integrate the different density dependencies observed in various tokamaks, and thereby a firm ground for the size scaling may also be established, which can well be extrapolated to a fusion reactor with an adequate precision.

Dependence of transport properties on the normalized gyro-radius ρ^* has been studied on ELMy H-mode plasmas with high triangularity δ in JT-60U [2.3-2]. The thermal diffusivity χ is expressed as $\chi = (T_e/eB)\,(\rho^*)^{\mu}\,F(\beta, \nu^*, \ldots)$, where F is a nondimensional function with β, ν^* etc. Because the ρ^* value of ITER is much smaller than that of large tokamaks, the ρ^* dependence of χ is an important subject to predict the transport properties of ITER plasmas. In ELMy H-mode plasmas with low δ value, the normalized thermal energy confinement time, $\tau_{th}T_e/eB_t$, was found almost independent of ρ^* due to the strong ELM activity occur in the high B_t shot [2.3-3]. The high δ configuration ($\delta = 0.35$) applied here is expected to suppress the ELM activity. A pair of NBI heated ELMy H-mode shots with B_t =1.86 T and 3.08 T are compared. Nondimensional parameters except ρ^* are the same and $T_i/T_e \approx 1$ in $1/3 < a/r < 2/3$ for both shots. It is found that the ρ^* dependence of χ_e is almost the same or somewhat stronger than that in L-mode plasmas, i.e., $\mu \approx 0.5$, while the χ_i becomes almost gyro Bohm type diffusion, i.e., $\mu \approx 1$. The confinement time is almost inversely proportional to $\tau_{th}T_e/eB_t \propto (\rho^*)^{-0.8}$ which is favorable for the future reactor. This results is similar to those obtained in JET and DIII-D.

The relative change of the electron and ion thermal diffusivity, $\delta\chi_e/\chi_e$ and $\delta\chi_i/\chi_i$, and that for the improvement of thermal energy confinement, δTH/TH, at the H-L transition has been studied in JT-60U ICC (Improved Core Confinement) H-mode plasmas with I_p = 1.6~3.5 MA and $B_t \approx 4.0$ T [2.3-4]. Here the change is defined as $\delta\chi = \chi(t_+) - \chi(t_-)$ across the transition at the time t. The improvement factor TH is determined on the basis of the L-mode thermal confinement time scaling. As for $\delta\chi_e/\chi_e$, it is large (0.5~0.6) even for small δTH/TH value (=0.15) and changes very little with the increase of δTH/TH. On the other hand, $\delta\chi_i/\chi_i$ increases with δTH/TH. The improvement of total thermal confinement in H phase is dominated by the reduction of ion heat transport. The relative change of the effective particle diffusivity, δD/D, is independent of δTH/TH.

The width of the edge pedestal Δr has been investigated for ELM-free H-mode plasmas in JT -60U [2.3-5]. The width plays an important role to determine the stability of ELM. Edge pedestals of electron and ion temperature profiles are measured over a wide range of plasma current from 1 MA to 4.5 MA. The results show that Δr is linearly scaled with $\sqrt{\varepsilon}\,\rho_{pi}$ as the prediction in Shaing's theory, where ε is the inverse aspect ratio and ρ_{pi} is the poloidal gyro-radius for thermal ions. The value of Δr is a factor ~4 larger than the theoretical prediction

In order to predict the threshold power for the L-H transition and the energy confinement performance in ITER, databases have been assembled and are being analyzed [2.3-6]. Data from JT-60U and JFT-2M contribute to these ITER database. The ITER Threshold Database includes data from 10 divertor tokamaks. This database gives a scaling of the threshold power of the form $P_{thr} \propto B_t\, n_e^{0.75} R^2 \times (n_e R^2)^{\pm 0.25}$, which predicts $P_{thr} \approx 100 \times 2^{0\pm 1}$ MW for ITER at $n_e = 5 \times 10^{19}$ m^{-3}. The ITER L-mode Confinement Database has also been assembled from 14 tokamaks, and a scaling of the thermal energy confinement time τ_{th}^{L} in L-mode and ohmic phases has been obtained. With the ITER parameters, τ_{th}^{L} is about 2.3 sec. For ignition in ITER, more than 2.5 times this value will be required. The ITER H-mode Confinement Database has been expanded from the data of 6 tokamaks to the data of 11 tokamaks. A τ_{th} scaling for the ELMy H-mode has been obtained by a standard regression analysis and predicts for ITER a confinement time $\tau_{th} \approx 6 \times (1 \pm 0.3)$ sec. The degradation of τ_{th} with increasing $n_e R^2$ (or decreasing ρ_*) is not found for ELMy H-mode. An offset-linear law scaling with a dimensionally correct form also predicts nearly the same τ_{th} value.

References

[2.3-1] Fukuda T., Sato M., Takizuka T., et al., 16th IAEA Fusion Energy Conference, Montreal, (1996) IAEA-CN-64/AP2-9.

[2.3-2] Shirai H., Takizuka T., Kamada Y., et al., "Nondimensional Transport Study on ELMy H-mode Plasmas in JT-60U", in JAERI-Research 97-047 (1997).

[2.3-3] Takizuka T., Shirai H., Kamada Y., et al., "Nondimensional Transport Experiment in JT-60U", in JAERI-Research 95-075 (1995) 22.

[2.3-4] Shirai.H, Takizuka T., Sato M., et al., "Analyses of Electron and Ion Transport Properties in JT-60U H-mode Plasmas with Improved Core Confinement", proc. 23rd EPS Conf., Kiev, Part I (1996) 339.

[2.3-5] Hatae T., Ishida S., Kamada Y., et al., "Edge Pedestal Width of H-mode Plasmas in JT-60U", in JAERI-Research 97-047 (1997).

[2.3-6] Takizuka T. and ITER Confinement Database and Modelling Expert Group, 16th IAEA Fusion Energy Conference, Montreal, (1996) IAEA-CN-64/F-5.

2.4 Current Drive Experiments

2.4.1 Neutral beam current drive (NBCD) [2.4-1]

Non-inductive current drive by the newly installed negative-ion-based neutral beam injector (N-NBI) has been demonstrated at beam energy of 350 keV. Up to 0.28 MA of plasma current was driven by N-NBI. The current drive efficiency of N-NBI defined by $\eta_{CD} = n_e I_{CD} R_p / P_{CD}$, where n_e, I_{CD}, R_p and P_{CD} being respectively average electron density, non-inductively driven current, plasma major radius, and power of the current driver, reached 0.8×10^{19} $m^{-2}A/W$. This value is 1.6 times higher than that of conventional positive-ion-based NBI (P-NBI) at 80 keV and consistent with the theoretical prediction.

The JT-60U's N-NBI was designed to deliver 10 MW of beam power at 500 keV for 10 s. Up to now 2.5 MW of N-NB power has been injected into plasmas at beam energy of 350 keV.

Non-inductive driven current and current drive efficiency of N-NBI were evaluated by injecting N-NB into P-NBI heated plasmas (with 4 MW of tangential and 4 MW of perpendicular beams). An example of such discharge is shown in Fig. 2.4.1-1. Before the N-NB pulse, 70% of plasma current was driven by P-NB and the bootstrap current. During 2 MW of N-NB pulse, the neutron emission rate S_n increased by a factor of 2 and the loop voltage V_l became slightly negative indicating that the plasma current was driven fully non-inductively. With the aid of a 1.5-dimensional time-dependent tokamak transport analysis code TOPICS and a current drive code ACCOME, the bootstrap, P-NB, and N-NB driven currents were estimated to be 0.27, 0.46, and 0.28 MA, respectively.

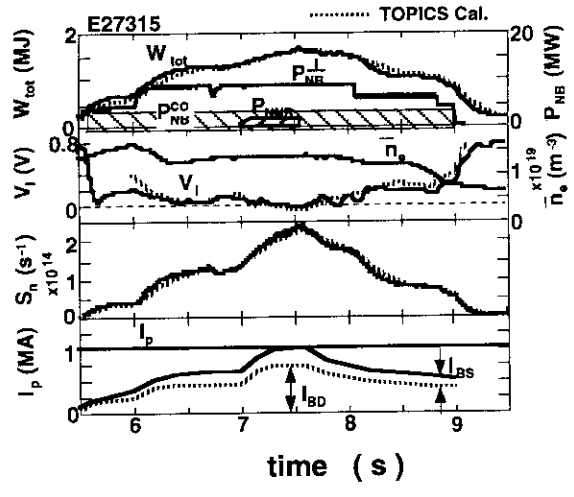

Fig. I.2.4-1 Time evolution of full non-inductive discharge by P-NB and N-NB. Total stored energy W_{tot}, NB power P_{NB}, loop voltage V_l, average density n_e, neutron emission rate S_n, plasma current I_p are shown.

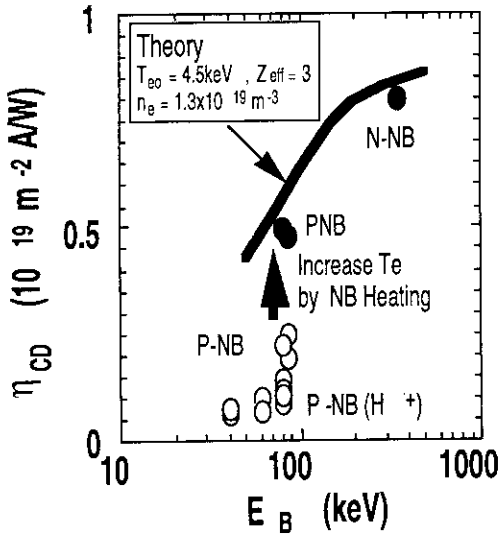

Fig. I.2.4-2 Current drive efficiency η_{CD} of NBCD as a function of beam energy E_B.

Figure 2.4.1-2 shows the current drive efficiency η_{CD} as a function of injected beam energy EB. Clearly, N-NB has efficiency higher than that of P-NB. The curve shows η_{CD} calculated

by ACCOME code with central electron temperature T_{e0} = 4.5 keV, effective ionic charge Z_{eff} = 3, and n_e = 1.3×10^{19} m–3. The experimentally obtained data are in reasonable agreement with theoretical prediction.

2.4.2 Lower hybrid current drive (LHCD) [2.4-2.2.4-3]

Current profile control by lower hybrid wave (LHW) was applied to the reversed shear plasmas. It has been demonstrated that the reversed shear configuration, otherwise relaxes to a monotonic shear profile, can be maintained by LHCD. It has also been shown that strong reversed shear with large area of shear reversal can be formed by LHW alone. The attainable normalized beta of such discharge is comparable to that obtained by current ramp-up method, and strong gradient is found in the electron temperature profile suggesting the improvement in confinement.

References

[2.4-1] Ushigusa K. and the JT-60 Team, to appear in Proc. 16th IAEA Fusion Energy Conf., Montréal, 1996, F1-CN-64/O1-3.

[2.4-2] Ide S., Naito O., Fujita T., *et. al.*, to appear in Proc. 16th IAEA Fusion Energy Conf., Montréal, 1996, IAEA-CN-64/E-3.

[2.4-3] Ide S., Fujita T., Naito O., *et. al.*, Plasma Phys. Controlled Fusion, **38**, 1645 (1996).

2.5 Radiative Divertor and SOL

2.5.1 Radiative divertor formation in the reversed shear plasma [2.5-1, 2]

The reversed shear plasma with an Internal Transport Barrier (ITB) has a potential to satisfy the target plasma conditions for a fusion reactor design. The radiative divertor formation with the improved energy confinement in the core plasma is a crucial requirement, and it was demonstrated for the first time in the reversed shear plasma. Full detached divertor condition was obtained for the reversed shear plasma (I_p = 1.2 MA, B_t = 3 T, P_{NBI} = 10-15 MW) with the ITB using a combination of neon and deuterium/hydrogen gas puffing. Total radiation loss power was increased up to 80% of the net input power for the central n_e = 4x10^{19} m^{-3}. The improved energy confinement within the ITB was maintained during the divertor MARFE for 3 sec. The results were the first demonstration of the compatibility of the radiative divertor with the ITB formation in the core plasma. The ITB was terminated by a beta-collapse during NB heating for the case of the deuterium (including neon impurity) plasma, while it was maintained for the case of the hydrogen plasma. An optimization of the gas puff sequence and the feedback control of the input power are required for the steady-state operation of the improved confinement plasma. During the sustainment phase of the ITB, the location of the minimum-q and the ITB shifted to the plasma center with the time constant of the current diffusion. The sustainment of the current profile is another important problem for realizing the steady-state operation.

2.5.2 Energy and particle confinement in high density ELMy H-mode

High density operation of the ELMy H-mode plasma has been performed in 1994-1995. Degradation of energy and particle confinements under the high recycling condition was investigated for high power neutral beam injection of 18-19 MW [2.5-3]; plasma parameters were fixed at I_p = 1-1.2 MA, B_t = 2-2.1 T, q_{95} = 3.3-3.5. The global energy confinement time τ_E and the H-factor H (compared with the ITER-89P scaling law for the L-mode) were reduced with increasing the plasma density n_e, which was caused by the decrease in the stored energy of fast ions due to a reduction in T_e. Here the thermal plasma energy was constant even for the increase in n_e. Global particle confinement time τ_p^G was evaluated using a neutral transport code for the divertor/SOL region, and it was found that τ_p^G greatly decreased from 0.13 to 0.08 s with increasing n_e due to an increase in the neutral particle influx from the divertor. Thus τ_p^G/τ_E decreased from 1.0 to 0.8 with increasing n_e for the ELMy H-mode plasma. This τ_p^G/τ_E is larger than that for the ELM-free H-mode plasma by a factor of 2-4, which is more favorable for achieving a cold and dense divertor plasma.

The increase in the neutral particle density inside the separatrix, n_0, was evaluated under the high density divertor condition. The n_0 near the X-point increased up to ~2×10^{16} m^{-3}, and it was by a factor of 10 larger than that at the midplane due to i) the short distance between the X-point and the divertor target plate and ii) the open divertor configuration. The transport of the neutral particles was calculated for the new (W-shaped) divertor configuration [2.5-4], which predicted that the inclined divertor plates and a dome in the private region can condense neutral particles in the divertor region. The effective formation of a dense and cold divertor plasma and the reduction of the neutral particles back-flow to the main plasma were also predicted, which will be investigated with their effects on the main plasma performance from 1997.

2.5.3 High density SOL plasma

Radial profiles of electron density at the midplane $n_{e,mid}$, temperature $T_{e,mid}$, and ion temperature $T_{i,mid}$ in the scrape-off layer (SOL) were investigated under radiative and detached divertor conditions in L-mode discharges (P_{NBI} = 4 MW) [2.5-5]. $T_{e,mid}$, and $n_{e,mid}$ profiles were measured with a fast reciprocating Langmuir probe. $T_{i,mid}$ profile at the edge was measured with charge exchange recombination spectroscopy system. The ratio of $T_{i,mid}/T_{e,mid}$ was found to be about 3 over a wide range of the plasma density, and the ion pressure was dominant. It was expected that $T_{i,mid}$ is higher than $T_{e,mid}$ due to the low parallel thermal conductivity of ion. The measured value of $T_{i,mid}/T_{e,mid}$ ~3 was consistent with the SOL/divertor two-point model.

Two (i.e. first and second) SOL regions with different characteristic lengths were measured both in the $n_{e,mid}$ and $T_{e,mid}$ profiles. The first SOL extended up to 10-15 mm outside the separatrix, where the parallel conduction is dominated. The profile had a small e-folding length. Effect of the connection length (safety factor) on the decay lengths of $n_{e,mid}$ and $T_{e,mid}$ (λ_{ne} and

λ_{Te}) was investigated. A regression analysis suggested that large dependence on the safety factor such as $\lambda_{ne} \sim q^{\alpha} T^{\beta}$, where $\alpha = 0.85$ and $\beta = 0.23$. λ_{Te} was larger by a factor of 1.5-2 than λ_{ne}, and λ_{Ti} was larger by a factor of 2.5-3 than λ_{Te} at the first SOL.

At the occurrence of the X-point MARFE, $T_{e,mid}$ at the separatrix was observed at 40-45 eV. During the X-point MARFE, λ_{Te}, λ_{ne} and λ_{Ti} increased substantially with a reduction in $T_{e,mid}$ and $n_{e,mid}$ at the plasma edge and in the first SOL. This is caused by the penetration of the intense radiation region into the main plasma near the X-point.

Parallel current $J_{//}$ flowing between the two strike points through the SOL was measured with the divertor Langmuir probes [2.5-6]. Location of the maximum $J_{//}$ corresponded to that of the peak of the ion flux Γ_{ion}. During the partial detachment of the divertor plasma, the locations of the peak $J_{//}$ and Γ_{ion} shifted from the separatrix to the outer magnetic flux surface. At the same time, the direction of $J_{//}$ was reversed due to the reversal of the in-out asymmetry in T_e profile. Thus not only Γ_{ion} but also $J_{//}$ changes the flowing root at the upstream during the divertor detachment.

References

[2.5-1] Itami K., Hosogane N., Asakura N. at al., Phys. Rev. Lett. 78, 1267 (1997).
[2.5-2] Itami K., Hosogane N., Asakura N. at al., to be published in Proc. 16th Int. Conf. on Plasma Physics and Controlled Nuclear Fusion Research, Montreal Canada, 1996, IAEA-CN-64/A-4-2.
[2.5-3] Asakura N., Koide Y., Shimizu K. et al., to be published in Plasma Phys. Control. Fusion, 1997.
[2.5-4] Hosogane N., Sakurai S., Shimizu K. et al., to be published in Proc. 16th Int. Conf. on Plasma Physics and Controlled Nuclear Fusion Research, Montreal Canada, 1996 IAEA-CN-64/GP-11.
[2.5-5] Asakura N., Koide Y., Itami K. et al., J. Nucl. Matter. 241-243, 559 (1997).
[2.5-6] Kumagai A., Asakura N., Itami K. et al., to be published in Plasma Phys. Control. Fusion, 1997.

2.6 Particle Confinement and Impurity Behavior

2.6.1 Particle confinement [2.6-1]

The density in the main plasma is maintained by not only the particle source in the main plasma but also the edge density. In order to understand the effects of the particle source distribution and the edge density on the global particle confinement, the local particle transport has been analyzed for L-mode plasmas. In this analysis, the densities maintained by the NBI source (n^{NB}) and wall-recycling source (n^{R}) and the base density (n^{Base}) were separated. Here, "base density" indicates the density that is not related with the particle source in the main plasma. The confinement times of the particles fueled by NBI (τ_p^{NB}) and that of the wall-recycling particles (τ_p^{R}) were estimated.

From the analysis in the steady state phase and the perturbed phase, the particle diffusion coefficient was estimated to be 1.0 m^2/s at the plasma edge and 0.1 m^2/s at the plasma center, and a large inward pinch velocity of 20 m/s was also obtained at the plasma edge. Using these estimated transport coefficients n^{NB}, n^{R}, and n^{Base} were separated. It was found that the base density is larger

than the other densities in all the plasma region and dominant at the edge region. The contributions of n^R, n^{NB} and n^{Base} to the total particle number were estimated to be 0.18, 0.22 and 0.6, respectively. τ_p^{NB} and τ_p^R were estimated to be 0.35 s and 0.14 s, respectively, and the ratio of τ_p^{NB} to τ_p^R was estimated to be 2.5. It was also found that τ_p^{NB} was not so large compared with τ_p^R although the penetration for the NBI source was about 10 times deeper than that for the wall recycling source. The high edge density and the large inward pinch gave the small τ_p^{NB} / τ_p^R.

Previously, τ_p^{NB} and τ_p^R had been estimated to be 0.9 s and 0.3 s from the analysis of the global particle balance, in which the base density had not been taken into account. The ratio of τ_p^{NB} to τ_p^R estimated from the global analysis was in agreement with the results obtained from the local analysis. However, τ_p^{NB} and τ_p^R estimated from the local analysis were smaller by 60% than those estimated from the global analysis. These results indicated the particle confinement can not be estimated from the particle number and the particle source in the main plasma. The base density should be considered for the investigation of the particle balance.

2.6.2 Active Control of Helium Ash Exhaust and Transport Characteristics[2.6-2]

In-out asymmetry of He flux in the divertor during the ELMy H-mode has been studied by scanning neutral beam power (PNB) and plasma current (Ip). The dependence of He exhaust on the ion grad-B drift direction, the plasma current and the toroidal magnetic field (BT) was investigated for the ELMy H-mode and L-mode. The He flux on the outer target was larger than that on the inner target in the cases of Ip = 1.0 MA, BT = 2.5 T, PNB = 18 MW. On the other hand, the He flux on the inner target was larger than that on the outer target in the case of Ip = 1.7 MA, BT = 3.5 T, PNB = 18 MW. The in-out asymmetry with the enhanced outboard He flux was remarkable for the ELMy H-mode with higher NB power heating and lower Ip. The in-out asymmetry of the He flux did not depend on the ion grad-B drift direction. However, the in-out asymmetry of the D flux could be reversed by the change of the ion grad-B drift direction (reversed BT and Ip). The asymmetry seemed to be determined by βp (including edge parameters: ne, Te, Ti et al.). It did not explicitly depend on NB power and Ip. This result suggested that the selective exhaust, for example He ash removal from the outboard divertor and fueled particle removal from the inboard divertor, may be possible.

Helium transport characteristics in reversed shear plasmas has been studied using a He beam (central fueling) and a short pulse He gas puff (edge fueling). In the reversed shear mode, the confinement is remarkably enhanced inside the internal transport barrier (ITB), which is formed near the position of minimum q. ne(r), Te(r) and Ti(r) profiles have large gradients at the ITB. The He particle confinement in the ITB was improved with the energy improvement. The He transport was found to be characterized by a large inward velocity near the ITB. However, the profile of He concentration (the ratio of the He density to the electron density) in reversed shear plasmas was almost flat because the electron density profile was similar to the He density profile.

The transport in the reversed shear mode is clearly different from that in the ELMy H-mode and L-mode. However, He particles inside the ITB was expelled when a partial collapse occurred as observed for ELMs. It suggested that Helium can be removed from reversed shear plasmas by frequent partial collapses.

2.6.3 Behavior of Neutral Deuterium and Helium Atoms in the Divertor Region [2.6-3, 4]

Understanding of behavior of neutral deuterium and helium atoms in divertor regions is necessary to control fueling and pumping in fusion plasmas. In the divertor region, the Doppler broadening of Dα and He I (667.8 nm) lines has been observed and analyzed to study the recycling and emission processes of neutral deuterium and helium atoms.

The Dα line profile was observed with wavelength resolution of 0.011 nm; this wavelength resolution corresponds to the temperature of deuterium atoms of 0.09 eV. The profile was simulated with a two-dimensional neutral particle transport code (DEGAS) using the electron temperature and density measured by Langmuir probes at the divertor tiles. The measured Dα line profile was well reproduced by this simulation, which showed that it is necessary to consider the emission from deuterium atoms excited at dissociation of deuterium molecules and ions. It was found that the reflection model using reflection coefficients overestimated the reflection of deuterium atoms at the surface of the divertor tiles by a factor of 2 - 3.

The profile of He I line was observed with wavelength resolution of 0.014 nm; this wavelength resolution corresponds to the temperature of helium atoms of 0.29 eV. In low-density divertor plasmas, the width of the observed He I line was close to the wavelength resolution, which suggested that the helium atoms are dominantly desorbed with the energy of the surface temperature of the divertor tiles. As the electron density of divertor plasmas increased and the electron temperature of them decreased, the line width increased. The temperature corresponding to the width of He I line was 1.7 eV for partially detached plasmas. Since it is expected that the helium atoms with such high energy significantly affect helium contamination of the main plasma and the pumping efficiency of He ash, it is important to understand the production mechanism of atoms with the high energy. It was shown that the heating of the helium atoms by the elastic collision with deuterium ions can qualitatively explain the mechanism.

References

[2.6-1] H. Takenaga, K. Nagashima, N. Asakura et al., "Effects of Source Distribution and Edge Density on Particle Confinement in JT-60U", to be published in Nucl. Fusion (1997).

[2.6-2] A. Sakasai, H. Kubo, K. Shimizu, et al., "Active Control of Helium Ash Exhaust and Transport Characteristics in JT-60U", Proc. of the 16th Int. Conf. on Plasma Phys. Control. Nucl. Fusion Res., Montreal, O2-6, AP-2-1 (R), (1996).

[2.6-3] H. Takenaga, H. Kubo, T. Sugie, et al., "Neutral deuterium and helium behavior in JT-60U divertor plasmas", Proc. 1996 Int. Conf. on Plasma Physics, Nagoya, 1 642 (1997).

[2.6-4] H. Kubo, H. Takenaga, T. Sugie et al., "Behavior of Neutral Deuterium and Helium Atoms in the Divertor Region of JT-60U", Proc. 24th EPS Conf. on Controlled Fusion and Plasma Physics, Berchitesgaden, (1997).

2.7 Fast Ion Study in ICRF Heating

In JT-60U, second harmonic ICRF minority heating of deuterium plasma in negative shear discharges was found to efficiently heat bulk plasmas inside the transport barrier. The plasma stored energy, the electron and ion temperatures in the plasma core remarkably increased after the onset of the ICRF injection and reached 5 MJ, ~7 keV and ~12 keV, respectively. [2.7-1] However, in reversed magnetic shear plasma, fast ion confinement is anticipated to be deteriorated because of weak poloidal magnetic field in the core. The JT-60U experiment indicated that confinement of energetic ions in reversed magnetic shear was inferior to that in the normal shear with positive magnetic shear. The experimental triton burnup ratio in the reversed shear was a half or a third of the expected, while that in the normal shear almost agreed with the calculation. The results indicate that a significant fraction of energetic tritons escaped from the plasma in the reversed shear, raising a concern on serious losses with MeV class ions in reversed shear operations of steady state tokamak reactors. Stochastic and collisional ripple losses are a probable explanation for the significant triton losses. [2.7-2] Toroidicity-induced Alfvén eigen (TAE) modes excited by ICRH were studied in a low-q plasma. Low shear TAE modes and bi-directional TAE modes were observed for the first time. In the low-q discharge similar to ITER configuration it is found that the location of TAE modes shifted from the outside to the inside of the q=1 surface following the expansion of the q=1 surface caused by current diffusion into core region accompanying decrease of li. The higher order TAE modes inside q=1 surface (tornado modes) are much more harmful for energetic ion confinement than the TAE modes outside q=1 surface. [2.7-3] The TAE mode, the ellipticity induced Alfvén mode (EAE) with mode number m and m+2 and the noncircular induced Alfvén eigen mode (NAE) were observed for the first time by means of Mirnov coil in the NBI and ICRF heated plasma of JT-60U [2.7-4].

Diagnostics of the highly energetic α-particles created by the D-T fusion reactions are necessary in a fusion reactor tokamak. Ion Cyclotron Emission (ICE) is one of the simplest and most promising diagnostics. It consists in measuring the radiation emitted by the ions rotating around the magnetic field lines at the first harmonics of cyclotron frequency (f ~ 10-200 MHz). The radiation detected is principally due to the fast ions, even if they are in a very small minority in comparison with the thermal ions. In an NBI-heated plasma, the perpendicular electric field spectra are consisted of narrow, regularly spaced peaks. Their frequencies correspond to the cyclotron harmonics of the main ion species taken at the plasma outer edge. In high βp discharges we detect emission peaks corresponding to the first three cyclotron harmonics of fusion tritons at the plasma center (R ~3.1-3.2 m) in a tokamak for the first time. The measurement of ICE during ICRF heating shows the redistribution of the emission peaks due to parametric instabilities. We observe good correlations between ICE at fixed frequencies and ELMs. We also observe oscillations in ICE due to the expulsion of fast ions from the plasma center during fishbone-type instabilities. We do not observe any evidence of correlation with TAE modes. [2.7-5]

References

[2.7-1] H. Kimura et al., Proceedings of the 16th IAEA Fusion Energy Conference, Montreal, 1997, paper F1-CN-

64/E-6 (IAEA, Vienna, to be published).
[2.7-2] K. Tobita, T. Nishitani, H. Harano, K. Tani, M. Isobe, et al., in Plasma Physics and Controlled Nuclear Fusion Research 1996 (Proc. 16th Int. Conf. Montreal, Canada 1994), IAEA, paper IAEA-CN-64/A5-6.
[2.7-3] M. Saigusa et al., Plasma Phys. Control. Fusion Res., 37, 295 (1995).
[2.7-4] G.J.Kramer et al., submitted to Phys. Rev. Lett.
[2.7-5] O. Da Costa et al, International Conference on Plasma Physics, Nagoya, 1996.

2.8. Plasma Control and Disruption

The fast current shut down scenario using the killer-pellet injection (KPI) has been demonstrated without the generating harmful runaway electrons (REs) in JT-60U. The "burst" like magnetic-fluctuations are enhanced by external helical magnetic-fields. The enhanced magnetic fluctuations can eliminate the relatively low-energy super-thermal (slideaway) electrons created just after the KPI, consequently the quick generation of REs which cause current tail is suppressed. [2.8-1]

In the experimental condition of NB power 32 MW, Ip=2.2 MA and Bt=4.1 T, in JT-60U, during ELMy H-mode phase, some of giant ELMs cause a plasma displacement, which mainly moves in the vertical direction over a maximum distance of ~ 4.7 cm. A large vertical displacement (VD) of ZJ occurs at giant ELMs. This phenomenon can be divided into two phases based on plasma movement. In phase I, a small βp-drop and a small RJ-shift are observed while in phase II, a l_i-drop of by ~ 0.25 and a large ZJ-drop of by ~ 4.7 cm occur. And this large VD in phase II has been confirmed by the soft X-ray emission. The large VD is always observed with a large decrease in l_i. Intense n = 1 ~ 3 modes are always observed at the giant ELMs accompanied by the large VD, which would explain the sudden l_i-drop. It is necessary to clarify the mechanism of VD at giant ELMs and work out effective measures to cope with giant ELMs when they occur. Here, the vertical position of the Ip-center (ZJ) is measured from the mid plane of the vacuum vessel, and the horizontal position of that (RJ) is the plasma major radius. [2.8-2]

Extremely fast vertical displacement events (VDE's) induced by a strong β_p collapse were found in a vertically elongated (κ ~ 1.5), high β_p (β_p ~ 1.7) tokamak with a resistive shell through computer simulations using the Tokamak Simulation Code. Although the plasma current quench, which had been shown to be the prime cause of VDE's in a relatively low β_p tokamak (β_p ~ 0.2), was not observed during the VDE evolution, the observed growth rate of VDE's was almost five times (γ ~ 655 sec^{-1}) faster than the growth rate of the usual positional instability (γ ~ 149 sec^{-1}). The essential mechanism of the β_p collapse-induced VDE was clarified to be the intense enhancement of positional instability due to a large and sudden degradation of the magnetic field decay n-index in addition to the significant destabilization due to a reduction of the stability index ns. The radial shift of the magnetic axis caused by the β_p collapse induces eddy currents on the resistive shell, and these eddy currents produce a large degradation of the n-index.[2.8-3]

References

[2.8-1] Y. Kawano, et. al., paper IAEA-CN-64/A3-4 in 16th Fusion Energy Conference, Montreal (1996).
[2.8-2] OHSAWA M., et al., ICPP96,12E04
[2.8-3] NAKAMURA K., Plasma Phys. Control Fusion 38 1791 (1996)

3. Design Progress of the JT-60SU

To realize the steady-state tokamak reactor such as SSTR, simultaneous achievement is required at high q (5-6) and high β_p (2-2.5), in addition to the alpha burning, of (1) high energy confinement (H-factor>2) under good particle controllability, (2) stable high normalized beta (β_N~3.5), (3) high bootstrap current fraction and high efficiency non-inductive current drive, and (4) heat load reduction and He ash exhaust with divertor. The JT-60SU machine has been studied to establish such a reactor relevant operation mode using deuterium as well as to contribute to the advanced steady-state ITER scenario [3-1].

3.1 Key Design Features

Major parameters of the recent JT-60SU design are shown in Table I.3-1. Firstly, a low unit weight w =(weight/magnetic energy) of 125ton/GJ is realized for the TF SC (super-conducting) magnets as compared with w = 1000ton/GJ of JT-60U Cu magnets. Primary candidate for TF SC cable is Nb_3Al with its good mechanical property. Ten units of the PF coils, 6 EF coils and 4 CS coils, can produce a wide variety of plasma shaping of elongation κ_x up to 2.0 and triangularity δ_x up to 0.8 for DN divertor. The total magnet weight is ~4000ton and is cooled down to liquid He temperature (4.2 ^oK) with a 40kW cryogenic system. To allow a wide variety of current profile control, both NBI (750keV) and ECW (220GHz) are considered as heating and current driver because of their remote coupling capability to the plasmas. The total heating power is 60MW and is larger than the H-mode power threshold of ~40MW. Demonstration of 5MA full current drive is planned for 1000s-1Hr at $<n_e>$~$8.8\times10^{19}m^{-3}$ which is around the Greenwald density limit [3-2]. Full current drive of 6MA at β_N=3 could be tested if the D-T operation is allowed. A plasma current of 10MA can be driven inductively for 200 s. The power supply (P/S) for the SC PF coils utilizes the present JT-60 P/S and two motor generators. New water-cooled 280MW thyristor P/S is enough for a long pulse operation. The vacuum vessel is designed to have one-turn resistance of 25μΩ. The growth rate of the vertical instability γ and stability margin $m_S=(n_S(\infty)+n)/|n|$ are $\gamma \leq$ 30/s and $m_S \geq 0.5$, respectively, with toroidally continuous divertor baffle plate. Active control coils are located between TF coils and the vacuum vessel.

3.2 Safety Issues

Material selection of the vacuum vessel is one of key issues to improve safety and to reduce the exposure dose. Feasibility of SUS316 with low cobalt concentration (0.05%) is studied. Inner wall is covered with 3cm W shield in order to allow human access inside the vessel, even after 1 year cooling down followed 10 years of high power deuterium experiments (with DD neutron production of 4×10^{22}/year). Total weight of the vacuum vessel is ~1600ton. In case of possible future DT operation, an additional-shield of ~2400ton (reduced activation ferritic steel F82H) is required. Radiation shield against DD neutrons and induced γ-rays consists of vacuum vessel

(40cm thick) and cryostat (50cm thick) to reduce the radiation dose rate at the site boundary. Additional shield inside the vacuum vessel and TF magnet with polyethylene blocks filled inside the TF shear-panel are enough to keep the radiation dose of the DT option to that for DD experiments. Tritium production from intense auxiliary heating of deuterium plasma is estimated to be 2000Ci/year. The fuel treatment and tritium removal systems are planned to have multiple confinement barriers and defense-in-depth philosophy, similar to the tritium process laboratory (TPL) at JAERI.

References

[3-1] M. Kikuchi et al., IAEA-CN-64/G-2-3(1996).

[3-2] K. Nagashima et al., to be published in Fusion Engineering and Design.

Table I.3-1 Major parameters of JT-60SU

Plasma current	10	MA	Flux swing	170V·s
Toroidal field at 4.8m	6.25	T	Divertor pumping	$20Pam^3/s$
Plasma major radius	4.8	m	DD neutron rate	$1x10^{18}/s$
Plasma minor radius	1.4	m	Elongation (κ_{95})	1.8
Triangularity (δ_{95})	0.4		Inductive flat top	200s
Heating power(NBI & ECH)	60	MW	Non-inductive pulse	1-1000hr
TF magnet energy	24	GJ		

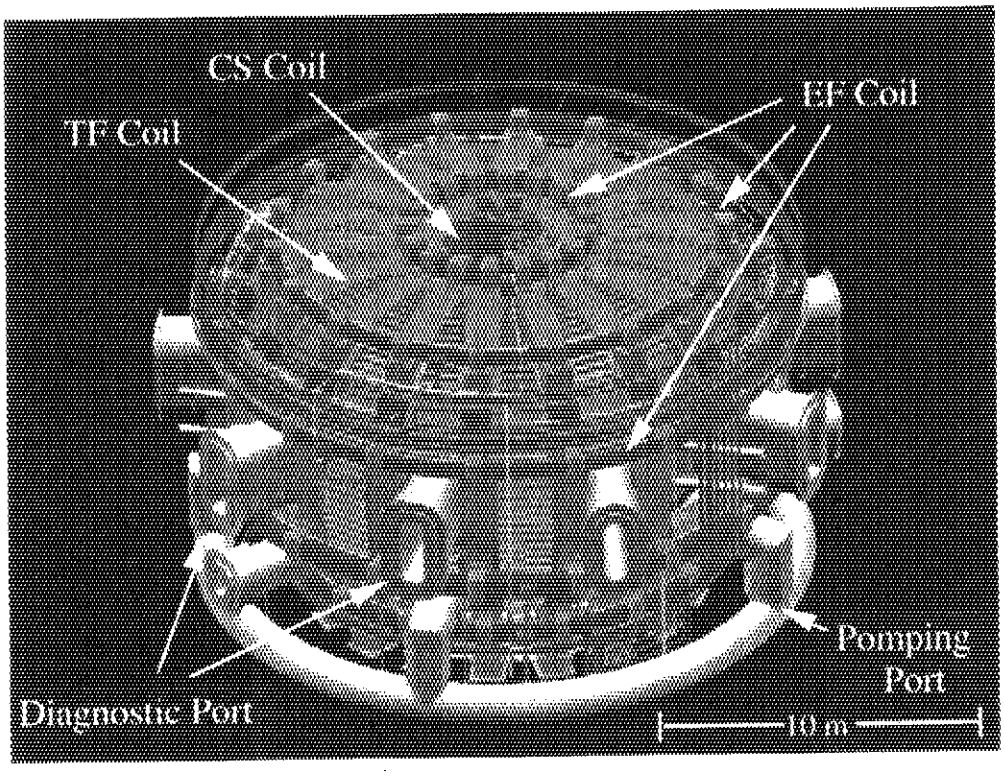

Fig.I.3-1 Birds' eye view of the JT-60SU

II. JFT-2M PROGRAM

Objectives of the JFT-2M program are (1) advanced and basic researches for the development of high-performance plasmas for nuclear fusion and (2) contribution to the physics R&D for ITER, with a merit of flexibility of a medium-size device (R=1.3 m, a=0.35 m, B_T=2.2 T and I_P=0.5 MA). Both international and domestic collaborations have been vigorously utilized to strengthen activities of JFT-2M. In the last fiscal year, the baffle structure for the closed divertor had been modified to have more closed geometry. In this fiscal year, the modified closed divertor was found to be more effective for compatibility of the H-mode and the dense and cold divertor plasma. Physics studies on H-mode also made progress, such that a region of suppression of the density fluctuation was found to coincide with that of a high shear region of the radial electric field. It was demonstrated that the m=2 tearing mode was suppressed by the O-mode ECH for the first time in an elongated plasma. Plasma coupling experiment of the combline antenna for FWCD was carried out in collaboration with General Atomics, demonstrating merit of load insensitivity of the antenna. Planning of the Advanced Material-Tokamak Experiments (AMTEX) was initiated, which will provide database on effects of ferritic material on tokamak plasma, including toroidal field (TF) ripple reduction. In this fiscal year, water leakage occurred at the inlet of cooling water to one of the TF coils. Replacement of all the inlet and outlet connectors to the TF coils with new-type ones has been completed within this fiscal year.

1. Experimental Results and Analyses

1.1 Closed Divertor

Handling of the heat load onto a plasma facing component, e.g. divertor plate, for a fusion reactor keeping the plasma in high confinement state is still an open question. One of the promising examples to solve this question is the dense & cold divertor which we found in D-III open divertor. But it was in L-mode due to high recycling and restricted in high density regime [1.1-1].

Our target had been to realize dense & cold divertor plasma and H-mode simultaneously, employing a closed divertor. It is expected that the closed divertor reduces recycling at the main plasma edge, keeping high recycling in the divertor region. The effect of baffle plate opening on neutral gas back flow from the divertor chamber had been examined. The shape of the baffle plates had changed from less closed configuration (CD1) to more closed configuration (CD2) in March, 1996. The edge of the outer baffle plate is located near the X-point at the position about 1.4 λ_Γ and 0.8-0.9 λ_Γ from the peak position of the particle flux profile near the divertor throat for CD1 and CD2, respectively, where λ_Γ is an e-folding length of the particle flux profile. In addition, the gap between inside hit point and the baffle plate for the private region was reduced from about 5cm to 2cm. In order to compare the baffle effect on the simultaneous realization of

a dense & cold divertor plasma and an H-mode, we tried to increase a gas feed rate, Q_H, shot-by-shot into the divertor chamber. Note that the gas was introduced after the H-mode transition for the low target density case where the spontaneous dense & cold state disappears. In CD1, the H-mode was compatible with a dense & cold divertor to some extent, but was degraded and then terminated when Q_H exceeds 2.8 Pam^3/s [1.3-2]. The divertor plasma was not enough cold (~15eV). With the reduced baffle opening in CD2, buildup of gas was established only in the divertor chamber to the extent of $Q_H = 4.0$ Pam^3/s without degrading H-mode [1.3-3]. Principal parameters at 100 ms after the beam initiation are shown in Fig. II.1.3-1. The divertor plasma is becoming much denser and colder (Fig. II.1.3-1(a)) compared to those of CD1 in accordance with sole buildup of neutral gas pressure in the divertor chamber while the main chamber pressure kept low by increasing of Q_H (Fig. II.1.3-1(d)). Neutral compression ratio (divertor pressure/main pressure: an index of baffling performance) exceeds 35. This ratio is doubled by applying divertor biasing.

Since the strong Q_H gives less affection on the main plasma parameters, i.e. electron density, plasma stored energy, radiation/charge-exchange loss power and neutral gas pressure as shown in Figs. II.1.3-1(b)~(d), we would say that the gas puffing from the closed divertor chamber has a capability of controlling dense & cold states independently of the main plasma even in H-mode. The suppression of the gas buildup of main chamber by a divertor shape optimization, which we have firstly shown experimentally, is the necessary condition of the divertor design for ITER.

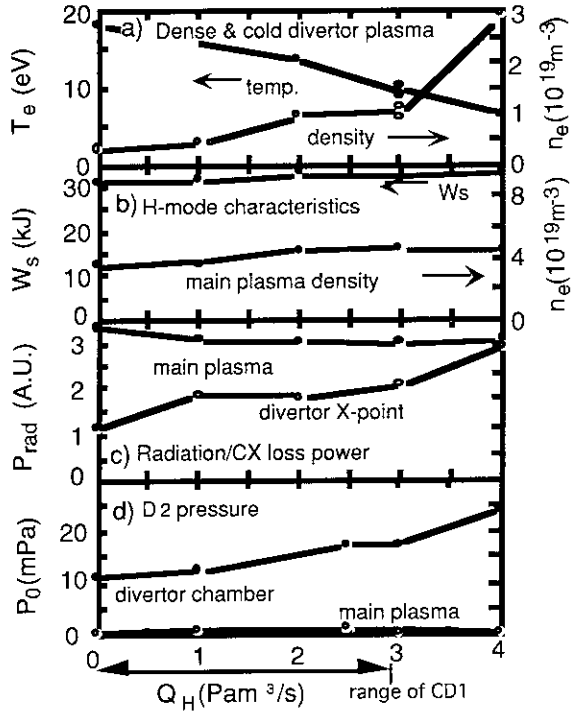

Fig. II.1.1-1 Main parameters during H-mode against gas feed rate, Q_H, a) electron temperature and density at the divertor plate, b) line averaged electron density and stored energy, c) radiation/CX loss power in the main plasma and the divertor X-point region, d) deuterium neutral pressure in divertor and main plasma periphery. P_{NBI} ~ 0.7 MW, B_T = 1.3 T and I_p ~ 220 kA.

References

[1.3-1] S. Sengoku, M. Shimada, N. Miya et al., Nucl. Fusion, **24**, 415 (1984).
[1.3-2] S. Sengoku and the JFT-2M group, Bull. Amer. Phys. Soc., **40**, 1765 (1995).
[1.3-3] S. Sengoku and the JFT-2M group, Bull. Amer. Phys. Soc., **41**, 1486 (1996).

1.2 Confinement Studies

Understanding the relation between the transport and the micro turbulence is one of the most important topics in the fusion plasma research. In JFT-2M, the turbulence is measured by a

microwave reflectometer technique. The reflectometer installed on JFT-2M is a 2 channel heterodyne system. The frequency of the launching waves can be tuned from 28 to 50GHz. The polarization of the wave is O-mode, so that the corresponding cut-off density is from 0.97 to $3.1\times10^{19}m^{-3}$. This range of density lies in the region of $0.5<r/a<1$ in a typical L-mode and $0.9<r/a<1$ in a typical H-mode. In the analysis, we consider that the received wave has two component at least. One is the reflected wave coming from the geometrical optics and the other is the waves scattered by the density fluctuations. This consideration allows us to analyze the density fluctuation by taking a complex spectrum under the runaway phase phenomenon [1.2-1].

Figure II.1.2-1 shows a temporal evolution of power spectra of the complex amplitude at an L/H transition. The fluctuations coming from the cut-off layer of $1.83\times10^{19}m^{-3}$ (inner cut-off) and $0.97\times10^{19}m^{-3}$ (outer cut-off) are shown in Fig.II.1.2-1(b) and Fig.II.1.2-1(c), respectively. The L/H transition occurs at 731 ms (from the reduction of D_α intensity shown in Fig.II.1.2-1(a)). The density fluctuation with frequency lower than about 100 kHz at the outer cut-off layer was reduced at the time of the L to H transition, while the density fluctuation at the inner cut-off layer was reduced with the delay of about 20 ms after the L to H transition. Figure II.1.2-1(d) shows the movement of the inner and outer cut off layers that are obtained by using the numerical low pass filter. The delay time of reduction of the fluctuation at the inner cut-off layer from the L/H transition might be the time to reach its position to the high shear of the radial electric field region [1.2-2]. It may support the model of the turbulence stabilization by an E×B induced poloidal flow.

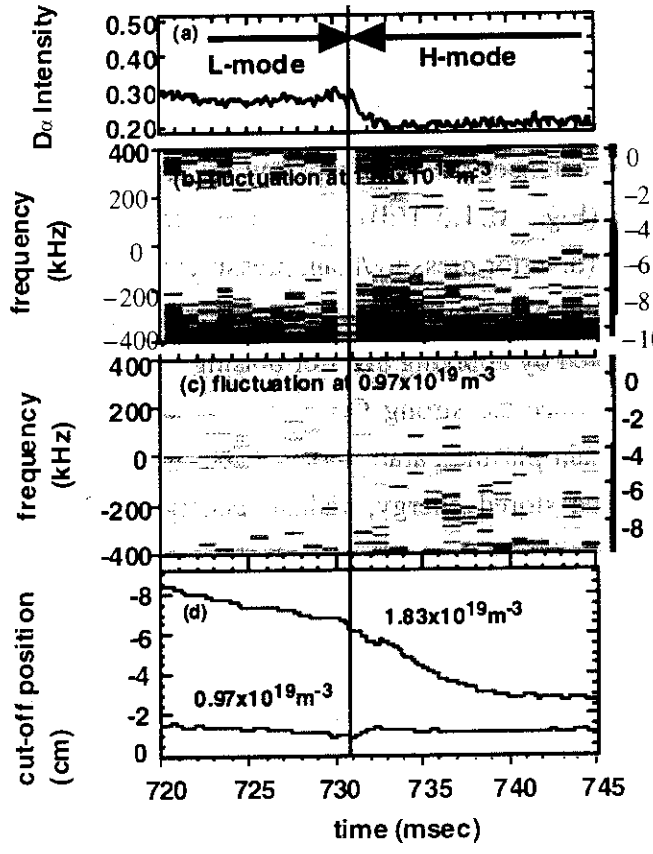

Fig.II.1.2-1 (a); D_α intensity. (b) and (c); Power spectra of the complex amplitude in logarithmic-scale (the more dark shows more week of the amplitude). (d); Movement of the inner and outer cut-off layer. The vertical axis shows the position of the cut-off layer from the separatrix. The sign of this axis is negative inside the separatrix.

References

[1.2-1] G.R.Hanson et al., Nucl. Fusion **32**, 1593 (1992).
[1.2-2] K.Ida et al., Phys. Fluids **4**, 2552 (1992).

1.3 Disruption Control by ECH

The power of the ECH system of the JFT-2M was increased up to 1MW in the last fiscal year in collaboration with the United States. The first ECH experiment after the power-up was carried out in this year. For the tokamak plasma of circular cross-section, we already found that avoidance of the disruption is possible by the local island heating of the tearing mode using the off-center heating by ECH [1.3-1,2]. We used the 2nd harmonic X-mode in those experiments.

In this year, we launched the fundamental O-mode into the elongated diverted plasma whose configuration may be realistic for a future thermonuclear fusion reactor. We found that the m=2 tearing mode which was observed in the single null divertor discharge (q_{95}=4.8, ellipticity=1.46, triangularity =0.42), was found to be suppressed by the off-central-heating (net power =0.2 MW), for the first time in such an elongated plasma [Fig. II.1.3-1]. The O-mode, whose single path absorption is less than the 2nd harmonic X-mode, was found to be effective for the suppression of the mode. We plan to continue the study with plasmas of larger plasma current and lower q value. Furthermore, we achieved the electron temperature of 2.5-3.0 keV, which is the highest value in JFT-2M, by the central heating (power=0.25 MW, line averaged density =$1.1\times10^{19}m^{-3}$). Such a parameter region is the target for the current drive experiments with the 200 MHz fast wave. We will continue the conditioning to get the higher power and higher plasma temperature.

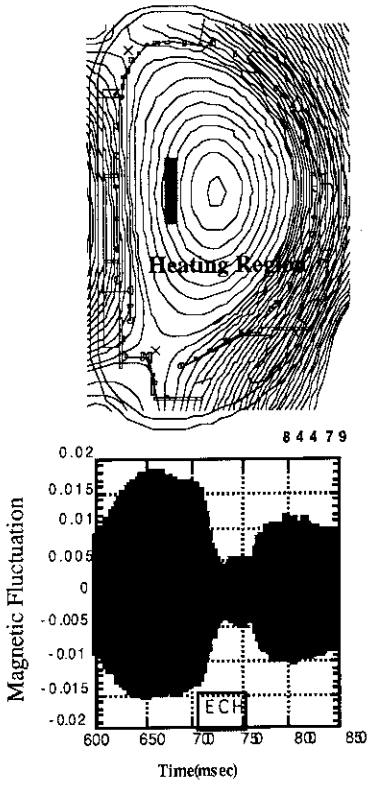

Fig. II.1.3-1 Suppression of the tearing mode by ECH in the diverted discharge with B_T= 1.87 T and I_p = 0.2 MA, Top: Magnetic surface at 0.725s, The heating position is 14 cm inside (plasma radius 27 cm). Bottom: Time evolution of the magnetic fluctuation (time derivative).

A localized current drive is possible by ECH. There is a possibility that we can avoid the tearing mode/disruption more effectively by the local current drive in the magnetic island of the tearing mode. It is expected that the current drive is dependent on the direction of the ray of the wave. In order to study the effect of the ray direction to the current drive, we designed a new launcher with mirrors, with which the ray direction can be changed. We did the engineering development in collaboration with the RF heating laboratory.

References

[1.3-1] K. Hoshino et al., Phys. Rev. Lett., **69**, 2208 (1992).

[1.3-2] K. Hoshino et al., in Radio Frequency Power in Plasmas, Boston 1993, AIP Conference Proceedings, **289**, 149 (1994).

1.4 Advanced Material - Tokamak Experiment (AMTEX) Program

Ferritic steel is one of the candidate materials for a DEMO fusion reactor, such as SSTR, because of its low activation under fast neutron irradiation. However, one concern is that their ferromagnetic properties would have harmful effects on plasma production, plasma control and confinement performance. In order to examine the effects, advanced material-tokamak experiments (AMTEX) are planned in JFT-2M. For AMTEX, the ferritic material F82H (8%Cr-2%W-0.2%V-0.04%Ta-Fe) [1.4-1] which has a low activation of 10^{-6} damping factor/century is considered. F82H begins to saturate at magnetic field strength (H)~ 0.2[MAT/m] and saturated magnetic flux density (B) is 2T with an external B of about 0.3T [1.4-2]. Although F82H is not saturated in low magnetic field discharge (for instance a Taylor discharge cleaning (B=0.07 T)), F82H is saturated in normal tokamak discharges (B≤ 2.2 T). The issues of AMTEX on JFT-2M are to clarify the effects of the ferritic steel on plasma production, plasma control and confinement property as well as plasma-wall interaction, and to obtain guidelines for the design of tokamaks with a small toroidal ripple. We have evaluated the error magnetic field from the ferritic steel by a computer simulation code. The magnetic field is calculated using a 3D static magnetic field analysis code ELF/MAGIC made by the ELF Corp.. The method is the same as that in the case of the SSTR [1.4-3]. If ferritic steel boards are located inside toroidal coils, they strengthen magnetic field between toroidal coils, while the toroidal magnetic field just inside the coils becomes weaker. Thereby, toroidal field ripple can be reduced. A ferritic board of 24 mm in thickness, 500 mm in height and 150 mm in width is assumed to be attached outside of vacuum vessel. The preliminary results in the case with and without ferritic steel board is shown in Fig.II.1.4-1. The ripple is significantly reduced in the plasma region in the case with ferritic steel boards.

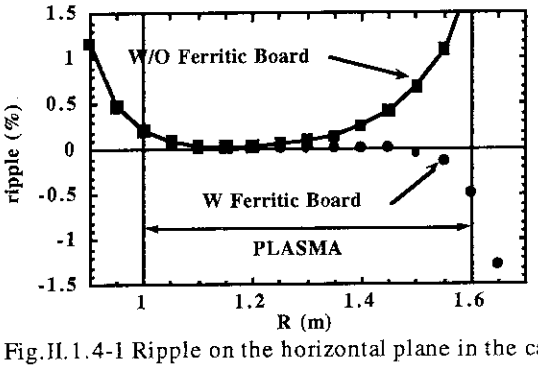

Fig.II.1.4-1 Ripple on the horizontal plane in the case with and without setting Ferritic board.

Reference

[1.4-1] M. Tamura *et. al.*, J. Nucl. Matter, **155**, 620 (1988).
[1.4-2] K. Siba and A Oyama, private communication
[1.4-3] S. Takeji *et. al.*, in Proc. of the 16th IEEE/NPSS SOFE, Illinois, **2**, 1214 (1995).

2. Operation and Maintenance

JFT-2M tokamak has been running for ITER physics R&D experiments. In this fiscal year, main apparatus (JFT-2M tokamak, heating apparatus and flywheel motor-generator for toroidal field coil) was smoothly operated from April to December according to the experimental plan. The total shots of 2249 were devoted to experiments on closed divertor, H-mode characteristics, electron cyclotron resonance heating and fast wave current drive. In the residual period, periodical

inspection and some repairing were carried out on each apparatus. Furthermore, a capacitor bank for the compact toroid injection was prepared, and technical problems to use ferritic steel on JFT-2M were discussed and basic design of plasma- materials test program has started.

2.1 Tokamak

Tokamak operation started in April after wall conditioning with baking and TDC. In May, small leak of cooling water from a joint to toroidal field coil was found, however, electrical insulation between coils and the earth was not degraded, so after temporary repairs tokamak operation was continued without 3 cooling channels. As main cause of water leak comes from superannuated seal material, regular examination and replacement of water joint for all toroidal coils were carried out in the periodical maintenance time. During closed divertor experiments, some troubles have occurred on electrical insulation of divertor plates by arcing, mineral-insulated cable disconnection by electro-magnetic force and current feed-through air leak by arcing, so preventive measures for each trouble have been taken in the maintenance time. In the vacuum system, old vacuum gages were replaced and a new He leak detector capable to distinguish He and D2 was installed. New experiments to inject a compact toroid into JFT-2M plasma has been planned and manufacture of the injector system has started in 2 year schedule by collaboration with Himeji Institute of Technology. Plasma-materials test program to support development of structure materials such as ferritic steel has started. Technical problems such as error field production, vacuum characteristics and electro-magnetic force were discussed and basic design of ferritic steel setup was decided.

2.2 Neutral Beam Injection System and Radio-Frequency System

Neutral beam injection system (NBI) has contributed to almost all experiments as a main heating apparatus. In order to reduce time needed for conditioning, a baking heater was newly installed on the manifold. Old vacuum pumps for NBI were replaced to new one. Electron cyclotron heating system(ECH) with maximum power of 1MW by 5 gyrotrons was adjusted to operate with long pulse by cooperating with GA technologies. These gyrotrons were applied to experiments on suppression of MHD fluctuation and current drive. Fast wave system with a comb-line antenna developed by GA technologies had been adjusted and experiments on coupling characteristics have been carried out before experiments on DIII-D.

2.3 Power Supply

DC generator with a flywheel which has capability of 51.3 MW through 4 seconds was operated smoothly and experiments on ECH have been carried out at 2.2 T. In the maintenance time, precise examination of main circuit switches were carried out to keep good conditions and a higher harmonics filter were added in the syristor circuit to reduce higher harmonics in the commercial line.

III. THEORY AND ANALYSIS

The primary objective of theory and analysis is to improve the physical understanding of the magnetically confined tokamak plasma. Remarkable progress has been made on understanding of physics of the reverse shear plasma such as reduced transport near the pitch minimum location for "semi-global" toroidal turbulence, stability properties of ideal MHD, TAE and kinetic ballooning modes. Progresses are also made on understanding of VDE mechanism and nature of divertor asymmetry using 5 point divertor model. New Implicit Monte Carlo method is also developed for the analysis of impurity ionization and recombination. Selective He ash exhaust is also demonstrated using OFMC code simulation.

The main focus of the NEXT (Numerical Experiment of Tokamak) project is to simulate tokamak plasmas using particle and fluid models on the developing technology of massively parallel computers. For core plasmas, three models are being developed; a particle model, a fluid model, and a particle/fluid hybrid model. For the divertor, particle and fluid models are being developed. The NEXT project involves research in parallel computing technologies.

1. Confinement and Transport

It is understood that drift waves in a toroidal geometry behave quite differently from a slab geometry. In a toroidal geometry, excited eigen-modes are radially extended to a semi-global width given by $\Delta r \sim (\rho_i L)^{1/2}$ [1-1]. This originates from a toroidal geometrical effect which couples the small scale ion gyro radius ρ_i with a scale length L of the plasma equilibrium. This understanding leads to a strategy where improved modes can be achieved by suppressing such prominent structures. We have investigated the role of magnetic shear and plasma shear rotation on the improved modes using toroidal numerical simulation and theory [1-2]. We found that the weak and/or zero magnetic shear breaks up the toroidal coupling and the associated semi-global mode structure, leading to a "discontinuity" (or "gap") between the turbulence inside and outside the q-minimum (q-min) surface. Such a discontinuity prevents particle motion across the q-min surface, suggesting an existence of a transport barrier. The discontinuity effectively works as a transport barrier when the q-min surface is locatedd just outside the maximum pressure gradient. This is consistent with recent JT-60U experimental results. It is also found that plasma shear rotation enhances the character of the discontinuity when the flow direction is in the same direction as the the mode rotation. This significantly suppresses the mode activity near the q-min surface.

Reference

[1-1] Y.Kishimoto, et. al. Phys. Plasmas 3, (1996) 1289.
[1-2] Y.Kishimoto et. al., 16th IAEA Fusion Energy Conf., Montreal, IAEA-CN-64 / DP-10.

2. Stability

Dynamics and acceleration mechanisms of vertical displacement events (VDEs) of elongated

tokamaks are investigated using the Tokamak Simulation Code. It was shown that disruption events, such as a sudden plasma pressure drop (β_p collapse) and the subsequent plasma current quench (I_p quench), can accelerate VDEs due to the adverse destabilizing effect of the resistive shell [2-1]. The essential mechanism of the VDE acceleration was clarified to be the intense enhancement of positional instability due to a large and sudden degradation of the magnetic field decay n-index. Additionally, in a tokamak with an up/down asymmetric shell with respect to the geometric midplane, the I_p quench also causes an additional VDE acceleration due to the vertical imbalance of the attractive force.

An amelioration of I_p quench-induced VDEs was experimentally established in JT-60U tokamak by optimizing the plasma vertical location (the neutral point) just prior to the disruption. The JT-60U vacuum vessel is shown to be suitable for preventing the β_p collapse-induced VDE. The neutral point of the ITER-EDA tokamak is found to lie at ~ 22 cm below the plasma magnetic axis of the nominal equilibrium [2-2]. Consequently, it was clarified that the ITER tokamak has an advantage of avoiding the fatal damage of the complicated structures of the bottom-divertor.

In recent experiments of JT-60U, the high performance plasmas have been obtained by the negative shear discharges. In most of such discharges, the β_p -collapse occurs following MHD activities with the fast growth rate of about $100\mu s$ and limits the maximum attainable β -value. It is important to clarify the feature of the ideal MHD stability and to achieve higher plasma performance. Figure 2-1 shows the n=1 toroidal mode stability limit against β_n and $q_{\min}$ for the JT-60U like plasma, where the pressure profile has the steep gradient just inside the radial position of $q_{\min}$. An area above the solid line is unstable. A feature of the stability limit is that when $q_{\min}$ is just below a rational surface, the stability limit becomes lower.

The effects of the q-profile and the pressure profile on the stability limit are investigated. In both profiles on inside and outside regions of $q_{\min}$, the stronger magnetic shear makes β -limit higher, and the stronger pressure gradient has lower β -limit. These show the way to get the higher performance plasma. [2-3]

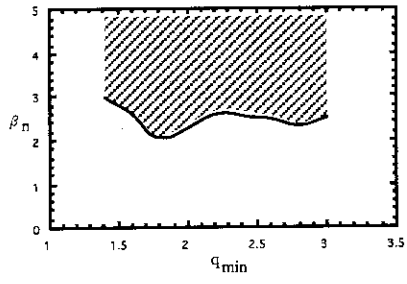

Fig.2-1 Ideal stability of n=1 mode

High energy particles produced by the nuclear fusion reaction or RF heating system resonance with a plasma wave. Among various waves which have the possibility to be excited, Toroidicity-induced Alfven Eigenmode (TAE mode) is considered to be the most important, because the velocity of the high energy particle is close to the Alfven speed. In the JT-60U experiment, the TAE mode in the negative shear plasma is rather stable than that in the positive shear plasma. A theoretical analysis for the TAE mode in the negative shear plasma shows that a large density gradient produced in the internal transport barrier makes the width of the gap of the

shear Alfven continuum spectrum narrower. Therefore, the TAE mode can not exist near the plasma center where the population of high energy particles is high, so that the TAE mode is stabilized[2-4].

The nature of the kinetic ballooning mode in the MHD second stability regime has been clarified through the behavior of the eigenfunction. It has been found to be a continuation of the MHD ballooning mode, not of the second mode with a smaller growth rate which coexists with the MHD mode. The kinetic shooting code has also been applied to the parameters of TFTR in which the kinetic ballooning mode was recently observed. The toroidal mode number and the frequency for the fastest growing mode have been found to be consistent with the experimental observations. Finite beta stabilization of the electrostatic ITG mode and destabilization of the ITG-driven ballooning mode have been demonstrated. The mode stability in the negative shear region, where the MHD ballooning mode is known to be stable, has also been studied. The kinetic ballooning mode persists for $s < 0$ with a narrow stable window near null shear [2-5].

A theory and a numerical method are presented for the asymptotic matching analysis of resistive MHD stability in a negative magnetic shear configuration with two rational surfaces. The theory formulates the problem of solving both the Newcomb equations in the ideal MHD regions and the inner-layer equations around rational surfaces as boundary value/eigenvalue problems to which the finite element method and the finite difference method can be applied. Hence, the problem of the stability analysis can be solved by a numerically stable method. The present numerical method has been applied to model equations having analytic solutions in a negative magnetic shear configuration. Comparison of the numerical solutions with the analytical ones verifies the validity of the numerical method proposed.

References

[2-1] Nakamura Y., Yoshino R., Pomphrey N., et al., "Acceleration Mechanism of Vertical Displacement Event and its Amelioration in Tokamak Disruptions", J. Nucl. Sci. Technol. **33**, No.8 (1996) 609.

[2-2] Nakamura Y., Nishio S., Yoshino R., et al., J. Plasma & Fusion Res. **72**, No.12 (1996) 1387.

[2-3] shii Y., Ozeki T., Tokuda S., and Takeji S., JAERI-Research 97-047, Section 2.5.

[2-4] Ozeki T., Azumi M., Ishii Y., et al., Plasma Phys. Control. Fusion 39 A371 (1997).

[2-5] Yamagiwa M., Hirose A., and Elia M., "Kinetic shooting code study of ballooning modes in a tokamak", Plasma Phys. Control. Fusion 39 531 (1997).

3. Divertor

A simple five-point model of the scrape-off layer (SOL) plasma outside the separatrix of a diverted tokamak has been developed to study the inside/outside divertor asymmetry [3-1]. The SOL current, gas pumping/puffing in the divertor region, and divertor plate biasing are included in this model. Gas pumping/puffing and biasing are shown to control divertor asymmetry. In addition, the SOL current is found to form asymmetric solutions without external controls of gas pumping/puffing and biasing.

A new "implicit" Monte Carlo (IMC) method has been developed to simulate ionization and recombination processes of impurity ions in divertor plasmas [3-2]. The IMC method takes into account many ionization and recombination processes during a time step Dt . The time step is not limited by a condition, $Dt << t_{min}$ (t_{min}; the minimum characteristic time of atomic processes), which is forced to be adopted in conventional Monte Carlo methods. We incorporate this method into a one-dimensional impurity transport model. In this transport calculation, impurity ions are followed with the time step about 10 times larger than that used in the conventional methods.

References

[3-1] N. Hayashi, T. Takizuka, A. Hatayama, M. Ogasawara, "Analysis of Divertor Asymmetry Using a Simple Five- point Model", JAERI-Research 97-018 (1997).

[3-2] A. Suzuki, T. Takizuka, K. Shimizu, et. al., "An Implicit Monte Carlo Method for Simulation of Impurity Transport in Divertor Plasma", J. Comput. Phys. **131** (1997) 193.

4. Burning

Helium ash removal is an important issue for determining the cost and viability of a fusion reactor based on the magnetically confiment scheme. The ash confinement time is dominated by the edge pumping rate rather than core transport. If helium ash is effectively exhausted in a peripheral region, the helium ash in the central region can be easily removed. A new method for helium ash removal is numerically confirmed by an Orbit Following Monte-Carlo simulation. The key point of the method is preferential coupling of an ICRF wave with He^+ ions without resonance with D^+ and T^+, where He^+ ions are produced by charge-exchange recombination with fuel neutrals near the peripheral region. He^+ ions are driven into the ripple trapped region of velocity space by the ICRF wave. The ripple trapped helium ions are then removed and transported to a pumping duct due to the grad-B drift motion. Numerical results[4-1] show that to reduce helium ash to about half of that without active ash removal and to keep a fusion output of 1.5GW in a reactor-grade tokamak, the required ICRF power is 10~15MW, when the ripple field is greater than 1.5%. In this scenario, it is enough to have an ICRF antenna array and a pumping duct between a pair of toroidal field coils.

References

[4-1] K.Hamamatsu, C.S.Chang et.al., IAEA-CN-64/DP-22 (Proc. 16th IAEA Fusion energy Conf.,Montreal, 1996).

5. Numerical Experiment of Tokamak (NEXT)

5.1 Gyrokinetic/Gyrofluid Model

A self-consistent particle-fluid hybrid simulation model has been formulated based on the nonlinear gyrokinetics in which the electron inertia effect is retained[5-1]. It has been shown that the present hybrid model possess an exact energy invariance. We can afford to use the time step in

the hybrid simulation determined solely by the mode frequency of interest.

A three dimensional gyro-fluid code has also been developed which employs a two field model including the electron kinetic effects. The m = 1 kinetic internal kink instability is simulated by the code. The results from the gyro-fluid simulation agree well with those from the gyrokinetic particle simulation for the linear and early nonlinear stages of the instability[5-2].

5.2 Divertor Simulation

Simulation codes play an essential role in understanding of physical processes in the divertor plasma where the plasma transport, the neutral transport and the impurity transport are strongly coupled with each other. Three representative codes with different purposes are presented [5-3]. A particle code, PARASOL, is being developed to verify the physical model used in fluid codes, such as sheath condition and the heat diffusivity. A fluid code, SOLDOR, is now under development to simulate the divertor plasma accounting for interactions with the neutral particles. A Monte-Carlo code, IMPMC, has been developed for the analysis of the impurity behavior in the divertor plasma. The optimization of these codes for massive parallel computers has just been started.

5.3 Massively Parallel Computing

The kinetic ballooning shooting code, KBSHOOT, developed at the Plasma Physics Laboratory, University of Saskatchewan, Canada, has been parallelized for running on the VPP500 machine. The CPU time has been reduced by a factor of three for the 4PE (Processing Element) mode and by a factor of eight for the 16PE mode, as compared to that of the original code with the 1PE mode[5-4].

Regarding the multiple-nodes simulation of the 1-D electrostatic PIC code, a test particle orbit separates from the orbit in the single-node simulation even for the exactly same stating conditions. Measuring the maximum Lyapunov exponent shows that the separation of particle orbits is not caused by accumulation of numerical errors but caused by the origin of chaos. Therefore, both results from different number of nodes are viewed as realization of an ensemble and equally reliable[5-5].

5.4 Interdisciplinary Research

The physics of disk-star system is clarified through MHD simulations[5-6]. The dipolar magnetic field of the protostar threads the protostellar disk in simulation. A current sheet inside the expanding magnetic loops gives rise to the magnetic reconnection followed by the generation of hot plasmoids. The plasma temperature rises sufficiently to emit hard X-rays to be observed by X-ray satellites such as ASCA. The simulation successfully explained the mass outflow phenomena in protostar as well as X-ray emission.

Generalized magnetic coordinates are constructed from a framework of quadratic flux minimizing surfaces. The coordinates smoothly reduce to straight field line coordinates where flux surfaces exist. A feature of the construction of such surfaces is an efficient identification of the size and phase of magnetic islands, and thus a new technique is enabled by which magnetic islands in the vacuum field of heliacs may be controlled[5-7]. The algorithm for constructing the coordinates is robust and flexible, and requires less field line tracing than present straight field line mapping routines.

References

[5-1] Tokuda S., Naitou H., Lee W. W, "A Particle-Fluid Hybrid Simulation Model Based on Nonlinear Gyrokinetics, " submitted to J. Plasma and Fusion Research.

[5-2] Naitou H., Kitagawa H., Tokuda S., "Linear and Nonlinear Simulation of Kinetic Internal Kink Modes, " J. Plasma and Fusion Research 73, 174 (1997).

[5-3] K. Shimizu, T. Takizuka, "Simulation of Divertor Plasma", J. Plasma and Fusion Research **72** (1996) 909.

[5-4] Yamagiwa M., Nemoto T., Hirose A., Elia M., "Parallelization of kinetic ballooning shootingcode KBSHOOT, " to be published in JAERI-Data/Code 97-032.

[5-5] Idomura Y., Tokuda S., Wakatani M., "Chaotic behavior in PIC simulation and its relation to computational errors, " to be published in Comput. Phys. Commun. 102 (1997).

[5-6] Hayashi M., Shibata K., Matsumoto R., "X-ray flares and mass outflows driven bymagnetic interaction between a protostar and surrounding disk, " Astrophys. J. 468, 37 (1996).

[5-7] S.R. Hudson and R.L. Dewar, "Manipulation of islands in a helical vacuum field, " Phyics Letters A 226, 85 (1997).

IV. TECHNOLOGY DEVELOPMENT

The Research and Development of nuclear fusion reactor technology has been focused on the ITER-related areas: brankets, fueling and pumping system, superconducting magnets, Neutral Beam Injection (NBI) heating system, plasma facing components, Radio-Frequency (RF) heating system, reactor structures, remote maintenance, tritium technology, and the analysis and assessment of nuclear fusion systems, etc. Major highlights of development for ITER in FY 1996 are as follows:

In the area of superconducting magnet, (1) 13.6 ton Nb_3Sn strand production was completed successfully, that achieved high performance of the ITER requirement on critical current density and low AC loss for the CS Model Coil and CS Insert Coil, (2) 3.3 km 46 kA superconducting cable production with 1080 strands was completed successfully, that is composed of 13.6 ton Nb_3Sn strand and 6.8 ton copper strand for the CS Model Coil.

Regarding the development of ITER plasma facing components for the full-scale length mock-ups, vertical target mock-ups and wing mock-ups, thermal cycling experiment was performed successfully to demonstrate durability of all the mock-ups at a transient heat load of 15 MW/m^2 for 15 sec for a repetition of 10^3 cycles.

A long pulse operation of a negative ion source was demonstrated at 30 kV and during 139 hours (equivalent to half year of the ITER operation) with a source plasma created in a water cooled chamber of 220 mm in diameter and 156 mm in height. Also in the CEA-JAERI joint experiment, a high current density D^- beam of over 20 mA/cm^2 was successfully produced at a source pressure of 0.3 Pa with the JAERI KAMABOKO source. As for the gyrotron development for ITER the maximum efficiency of 40% was obtained with the depressed collector at 170 GHz for 50 msec and long pulse operation up to 10 sec was demonstrated at 175 kW limited by the window temperature.

1. Blanket Technology

Following the achievements of the last fiscal year, blanket technology development has progressed steadily. Continued R&D activities within the framework of ITER/EDA have advanced to the successful fabrication of a medium-scale shielding blanket mock-up. Thermomechanical performance tests using this mock-up showed their satisfactory performance. Fundamental R&D of the breeding blanket have also continued, and design-oriented engineering data on a pebble bed has been obtained. Application of the Hot Isostatic Pressing (HIP) technology to a reduced activation ferritic steel, F82H, resulted in successful fabrication of a first wall panel.

The development of fueling and pumping technologies this year included a simulation

study on an electromagnetic railgun pellet injector and performance tests of a root pump. The development of a high-accuracy, high-stability vacuum thermobalance has been completed.

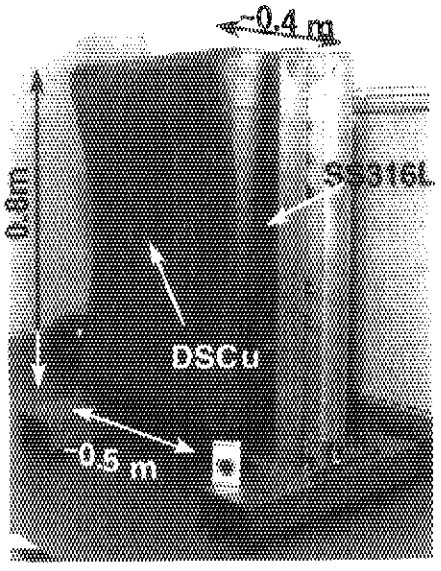

Fig. IV.1.1-1 Medium-scale shielding blanket mock-up

1.1 Development of a Shielding Blanket

1.1.1 Fabrication of a Medium-scale Blanket Mock-up and Preparation of the Test Facility

Based on the experience of successfully fabricated small-scale shielding blanket mock-up and several types of first wall mock-ups prior to 1996, a medium-scale shielding blanket mock-up was fabricated in 1996 [1.1-1, 1.1-2]. The medium-scale mock-up includes major design features of the ITER shielding blanket, i.e., austenitic stainless steel (SS316L) coolant tubes embedded within the first wall (FW) heat sink of alumina dispersion strengthened copper (DSCu), drilled coolant channels in forged SS316L shielding block and a poloidally curved FW and shielding blocks. The mock-up width and coolant tube/channel pitches vary in the poloidal direction. The final mock-up is shown in Fig. IV.1.1-1. The dimensions are a width of 455-513 mm, a height of 800 mm and a thickness of 329-369 mm. For this fabrication, a simultaneous HIP process (1050°C, 150 MPa for 2 hr) of DSCu/DSCu, DSCu/SS316L, and SS316L/SS316L was applied as it was for the fabrication of previous mock-ups. Metallographic examination of pieces cut from the edge of the HIPed mock-up confirmed good bondability of the HIPed joints. Thus, the basic technology and procedures for shielding blanket fabrication have been developed. A prototype ITER shielding blanket will be fabricated in 1997 to demonstrate its fabricability and to allow an assembly test of blanket modules onto the backplate.

In parallel with the mock-up fabrication, a test facility for thermomechanical and thermal-hydraulic tests of blanket mock-ups was prepared. The major components of this facility are an infrared lamp heater (160 kW), a vacuum vessel (ca. 1.5 m in diameter and 2.4 m high) to provide the vacuum atmosphere for the thermal insulation, and a water coolant circulation loop. The small- and medium-scale shielding blanket mock-ups will be tested in this facility in 1997.

1.1.2 High Heat Flux Testing of HIPed First Wall Panel [1.1-3]

High heat flux testing of a HIPed first wall panel with built-in circular cooling tubes (300 mm length × 132 mm width × 27 mm thickness) was performed at the electron beam facility, JEBIS, at the Naka Establishment of JAERI. The objectives of this test were to examine the thermomechanical performance of the panel, including the integrity of the HIP bonded interfaces and to examine the relation between the design fatigue curve and the experimental results. The test

conditions applied in these tests averaged 5.0 - 7.0 MW/m^2, much higher than the ITER normal operation conditions, 0.5 MW/m^2, with 2500 repetition cycles to accelerate fatigue testing. During these tests, no cracks or other damage was observed. Further, no degradation in heat removal performance was observed from temperatures measured by thermocouples embedded within the panel. The thermomechanical integrity of the panel was confirmed within the parameters tested, and the fatigue lifetime of the panel was found to be much longer than the design fatigue curve of this material, even beyond the raw fatigue data.

1.1.3 Fatigue Test of First Wall Structure Model with Built-in Circular Tubes[1.1-4]

Low-cycle fatigue tests using HIPed DSCu/SS first wall structure model specimens with built-in circular SS cooling tubes were performed. Typical test specimens were 20 mm in length and 6 mm in thickness for DSCu, and 10 mm in diameter and 1 mm in thickness for the SS cooling tubes. The objectives of these tests were to examine the fatigue lifetime and fracture behavior of the first wall structure under repeated mechanical loads, especially the effect at the DSCu/SS HIPed interface. Test conditions applied were strain ranges of 0.2, 0.3, 0.5, 0.7, and 1.0% at a strain rate of 0.1%/sec. Initial cracks in all test specimens were observed on the inner surface of the SS cooling tubes. Elastoplastic analysis was performed to evaluate the maximum strain on inner surface of the SS cooling tubes. The fatigue lifetime of the first wall obtained by these tests was found to be beyond the raw material fatigue data.

References

[1.1-1] Sato S., Kuroda T., Hatano T., et al., to be published in Proc. of 4th ISFNT, Tokyo (1997).
[1.1-2] Yamada H., Sato S., Osaki T., et al., to appear in 17th SOFE, San Diego (1997).
[1.1-3] Hatano T., Suzuki S., Yokoyama K., et al., to be published in Proc. 4th ISFNT., Tokyo(1997).
[1.1-4] Hatano T., Hashimoto T., Kitamura K., et al., to be published in Fusion Eng. Des (1997).

1.2 ITER Blanket Design

1.2.1 Design of Shielding and Breeding Blankets

For the shielding blanket with welded attachment to the backplate, 3-D thermo-mechanical analyses using the analysis model shown in Fig. IV.1.2-1 were performed for steady state, and the plasma start-up and shutdown transient conditions. Local stresses at the attachment root of the blanket module top and bottom regions were quite high due to the effect of thermal bowing of the module. Design

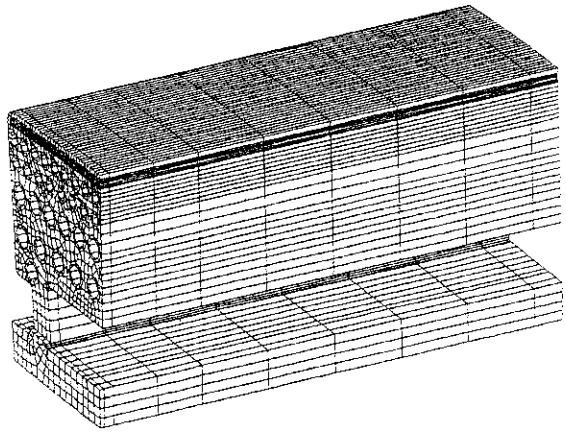

Fig. IV.1.2-1 3-D analysis model of shielding blanket

modifications of these regions are needed. Electromagnetic stress analyses were also performed. By introducing radial slits within the FW DSCu heat sink between adjacent coolant channels, the eddy current flowing through the attachment was reduced to about 60% of the total toroidal current [1.2-1]. Thus a reduction of electromagnetic force acting on the blanket module, especially the shearing force, is expected. The results of stress analyses for the blanket-backplate-support system under VDE disruption loads showed reinforcement of the backplate, especially at its bottom, was required, e.g., an increase in the thickness and/or the addition of a stiffening rib in the shape of a toroidal ring [1.2-2].

A multi layered pebble bed type blanket was designed as a proposed ITER breeding blanket [1.2-3]. With a Li_2O breeder and a Be neutron multiplier, both in the form of pebbles, a net tritium breeding ratio of 0.8 can be achieved. The results of a thermal analysis showed that the temperatures of Li_2O and Be would be maintained within their nominal ranges if the edges of the breeder cans were modified slightly.

1.2.2 Shielding Design

Two-dimensional shielding analyses have been performed on the maintenance and test module mid-plane ports in ITER[1.2-4]. The nuclear responses in the TF and PF coils around these ports have been calculated. Shield plugs with 20 mm-wide gaps between the blanket modules exist in both ports. For the test module port, shield plugs are installed at the back of a 500 mm-thick test module. To satisfy design limits, it was found that 540 and 150 mm thick shield plugs are required for the maintenance and the test module ports, respectively. In addition, the nuclear response as a function of the gap width has been also estimated. For a 50 mm-wide gap, it was found that 750 and 390 mm thick shield plugs are required for the maintenance and test module ports, respectively. Two-dimensional Sn radiation transport analyses were performed using the detailed toroidal cross-section model that included three NBI ports, and two non-NBI ports with shield plugs in their openings. Nuclear responses in the TF coils around NBI ports also satisfied the design limits.

Reference

[1.2-1] Kitamura K., Komatsuzaki M., Nishio S., et al., JAERI-Tech 96-031 (1996).
[1.2-2] Kitamura K., Koizumi K., Shimane H., et al., JAERI-Tech 96-049 (1996).
[1.2-3] Miura H., Kitamura K., Takatsu H., et al., to be published in Proc. 19th SOFT, Lisbon (1996).
[1.2-4] Sato S., Takatsu H., Utsumi T., et al., to be published in Proc. of 4th ISFNT(1997).

1.3 Development of a Breeding Blanket

1.3.1 Engineering Tests of Layered Pebble Blanket

Engineering tests of layered pebble blanket elements were performed to justify and specify the layered pebble blanket concept. This year, R&D activity focused on compatibility

between the breeder (Li_2O) and the multiplier (Be) material, and the structural material (low activation ferritic steel F82H) It also assessed the effective thermal conductivity of the Li_2O and Be pebbles.

The compatibility of Be and F82H was tested at 700 to 850°C for 3000 hours. Metallographic observations were performed after the compatibility tests and the corrosion zone lengths were measured. It is very important to obtain engineering data for the growth rate of the corrosion zone to allow appropriate materials selection and certification of design limits (lifetime, acceptable temperature range, and so on). As a result of these compatibility tests, it was determined that the compatibility performance of F82H was better than that of SUS316 [1.3-1]. Also, the growth rate at 600°C is estimated to be negligibly small (2.63×10^{-11}cm). Thus, it is concluded that compatibility will not be the temperature-limiting issue, since the design temperature limit is 600°C to avoid excessive Be swelling.

Measurements of the effective thermal conductivity of Li_2O and Be pebbles were performed from 400 to 650°C, for which measurement data had not yet been obtained. The results showed good agreement with the extrapolation of previous work. Thus, the design value for effective thermal conductivity was confirmed to be appropriate in the high temperature range. Further effort will be focused on the effective thermal conductivity of binary pebble bed.

1.3.2 Trial Fabrication of Small-Scale First Wall Panels Made of Reduced Activation Ferritic Steel, F82H, by Hot Isostatic Pressing Method [1.3-2]

A reduced activation ferritic steel, F82H, is the primary candidate structural material of the pebble-bed-type solid breeder blanket for DEMO reactors in JAERI [1.3-1]. To develop the necessary fabrication technology for the first wall and blanket box structure, fabrication of small-scale first wall panels fabricated from F82H has been attempted by applying the HIP (Hot Isostatic Pressing) bonding method. In previous studies, the optimum HIP conditions (the 1040°C, 150 MPa fro 2 hours) and optimum post heat treatment after the HIP process (tempering at 740°C for 2 hours) were determined [1.3-3, 1.3-4].

By applying the above conditions, two flat panels, each with ten cooling channels, have been successfully fabricated. Each panel consists of 1.5 mm-thick rectangular cooling channels (8 mm-square inner cross section) sandwiched between 2.5 mm-thick surface plates with a 4.5 mm-thick backing plate. Overall, the panels are 250 mm long, 120 mm wide, and 18 mm thick. A

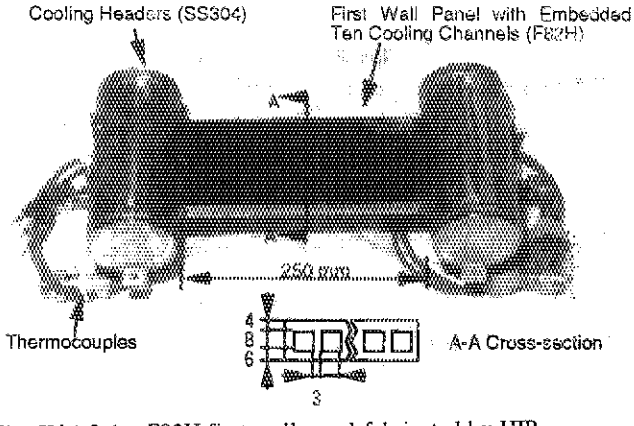

Fig. IV.1.3-1 F82H first wall panel fabricated by HIP bonding method.

fabricated panel is shown in Fig. IV.1.3-1. One panel has been destructively tested to examine the metallurgical bonding of the elements. This examination confirmed sound HIP bonding. The other panel, shown in Fig. IV.1.3-1, is to be thermomechanically tested to assess its thermomechanical responses and lifetime under the anticipated DEMO heat load conditions.

1.3.3 Test Program Development and Design of Test Module

Based on a Test Blanket Working Group (TBWG) decision, four horizontal ports were assigned for the test blanket modules. One of the ports will be used for the test module(s) of the ITER breeding blanket. These modules will be installed during the Enhanced Performance Phase (EPP). The other three ports will be used to test DEMO blanket test modules from each party. Two test modules will be installed in one port. Attachment/remote handling systems for the test modules and space and location requirements of ancillary systems were also decided and agreed to by the ITER JCT. Tests of two DEMO blanket modules, a water-cooled/ceramic breeder and a helium-cooled/ceramic breeder, both with Li_2O breeder/Be multiplier pebbles and F82H structural materials, were proposed by Japan. General Design Requirement Documents (GDRD) and Design Description Documents (DDD) including the design and major performance parameters of the test modules and ancillary systems were prepared [1.3-5].

References

[1.3-1] Takatsu H., Kawamura, H. and Tanaka, S., to be published in Proc. of 4th ISFNT, Tokyo (1997).
[1.3-2] Furuya K., et al., to appear in 8th ICFRM., Sendai, Oct. 26-31 (1997).
[1.3-3] Kurasawa T., Takatsu, H., Sato, S., et al., J. Nucl. Mater. 233-237 (1996) 313-318.
[1.3-4] Oda, M., Kurasawa, T., Kuroda, T., et al., JAERI-Tech 97-013 (1997).
[1.3-5] Miura H., Sato S., Enoeda M., et al., to be published as JAERI-Tech (1997).

1.4 Fueling/Pumping and Vacuum Technology

1.4.1 Simulation Study of the Railgun

An electromagnetic railgun injector has been studied to develop a repetitive and speed-controllable pellet accelerator for reactor-like plasmas. A final goal of this R&D is to obtain injection technology with the following characteristics. 1) Variable pellet speeds of 1-5 km/s during repeated injections. 2) Pellet injection rates of 1-2 Hz. 3) Plasma armor produced by a laser to reduce rail damage from accelerated pellets. This fiscal year, we investigated the effects of electromagnetic force acting on the plasma armature and the current distribution in the rail conductors using a two-dimensional simulation code. A calculation for augmented rails with a flat top rail current of 30 kA, determined the electromagnetic force is about 4.5 times larger than that in the normal rails (single rail). This enhancement is due to the magnetic flux density increase from the use of the augmented rails. The current in the rail cross section accumulates near the rail bore and the current in the augment rail distributes near the peripheral region of the main-rail side.

The amount of heating by this surface current on the tungsten alloy rails is very small, i.e., about 0.9 kW/mm^3, which results in a temperature rise of about 0.3°C during 1 ms acceleration period.

1.4.2 Measurement of Pumping Characteristics for Root Pumps

The ITER torus mechanical pumping system is comprised of a three-stage pumping system, with a four-stage dry-piston pump rated at 180 m^3/h as the final stage. Root pumps are being considered for the first two-stages of this mechanical pumping system to provide the high volumetric throughputs required. However, because of the danger of a hydrogen gas explosion, measured data are not available for compression ratios and pumping speeds of root pumps for light gases (H_2, D_2, He). This fiscal year, the compression ratios and pumping speeds of commercially available root pumps produced by the EDWARDS HIGH VACUUM Co. have been measured for light gases using PNEUROP standard method. The measurement of the pumping speeds for H_2, D_2, He, and N_2 has been completed. The measurement results, certify that the catalog values have less than 10% error.

1.4.3 Development of a High-Accuracy High-Stability Vacuum Thermobalance[1.4-1]

Impurities in a fusion plasma not only decrease the fuel (hydrogen isotopes) density but also increase radiation losses in the plasma and degrade the confinement of the plasma. A major impurity release is the outgas from the inner wall materials in the fusion machine. Therefore, it is important to measure the outgas quantities of candidate wall materials when addressing materials selection. This year, to directly measure outgas quantities of outgas from fusion materials, we developed a vacuum thermobalance capable of continuously measuring a weight of up to 20 grams with an accuracy of as high as one part in twenty million. This vacuum thermobalance has reduced the adverse thermal effects by the use of a proprietary technology. By using this vacuum thermobalance, it has become possible to measure the gas adsorption/desorption properties of materials which are important factors when characterizing fusion materials, with high accuracy under real-time conditions.

References

[1.4-1] Hamazaki S., Abe T., Murakami Y., J. Vac. Soc. Jpn. 36, 263 (1993). (in Japanese)

2. Superconducting Magnet Development

JAERI has been developing superconducting magnet technology development under the Engineering Design Activities of the ITER Program. In FY 1996, the ITER model coil development achieved the following;

(a) Successful completion of production of 13.6 tons of Nb_3Sn strand, that achieved high critical

current density (higher than 550 A/mm^2 at 12 T) and low AC loss (less than 200 mJ/cc-strand for a bipolar magnetic field of +/- 3 T) for the Central Solenoid (CS) Model Coil and CS Insert Coil.

(b) Successful completion of the production of 3.3 km of 46 kA superconducting cable having 1080 strands, which is composed of 13.6 tons of Nb_3Sn strand and 6.8 tons of copper strand for the CS Model Coil and CS Insert Coil.

(c) Development and testing of Butt-type joint of the 46 kA superconductor for CS Model Coil.

(d) Development of 1.0 ton mass-production technology of Nb_3Al strand for the Insert Coil.

(e) Construction of the 50 kA conductor and a conductor joint test facility, which has the capability to test a Force-cooled sample in a vacuum up to 11 T in a vacuum.

In the following sections, the technical achievements obtained from these research activities and structural material development are described.

2.1 Production of Nb_3Sn Conductor

The superconducting conductors for the CS Model Coil are fabricated in collaboration with partner Home Teams. There are three processes for fabrication of the superconducting conductor; the fabrication of Nb_3Sn superconducting strand having a 0.81 mm diameter, the cabling process that about 1000 strands are cabled, and the jacketing process where the cable is inserted into conduit and the conduit is compacted. Figure IV.2.1-1 shows the fabrication flow of Nb_3Sn conductor.

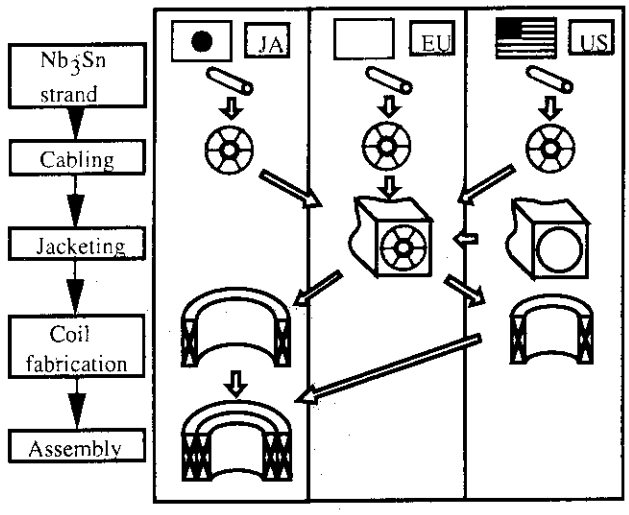

Fig. IV.2.1-1 Fabrication Flow

The total weight of the superconducting conductor for the CS Model Coil will be 26 tons. In Japan, 13.6 tons of the superconducting strands have been fabricated and the cabling process for these strands is completed. These Japanese cable were wound on a 2.5 m-diameter drum of 2.5 m diameter and shipped to Italy for the jacketing process. During transportation, the cable was protected from dust by vacuum packing. The conductors jacketed in Italy are wound on a 4 m-diameter drum and returned to Japan. Fourteen of the conductors among 16 conductors used for the outer module coil have been transported from Italy to Japan and wound into the coil.

2.2 Development of the Winding Technique

The outer module, which is composed of eight layers wound with two conductors in hand, has an outer diameter of 3618 mm and a weight of 50 tons. The cable-in-conduit conductor

having an Incoloy 908 jacket with as square outer cross section (46 × 46 mm) was used in the outer module. The development of the layer winding method for the CS Model Coil is a key for ITER R&D item because the tolerance in the radial direction of each layer is within ±1.5 mm. In addition to this tolerance, considering the strain applied during handling and fabrication, the free winding radius of the layer and the variation of curvature are specified to be +10, -50 mm and ± 2 mm at the winding process, respectively.

The winding system is shown in Fig. IV.2.2-1. The winding system involves an uncoiler for the conductor, a bender to straighten the conductor, and a forming bender to obtain the winding radius. The conductor delivered from the EU is installed on the uncoiler. The conductor is straightened by the bender and the required radius for winding is formed by the forming bender. A shot peening process is simultaneously applied to the conductor surface at the outlet of the forming bender to avoid stress acceleration grain boundary oxidization (SAGBO) of the Incoloy 908 jackets during heat treatment for Nb_3Sn reaction. Finally the formed conductor is wound on a mandrel. The winding speed is about 1 m/min.

For the R&D of the winding technique, trial windings using dummy conductors (around 100 m in length) and empty jackets were formed to study the deformation characteristics of the conductor during the winding process. Based on these R&D results, the winding technique, in which the formed condition of each layer fabrication is normalized, was developed. The winding of the first layer and the second layer for the outer module was successfully completed in December 1996 and March 1997, respectively.

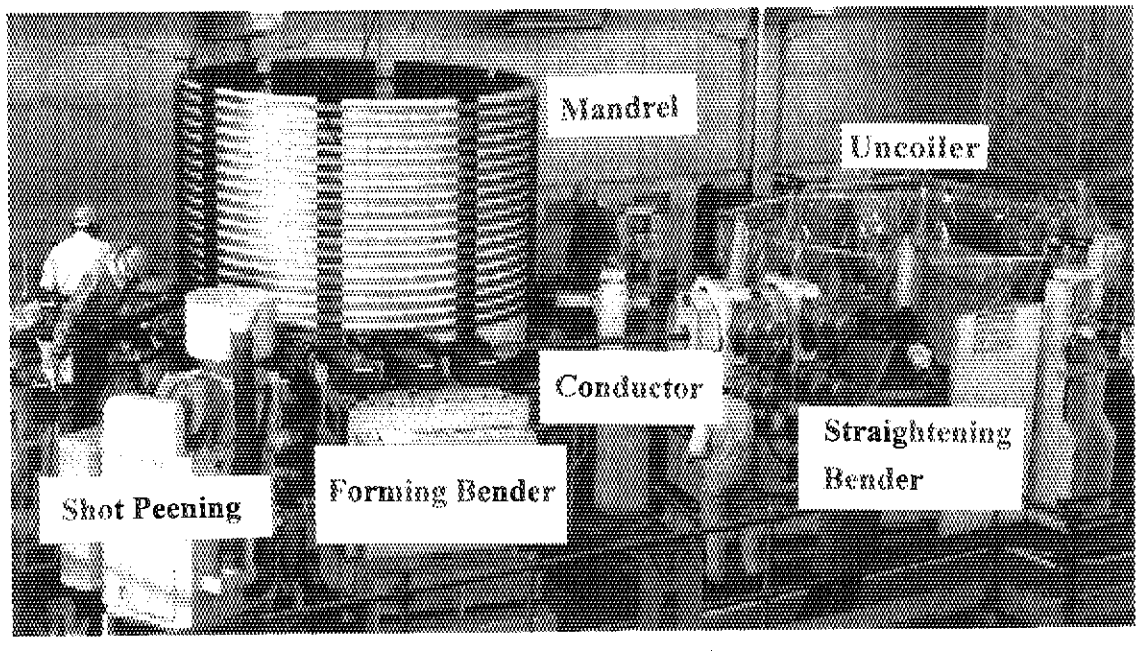

Fig. IV.2.2-1 Winding System

2.3 Development of CS Model Coil Joint

The conductor joint is a key technology for a superconducting coil. JAERI is developing two types of the 46 kA Nb_3Sn conductor joints for the outer module of the CS Model Coil, as shown in Fig. IV.2.3-1. One is a butt-type joint ((A) in the fig.) for the 15 joints between the coil layers. The other is a lap-type joint (B) for the two terminal joints, one to a bus bar and the other to the inner module.

For the a butt-type joint, the superconducting cable from the winding part and the hairpin cable are connected by a diffusion bonding technique. The AC losses of this joint are very small compared with the lap-type joint, because the size of compacted cable is small. A full-size sample of this joint was fabricated and tested. The DC resistance measured by a calorimetric method was 6.3 n Ω at an operating current of 50 kA and a background field of 5 T. The Joule loss and temperature increase of the coolant due to this loss are estimated to be 13 W and 0.2 K under the operating conditions of the joint. The AC losses measured by a calorimetric method were 0.24 W, very small as expected. The temperature increase of the coolant due to this loss is estimated to be 0.003 K. These results indicate the performance of this joint makes it suitable for the outer module. However, during the DC operation test, an instability was observed at lower current than expected. Though the current at which the instability occurred is higher than the operating current of the outer module, we are studying the cause for improvement.

For a lap-type joint, the necessary inspections, for example, the helium leak test, high voltage test, etc., can be done before the layers are connected. This is important for quality control. Brazing is used as the interface between the sleeve and the superconducting cable to obtain good electrical and mechanical contact. A full-size sample of this type joint also was tested. The measured DC resistance was 6.4 n Ω at the same conditions as for the butt-type joint.

2.4 Nb_3Al Insert Coil

The critical current of Nb_3Al is less sensitive to strain than that for Nb_3Sn. This characteristic is important for a high-field large coil for a fusion magnet. JAERI has advanced the development of Nb_3Al conductors, since 1986. In 1995 JAERI succeeded in developing a 40 kA-class conductor, which is required

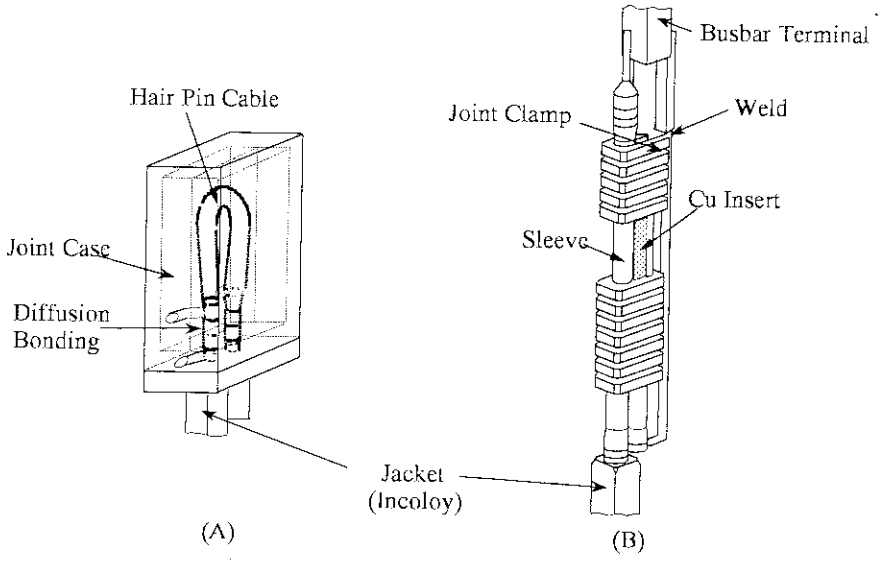

Fig. IV.2.3-1 CS Model Coil Joint

in ITER magnets [2.4-1]. Therefore JAERI is projected to fabricate and test a Nb_3Al Insert in the EDA for ITER for the purpose of demonstrating the applicability of a Nb_3Al conductor for the ITER-TF coil. Much effort was needed to overcome the technological obstacles, the manufacturing of the long length strand and to obtain the necessary yield rate for a large-scale production. Nb_3Al strands are now being produced.

The ITER-TF coils require generation of 12.5 T in a volume of 12 × 18 m. The bending strain is estimated to be ±0.4% when the React-and-Wind method is employed in winding the ITER-TF coil. To simulate this strain, the diameter of Nb_3Al Insert is expanded after the heat reaction.

The CS Model Coil and Insert are required to be cooled from R.T. to 4.5 K in 250 hr without thermal stress damage. A cool-down simulation was performed to verify the Nb_3Al Insert satisfies this requirement. The cool-down characteristic of Nb_3Al Insert is also studied[2.4-2].

References

[2.4-1] Nunoya Y. et al., : ICEC16/ICMC Proc. Elsevier Science, UK, (1997)p.1665.
[2.4-2] Koizumi N. et al., : ICEC16/ICMC Proc. Elsevier Science, UK, (1997)p.794.

2.5 Development of 46 kA Conductor Test Facility

A full-size conductor test is required before fabrication of the large coils. JAERI has developed the conductor test facility for the large current conductor. The capacity of this facility is listed in Table IV.2.5-1. The arrangement of main components in this facility is shown in Fig. IV.2.5-1. The sample is cooled by supercritical helium (SHe), which is generated by the refrigerator/liquefier. The coolant temperature is controlled within the range of 6-11 K by heaters attached to the inlet pipes. The magnetic field is applied to the sample by two pairs of superconducting split coils, which are cooled by liquid helium. The superconducting split coils consist of a pair of NbTi split coils and another pair of Nb_3Sn split coils. These coils can generate a maximum field of 17 T when the central field on the sample is 11 T. There is a vacuum chamber for the sample to isolate thermally the sample from the liquid helium. The 50 kA force cooled current leads were developed as test samples for this facility. Before a sample test, a performance test of these current leads was carried out in this facility as shown in Fig. IV.2.5-2. These current leads can operate stably up to 60 kA. Their performance is excellent, as expected. The force cooled current leads are compact compared with vapor cooled leads, because the liquid helium reservoir not necessary for the force cooled ones. The force cooled leads can be used in both vertical and also horizontal positions. This facility is completed and will be used for the superconducting

Table IV.2.5-1 Testing capacity of the 46 kA conductor test facility

Maximum sample field	11 T
Maximum sample current	60 kA
Maximum sample length	3.2 m
Available sample volume	102 × 170 mm²
Testing conditions	
Temperature	6 - 11 K
Inlet pressure	2 - 8 bar
Mass flow rate	≦ 10 g/s per conductor

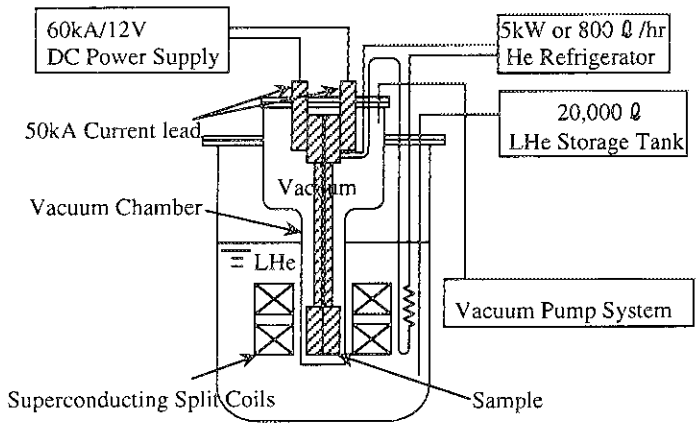

Fig. IV.2.5-1 Test facility for 46 kA superconductor cooled by supercritical helium

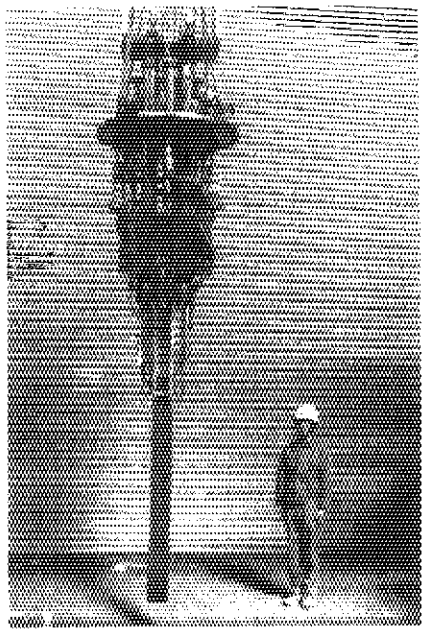

Fig. IV.2.5-2 46 kA superconductor joint sample with 50 kA current leads

performance tests of the 46 kA conductor, and conductor joint, for the CS Model Coil and the Insert coils.

2.6 Development of Structural Materials

The ITER TF coil case will require large cross-section forged plates. In addition, a 0.2% yield strength over 1000 MPa and fracture toughness of over 200 MPa$\sqrt{m}$ (ITER Target) at 4 K are required for these plates. Therefore, as an ITER task, we performed trial fabrication of 110 mm thick hot rolled plates and weld joints of JJ1 and JK2 stainless steels developed for the ITER magnet system to evaluate their mechanical properties at 4 K. The strength and the fracture toughness of their base and weld metals at 4 K, even if 110 mm thick weld metal, had higher values than the NIST Trend Line (cryogenic materials on the market). For JJ1, we succeeded in the trial fabrication of a 500 mm thick forged block. Its mechanical properties satisfied the ITER Target[2.6-1]. This demonstrated that heavy-section forged plate with a thickness up to 500 mm can be supplied.

We also evaluated the 4 K mechanical properties of Incoloy 908 jacket material used in the CS Model Coil to confirm the reliability of the base metal and the weld metal. The strength and fracture toughness of Incoloy 908 were found suitable for the CS Model Coil.

We also evaluated the mechanical properties of pure Ti, which has a high potential for the jacket material, as well as Incoloy 908, at 4 K. The details are described in Ref.[2.6-2].

References

[2.6-1]K. Ishio et al., To be published in Advances in Cryogenic Engineering Materials Vol. 44, 1998
[2.6-2]H. Nakajima et al., : ICEC16/ICMC Proc. Elsevier Science, UK, (1997)p.1895

3. Beam Technology

3.1 Development of Negative Ion Beam Technologies

Neutral beam (NB) injection has the capability to simultaneously heat a plasma, drive a plasma current for steady-state operation, and control plasma rotation for stable operation. For these purposes, it is essential to inject high energy and high power neutral beams. To produce such high energy neutral beams, it is necessary to create negative ion beams that have a high neutralization efficiency, 60%, even at the high beam energies required in future fusion reactors. Presently two major programs for negative-ion-based NB (N-NB) systems are progressing at JAERI. One is the development of a 1 MeV accelerator for ITER, and the other is the negative-ion-based NBI for JT-60U.

3.1.1 Demonstration of Negative Ion Beam Acceleration

In the N-NB system for ITER, a 40 A, 1 MeV D^- beam is required. To realize such a high current, high energy N NB system, it is essential to provide a high current negative ion beam acceleration up to an energy of 1 MeV. For this purpose, a test bed called MeV Test Facility (MTF) and a 1 MeV ion source/accelerator have been newly fabricated. Cockcroft-walton type acceleration power supply of the test bed has capacity of 1 MV, 1 A for 60 s. The acceleration power supply, source power supplies for operating the ion source (arc, filament, etc.) and the 1 MeV ion source/accelerator are installed in vessels containing SF_6 gas at 6 bars. The ion source is a Cs-seeded volume type with a semicylindrical geometry (KAMABOKO type) that can be operated at a gas pressure of less than 0.3 Pa to reduce the stripping loss of negative ions in the accelerator. The accelerator is the same type as the reference design for ITER, i.e., a multiaperture, multigrid (MAMuG) type, which has a 3 grid extractor and a 5 stage accelerator. Each grid has 49 apertures. Five acceleration grids are insulated by five insulators, each of which is made of fiber reinforced plastic (FRP), and is 1.8 m in diameter and 24 cm in thickness [3.1.1-1].

The accelerator was conditioned first without the beam. Voltage breakdowns due to outgas from the insulator often occurred at the beginning of this operation. By conditioning the accelerator, the breakdown voltage gradually increased, and finally attained 820 kV. After that, a 805 keV, 150 mA (drain current) H^- beam was produced for 1 s. No degradation of breakdown voltage due to the beam acceleration was observed. A small amount of Cs was injected into the plasma generator to increase the negative ion current and to examine the influence of the cesium on the breakdown voltage. The breakdown voltage characteristic was not degraded by the Cs seeding. A small divergence beam, less than 5 mrad, was successfully obtained at an optimum perveance of 3.2×10^{-11} $A/V^{3/2}$ [3.1.1-2, 3.1.1-3].

To improve the breakdown voltage characteristics further, new insulators were fabricated and installed on the accelerator. The thickness of the insulators was increased to 33 cm.

The accelerator power supply was also modified to suppress the energy input to the ion source/accelerator. The protection resistance connected to each acceleration stage were increased.

References

[3.1.1-1] M. Hanada et al., "A 1 MeV, 1 A Negative Ion Accelerator Test Facility ",Proceedings of the 18th Symposium on Fusion Technology, Karlsruhe, 617 (1994)

[3.1.1-2] T. Inoue et al., "High energy acceleration of H^- ion beam at MeV Test Facility", Proceedings of A Joint Meeting of the 7th International Symposium on the production and Neutralization of Negative Ions and Beams and 6th European Workshop on the Production and Application of Light Negative Ions, BNL,(1995)

[3.1.1-3] K. Watanabe et al., "Recent Progress of High-Power Negative Ion Beam Development for Fusion Plasma Heating", Radiat. Phys. Chem. 49.6.631-639(1997)

3.1.2 Long Pulse Operation of a Negative Ion Source

To demonstrate a long pulse operation of a negative ion source, the JAERI Steady State Negative Ion Source has been tested at ITS-2M in JAERI. For the steady-state operation, the source chamber and the acceleration grids are well cooled by water. The dimensions of the source chamber are 220 mm in diameter and 156 mm in height. The accelerator has 4 grids, out of which a plasma grid facing the source plasma has a bellows mechanism to absorb the thermal expansion. This enables to keep the temperature of the plasma grid more than 200 ℃, where the negative ion production is enhanced and the extracted electrons are reduced. After injecting 400 mg of Cs into the source, the ion source was operated stably for 139 hours, i.e., without a significant reduction of beam current and without the degradation of breakdown voltage. This operation time is equivalent to half year operation of the ITER N-NB system.

Small copper plates were placed at various places in the extractor and in the beamline to quantify the amount of cesium flowing from the plasma generator. After the 139 hour operation, the quantity of Cs on the plates was measured by ICP (Inductively Coupled Plasma) mass analysis. It was found that the quantity of Cs decreased with the distance from the plasma generator. The total amount of Cs that exited the source was less than 40 mg, i.e., 10% of the injected Cs. The source chamber retained 90% of the original Cs.

The weight loss of the tungsten filaments after the 139 hour operation was measured to clarify dominant factors of filament lifetime. The averaged weight loss of 6 filaments was 2.5%. A large reduction of the diameter was observed where the minus side was terminated. The diameter was reduced from 1.21 to 1.14 mm near the minus terminal while there was almost no reduction near the plus terminal. This nonuniform erosion is thought to be caused by evaporation. Since the arc current flows from the source plasma into the filament, the minus terminal is heated more and evaporates. Once the diameter is reduced, the resistance of the filament increases, resulting in a further increase in temperature and the accelerated reduction of the diameter at the minus terminal. Assuming the filament temperature to be 2850 K, the consumption rate calculated from the evaporation rate agrees well with that obtained in this experiment. Taking this filament

temperature as the ITER design value, the lifetime of the ITER filaments is estimated to be more than one year, longer than the maintenance period required for the ITER-NBI (half a year).

3.1.3 Study to Improve a Negative Ion Source

A high current density D^- ion beam, more than 20 mA/cm^2, has been successfully produced at a source pressure of 0.3 Pa in the JAERI KAMABOKO source. Following the success of the high current density D^- ion beam production, the source was modified to reduce the extracted electron current. By increasing the magnetic filter strength from 800 to 1800 Gauss·cm, the extracted electron current was decreased to half the D^- ion beam current while the D^- ion beam current was maintained at 1.4 A [3.1.3-1]. The current density, the source pressure, and the ratio of the extracted electron current to the beam current satisfy the ITER requirements.

References

[3.1.3-1] C. Jacquot, D. Riz, T. Trainham et al., " Negative D^- Ion Source Relevant for Application to ITER Neutral Beam Injectors ", Proc. of the 19th Symp. on Fusion Tech., Lisbon (1996)

3.1.4 Test of the Negative Ion Source in JT-60 Negative-Ion-Based NBI

A negative-ion-based neutral beam injector (N-NBI) of 500 keV, 10 MW D^0 was constructed in February 1996. This is the worlds first N-NBI system. It is shown in Fig. IV.3.1-1. The injector has two large ion sources, each is designed to produce 500 keV, 22 A D^- ion beams for a pulse duration of 10 s [3.1.4-1]. Negative ions are produced in a large KAMABOKO source at a low gas pressure. The magnetic filter, called a PG filter, is used to enhance the negative ion yield and to reduce the extracted electron current. The negative ions produced are extracted from a multiaperture extractor that has 1080 apertures within an extraction area of 45 × 110 cm. The extracted negative ions are accelerated to 500 keV in a 3 stage electrostatic accelerator.

From a single ion source, a 13.5 A, 400 keV D^- and a 18.4 A, 350 keV H^- beams have been produced to date. The beam power has attained 6.4 MW with hydrogen, from which a power of 3.2 MW has been injected into JT-60U to demonstrate a plasma

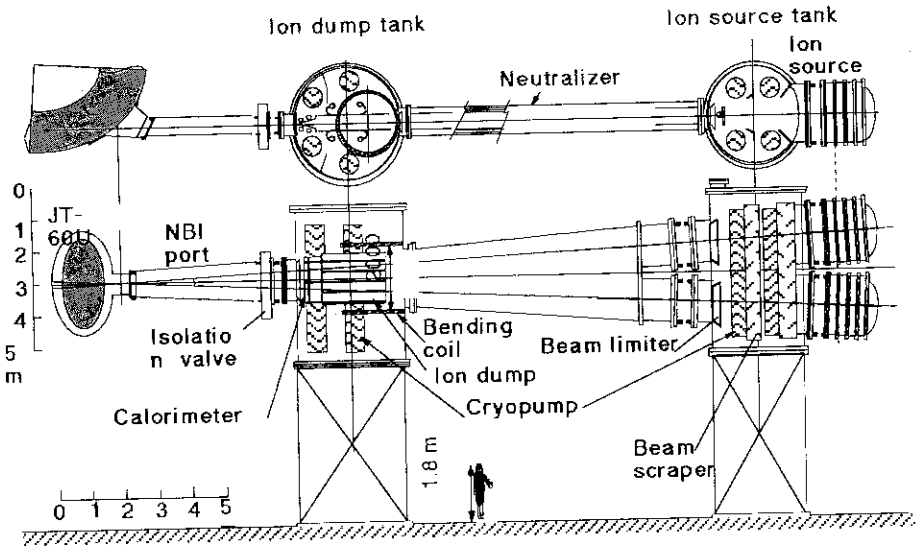

Fig. IV.3.1-1 A 500 keV, 10 MW negative-ion-based NB system for JT-60U

current drive. The optimum source pressure, that gives the highest beam current, was 0.2 Pa. This allowed a reduction of the stripping loss and an increase in the acceleration efficiency. In addition, the ratio of the extracted electron current to the beam current was no more than 0.5 even in D_2 operation. In conclusion, there has been no fundamental problems in achieving full performance. Both the source pressure and the extracted electron current satisfy the ITER requirements. In addition, the beam current has attained half the value required for ITER (40 A) [3.1.4-2].

References

[3.1.4-1] M. Kuriyama et al., "Negative-ion based NBI system for JT-60U", Proceedings of the 16th Symposium on Fusion Engineering, Champaign, (1995)

[3.1.4-2] K. Watanabe et al., " Beam Acceleration Test in Negative-ion based NBI System for JT-60U", Proceedings of A Joint Meeting of the 7th International Symposium on the production and Neutralization of Negative Ions and Beams and 6th European Workshop on the Production and Application of Light Negative Ions, BNL, (1995)

3.1.5 Engineering Design and R&D for ITER NBI

Engineering design studies of the ITER NBI system have been divided among the EU, Japan, and Russia. The Japanese design tasks are composed of five studies, which are the negative ion source/accelerator, the power supply, the neutronics, maintenance and the passive magnetic shielding. The negative ion source/accelerator is the key component in ITER-NBI system. A KAMABOKO source, the same type as the negative ion source for JT-60U, is adopted for the ITER NB system. The dimensions are 3 m in diameter and 2.7 m in height. The total weight is about 20 tons. The ion source/accelerator is designed to produce a 1 MeV, 40 A D^- beam with a beam divergence of less than 5 mrad. The ion source is also required to operated at a low operating gas pressure, 0.3 Pa, for more than 1000 s. In addition to the ion source/accelerator, the other engineering design studies also made progress in FY 1996 [3.1.5-1].

In the present design, the ion source/ accelerator is surrounded by insulation gas to provide a high voltage insulation, as shown in Fig. IV.3.1-2. The gas molecules are exposed to radiation from the reactor, and are ionized and dissociated during ITER operation. This may result in degradation of the

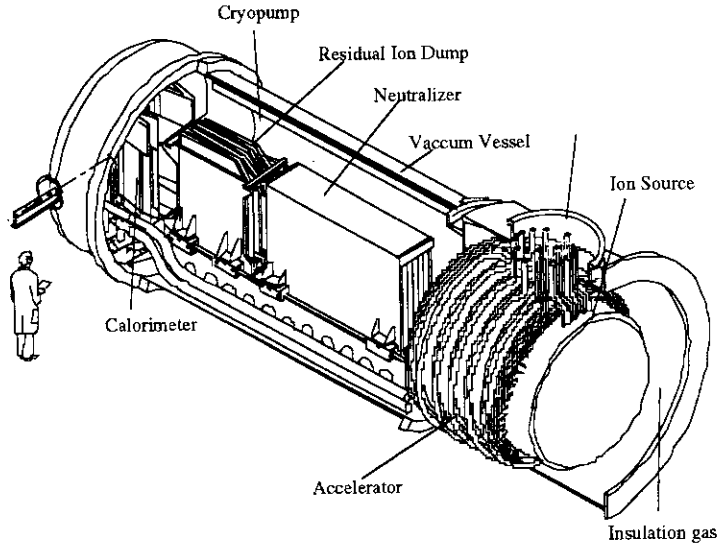

Fig. IV.3.1-2 The ITER neutral Beam Injector based on high energy negative ion beam.

breakdown voltage and in a power loss of the NB system. To examine the possibility of degradation of the gas insulation, the influence of radiation on insulation gas was examined. The experiment was performed in a small chamber, containing a pair of electrodes. The chamber was alternately filled with SF_6, C_2F_6, and CO_2. The chamber was irradiated by Co^{60} gamma rays. The following points were clarified in this experiment;

(1) The ionization current increases linearly with gap length between electrodes, gas pressure, dose rate and molecular weight.

(2) The breakdown voltage is decreased only by 10% with a dose rate of 0.45 Gy/s.

References

[3.1.5-1] R. Hemsworth et al., "Design of the ITER Neutral Beam Injectors", Rev. Sci. Instrum., 67, (1996).

3.2 Application of High Intensity Ion Beam Technologies

3.2.1 Development of Super Low Energy Ion Source

Our beam technology is applied also to the development of a super low energy ion source. A target of the development is to produce steady-state positive and negative ion beams of more than 1 A at a low energy, 200 eV. To produce such a high current beam at low energy, the electrical field for ion extraction should be strengthened against the space charge, therefore both the slit width and the gap length between electrodes should be reduced. Also the electrodes have to be thin to allow the electrical field to penetrate into the source plasma sufficiently. To obtain proper beam trajectory, the slit width and thickness of the electrodes are required to be less than 1 mm. In addition, the electrodes are required to have a cooling structure for the steady-state operation. It is very difficult to machine such an electrode and to braze cooling channels on this thin electrode. To overcome these manufacturing difficulties, a tungsten wire is utilized. Tungsten wires of 0.5 mm diameter are strung every 1 mm to make slits of 0.5 mm width. For steady-state operation, the wires are kept taut by springs to absorb thermal expansion. The ions obtained were extracted typically at 900 eV, and then decelerated to 250 eV. A 0.5 A, 250-eV H^- beam has been successfully produced at steady state to date. To enhance the reliability and to simplify the structure of the electrode, a new electrode has been fabricated using a photo etching technique.

3.2.2 Development of the Ion Source for High Energy Accelerator

A high brightness proton ion source is required for a fast neutron source (FNS). A 67 mA, 50 keV D^+ ion beam, whose proton ratio should be more than 65%, is required. To satisfy this requirement, a bucket ion source with a 120 mm inner diameter and a 130 mm height has been developed. To enhance the proton ratio, a transverse magnetic field was created in the plasma generator. Through a single 12 mm diameter aperture, a 130 mA, 50 keV hydrogen positive ion beam has been successfully produced at an arc power of 3 kW. The beam current obtained is equivalent to a deuterium positive ion beam current of 71 mA, which is higher than the

required D+ ion beam current. The proton ratio of the beam and the beam divergence angle have achieved 80% and 13 mrad, respectively. The beam current, the proton ratio, and the beam divergence satisfy the requirements for the FNS [3.2.2-1].

References

[3.2.2-1] Y. Okumura, Private Communication.

4. RF Heating Technology

Radio-frequency (RF) waves are a key tool for heating and current drive of a tokamak fusion reactor. Development of high-efficiency RF sources and tritium barrier windows for electron cyclotron heating (ECH: 100-300 GHz), high-performance launching systems for the lower hybrid current drive (LHCD: 2-8 GHz) and the ion cyclotron range frequency (ICRF: 40-200 MHz) are the main efforts of JAERI to advance RF heating technology. The most emphasized activity in FY 1996 was the development of the high-power gyrotron. This activity aims at a final target of 170 GHz/1 MW/CW, and the development of the tritium shielding window, which is used as the output window of the gyrotron.

4.1 Gyrotron Development

The gyrotron is a high-power millimeter wave source and is a key component of the ECH system. Under the task agreement of ITER/EDA, the 170 GHz gyrotron development has been ongoing since 1995. First, we fabricated a demountable gyrotron and performed an oscillation test at very high order volume mode $TE_{31,8}$, which is relevant to 1 MW/CW oscillation. A stable 1.13 MW oscillation was obtained with an efficiency of 30% at a pulse duration of 0.4 ms. Following this, we designed and fabricated the first long-pulse gyrotron and obtained a pulse duration of 2.2 s at 230 kW and 0.6 s at 525 kW. In 1996, based on the results obtained in 1995, the long-pulse gyrotron was modified to improve the output window and to provide an electron gun (MIG) and a cavity. A silicon nitride window, which was developed in collaboration with NIFS, was used. Figure IV.4.1-1 shows the output power and efficiency dependence on beam current at short-pulse operation. The oscillation mode is $TE_{31,8}$ and the beam voltage is 85 kV. An output power of 750 kW was obtained at I_C=40 A. The efficiency was 22%. The power without a depressed collector was 500 kW at a beam voltage of 85 kV and a beam current of 28 A, where the efficiency was 36% (η_{CD}=1.7). A maximum

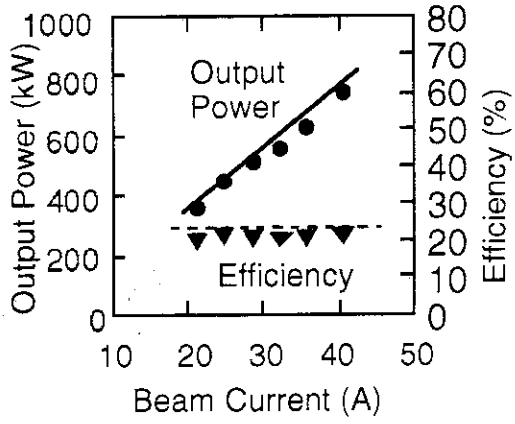

Fig. IV.4.1-1 Dependence of output power and efficiency on beam current. Beam voltage is 85 kV.

efficiency of 40% was obtained at a depressed voltage of 43 kV (η_{CD}=2), but the power decreased to 470 kW due to a influence of the trapped electrons. The pulse extension was carried out at P_{RF}=520 kW, 210 kW and 175 kW. At P_{RF}=175 kW, the window temperature stabilized at ΔT= 120°C and 10 s operation was attained. Here, the 10 s is limited by the capacity of the power supply system. However, so called thermal runaway was observed above 210 kW. At P_{RF}=500 kW, the maximum pulse duration was 0.75 s., which was limited by the increase in the window temperature (efficiency was ~34% with the depressed collector). For further pulse extension/power enhancement, materials of lower loss tangent are required. The major results are summarized in Table IV.4.1-1.

Table IV.4.1-1 Major performance of 170 GHz gyrotron

Power	pulse dur.	eff.
750kW	0.4ms	22%
500kW	50ms	36%(D/C)
470kW	50ms	40%(D/C)
520kW	0.75s	34%(D/C)
340kW	2s	20%
210kW	4s	18%
170kW	10s	30%(D/C)

(D/C:Depressed Collector)

References

[4.1-1] Sakamoto K., Kasugai A., Takahashi K. et al., "Stable, Single-Mode Oscillation with High-Order Volume Mode at 1 MW, 170 GHz Gyrotron", J. Phys. Soc. Japan, 65, 1888-1890(1996).
[4.1-2] Kasugai A., Sakamoto K., Tsuneoka M., "Development of 170 GHz long pulse Gyrotron with Depressed Collector", Proc. of 19th Symp. on Fusion Tech. Portugal (1996).
[4.1-3] Sakamoto K., Kasugai A., Takahashi K. et al., "Development of 170 GHz High Power Long Pulse Gyrotron for ITER", Digest of 21st Int. Conf. on Infrared and Millimeter Waves, AT1, 14-19(1996).

4.2 Development of Transmission Line and Launchers

4.2.1 ECH Window

A high power test of a synthesized diamond disk was performed under the ITER international collaboration. A diamond has extremely high thermal conductivity and a low RF absorbing ratio (loss tangent). Diamond is, therefore, expected to be an ideal material for a tritium shielding window and a gyrotron window for 1 MW/CW RF transmission at 170 GHz. Using a JAERI test stand, 160 kW level RF was transmitted through the diamond disk (~100 mm in diameter, 2.2 mm in thickness). The diamond disk is shown in Fig. IV.4.2-1. In Fig. IV4.2-2, the time dependence of the edge temperature (experiment and theory) is shown. The transmitted power is 165 kW, and the pulse duration is 57 ms. Good agreement was obtained between the experiment and theory, where a loss tangent of

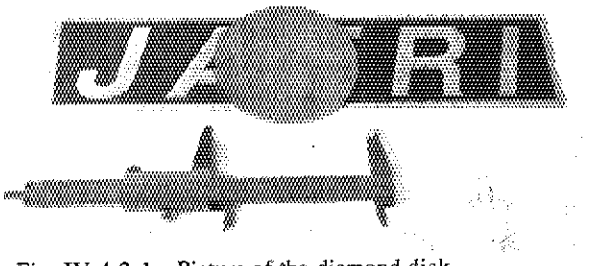

Fig. IV.4.2-1 Picture of the diamond disk.

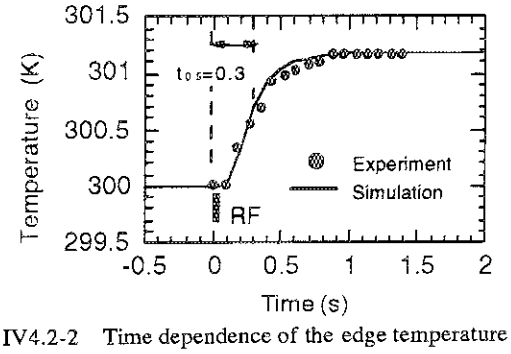

Fig. IV4.2-2 Time dependence of the edge temperature of the diamond disk.

1.3×10^{-4} and a thermal conductivity of 1800 W/m/K are assumed[4.2-1]. If this diamond disk is used, a 1 MW transmission is possible with an edge-cooled, single-disk window.

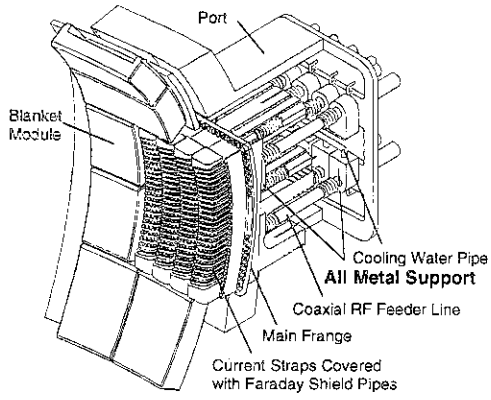

Fig. IV.4.2-3 Cutaway view of ITER ICRF antenna. AMSs are used to support the inner conductor of the transmission line.

4.2.2 LHRF Antenna [4.2-3]

A Carbon Fiber Composite (CFC) mock-up of a Lower Hybrid Current Drive antenna module was fabricated for the development of a heat resistant LH antenna front that faces to the plasma. This module is made of CFC plates and copper coated rods to reduce RF losses. The breakdown-voltage, RF properties, and outgassing rates for a long pulses at high RF power were tested at the Lower Hybrid test bed facility of Cadarache as a collaborative activity. After short pulse conditioning, long pulses with a power density ranging between 50 and 150 MW/m^2 were obtained with no breakdowns. The outgassing rate of Cu-plated CFC during RF injection is about six times larger than that of a Dispersion Strengthened Copper (DSC) module at a module temperature of 350°C.

4.2.3 ICRF Antenna [4.2-4,5]

All-metal antenna supports (AMSs) are a key element of the ICRF all-metal antenna. As the ITER R&D task, a full-size mock-up of the all-metal antenna support (AMS) for the ITER ICRF antenna was fabricated and the RF characteristics were measured. In present ICRF antennae used in large Tokamaks, a ceramic support is used for the central conductor. However, in ITER, enhancement of the dielectric loss tangent of a ceramic support due to neutron irradiation would significantly limit the power injection capability of the antenna. AMSs shown in Fig. IV.4.2-3 will enable the ceramic vacuum windows to be placed outside the vacuum vessel main flange where neutron flux is attenuated by the neutron shielding in and around the port.

Testing confirmed that the mock-up AMS (Fig. IV.4.2-4) has reasonably good RF characteristics, which are close to those calculated. The power reflection coefficient is ~ 1% at 60 MHz, which is the main frequency, and is less than 5% over the range of 55 - 70 MHz. The reflection level of the AMS meets the requirements of ITER antenna system specifications. Design of another full-size mock-up for high power testing was done using the experience gained from the low-power mock-up. Fabrication of this improved design is planned for 1997.

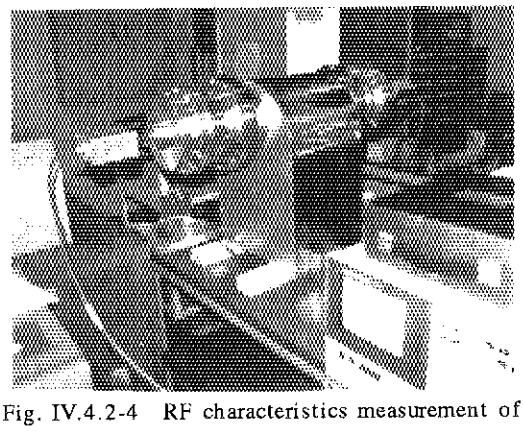

Fig. IV.4.2-4 RF characteristics measurement of the Full- size AMS mock-up.

References

[4.2-1] Kasugai A., Sakamoto K., Takahashi K., et al., JAERI-Research 97-020.

[4.2-2] Takahashi K., Kasugai A., Sakamoto K., et al., "Measurement of Temperature Dependence of Dielectric Permittivity of Sapphire Window for High Power Gyrotron", Jpn. J. Appl. Phys., 35, 4413-4416(1996).

[4.2-3] Maehara S., Seki M., Suganuma K., et al., JAERI-Research 96-036.

[4.2-4] Moriyama, S. Arai H., Ohta K., et al., "Final Report on Design Task: Development of all-metal Vacuum Transmission Line (Task G51 TT Sub task T238.1/1)", ITER Report 1997.

[4.2-5] Moriyama S., Kimura H., Saigusa M., et al., "All Metal Support for a Central Conductor of the ITER ICRF Antenna System", Submitted to Fusion Engineering and Design, (Proc. Fourth International Symposium on Fusion Nuclear Technology, 1997.4).

4.3 Millimeter Wave Free Electron Laser

A 2 MeV induction linac system was installed and tested using a dummy load. The installation of the diagnostic system for the induction linac and the checkout of the interlock system was completed. The electron beam acceleration test will be started soon. The design and fabrication of the next stage system, a 5 MeV/5 kA/160 ns class induction linac (JLA), was continued.

5. Tritium Technology

Studies on tritium technology have been continuously performed in the Tritium Process Laboratory (TPL) at the Tokai Establishment of JAERI. Some new activities regarding the studies of tritium safety technology and tritium processing technology were initiated FY 1996. Safe operation, of the TPL tritium facility, itself, is a valuable on-site experience that proves tritium can be safely handled in Japan.

5.1 Development of Tritium Safety Technology

At TPL, to establish safety technology for handling tritium in a D-T fusion reactor, research and development are being focused on (1) an advanced tritium removal system, (2) tritium accountancy, and (3) a study of tritium-material interactions and waste processing. For development of tritium confinement and removal technology for the ITER Atmosphere Detritiation System, application of a gas separation membrane module (hollow fibers of polyimide, process flow: 10 m^3/h) has been tested for recovery of hydrogen gas, moisture, and tritium gas from the atmosphere in a glove box filled with argon gas. The results of this test using the high permeability membrane module showed good performance and an increase of the processed gas flow [5.1-1]. To establish the "in-bed" tritium accounting technology for the ITER-scale tritium storage system, gas flowing calorimetry has been studied using a scaled ZrCo bed (25 g tritium capacity). Up to 20 g of tritium has been stored and measured in the bed with an accuracy satisfying the target accountability to measure ± 1 gram of tritium per 100 g stored at ITER. The

stability of the measurement and the integrity necessary for a seven month storage period was confirmed.

For prediction of tritium behavior in plasma facing components, investigations of hydrogen isotope permeation through, retention in and release from plasma facing and heat sink materials have been carried out. The experimental conditions were incident ion flux (Φ_i) = 3.8 $\times 10^{18}$ ~ 1.2 $\times 10^{19}$ D^+/m^2s, target temperature = 373 ~ 673 K, and incident D^+ ion energy = 200 ~ 2000 eV. Sample membranes of copper, stainless steel, and beryllium were tested. For beryllium, the activation energy obtained for its diffusion coefficient was close to that of beryllium oxide. This implies that the diffusion process of deuterium implanted into the surface of the beryllium sample was controlled by diffusion in the oxide layer.

The radiolysis of water containing a high concentration of tritium (max. 53.35 Ci/cm^3) was studied. The products of radiolysis were analyzed by pressure measurement, ultraviolet spectroscopy, and mass spectrometry, as a function of tritium (HTO) concentration. The ratio of the amount of gas produced by decomposition of water and the amount of helium 3 produced by tritium decay (G_T) was observed to increase with a decrease in the tritium concentration, as shown in Fig. IV.5.1-1 [5.1-2].

Interactions between water containing a high concentration of tritium and metal were studied from the aspect of corrosion and hydrogenation. After the exposure of zircaloy to water vapor containing tritium, the distribution of tritium was observed by autoradiography. The results showed a correlation for areas where additional elements like chromium and nickel were condensed and areas where tritium was located at high density.

References

[5.1-1] Hayashi T., Okuno K., Ishida T. et al., ISFNT4, April 6-11, 1997, Tokyo, Japan.
[5.1-2] Itoh T., Hayashi T., Okuno K., ISFNT4, April 6-11, 1997, Tokyo, Japan.

5.2 Development of Tritium Processing Technology

The development of the plasma exhaust processing system continued as an ITER R&D task. Based on the results obtained in the previous year, a closed loop fusion fuel processing system based on this JAERI developed technology was designed, fabricated, and tested. To satisfy the requirements of ITER, modification of the system to a three-stage process to accept

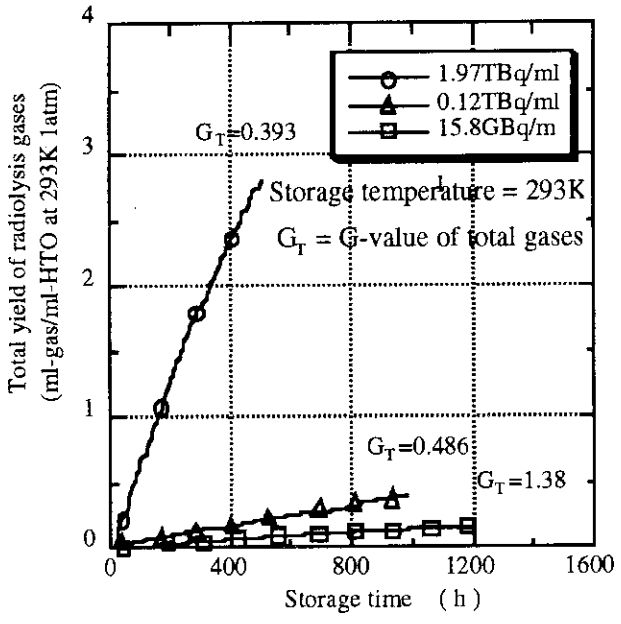

Fig. IV.5.1-1 Total yield of radiolysis gases with storage time of various tritium concentration.

various inputs has been proposed. It needs to be operated in the flexible modes shown in Fig. IV.5.2-1. This system is composed of a front end comprised of a combined palladium diffuser - vacuum pump and an electrolysis cell, a small loop palladium diffuser and an electrolytic reactor, and a catalyst bed-cold trap (or molecular sieve beds) polishing chain.

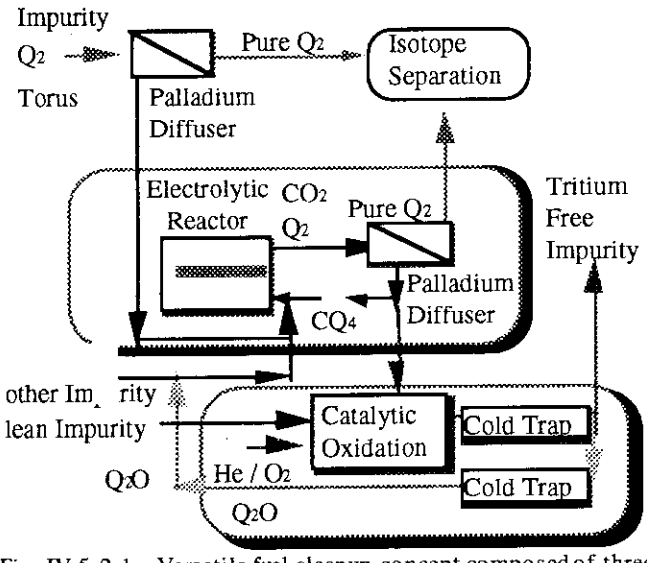

Fig. IV.5.2-1 Versatile fuel cleanup concept composed of three stages. (Q: any mixture of H, D and T.)

Each of these three processes handles different types of tritiated gases, and is operated independently. In the first system, the torus plasma exhaust is purified by the front end to feed Isotope Separation System (ISS). In the second, the impurity processing loop decomposes tritiated compounds and recovers tritium. Impurities contained in the plasma exhaust, other tritiated effluents, and regenerated tritiated water from the next recovery system are the major sources of tritiated impurities. The third tritium recovery system mainly accepts other process exhausts from vacuum pumping and analysis, which are expected to contain minor tritiated species. Experiments were conducted with the existing Fuel Cleanup apparatus to test the concept, followed by a major modification of the loop with the new processing unit composed of the palladium diffuser and the electrolytic reactor. Component testing of the electrolytic reactor also continued. An example of the experimental results obtained from the electrolytic reactor is shown in Fig. IV.5.2-2. A gas containing CH_4 and H_2O impurities was batch processed with the electrolytic reactor four times. The initial compositions of CH_4 and H_2O were ~10%, while the exhausted tritium from the residue of the process gas ranged from 39 to 720 mCi, suggesting a DF of approximately 1000 or higher was consistently obtained from this operation.

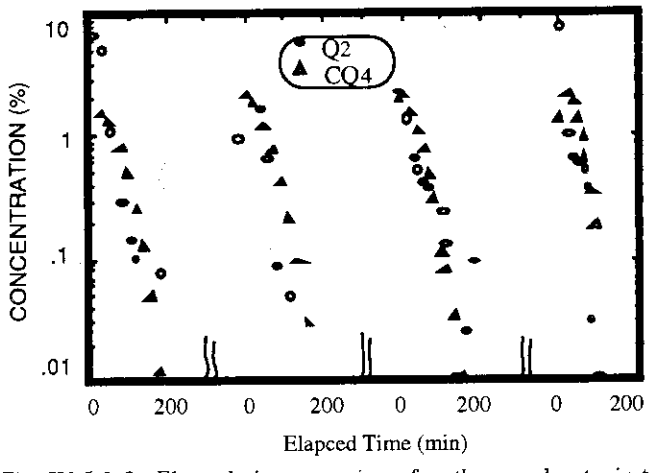

Fig. IV.5.2-2 Electrolytic processing of methane and water in the closed loop simulating electrolytic reactor at 50% efficiency by simultaneous oxidation and reduction. Consecutive 4 runs are shown.

The most promising approach for the Hydrogen Isotope Separation System in the fusion fuel cycle is a cryogenic distillation (CD) column. In simulation studies, control systems have been designed. Fig. IV.5.2-3 shows a proposed control system for a CD column [5.2-1]. A combination system of

feedforward and feedback control loops was found to be quite effective in maintaining the product purity of the column. A thermal diffusion column (TD) is attractive for the separation of small amounts of hydrogen isotopes. A series of experiments was carried out with the H-T system. This demonstrated that the TD column could recover the tritium from the H-T mixture. In addition, it was found that the separation factor of the column could greatly be increased by cooling the column wall with liquid nitrogen. In ITER, an appreciable amount of tritiated water is expected to be exhausted. A combination system of water distillation and Vapor Phase Catalytic Exchange (VPCE) columns was chosen to process the tritiated water in ITER. The design study of this combination system has been performed [5.2-2]. A basic experimental study for the VPCE column has also begun.

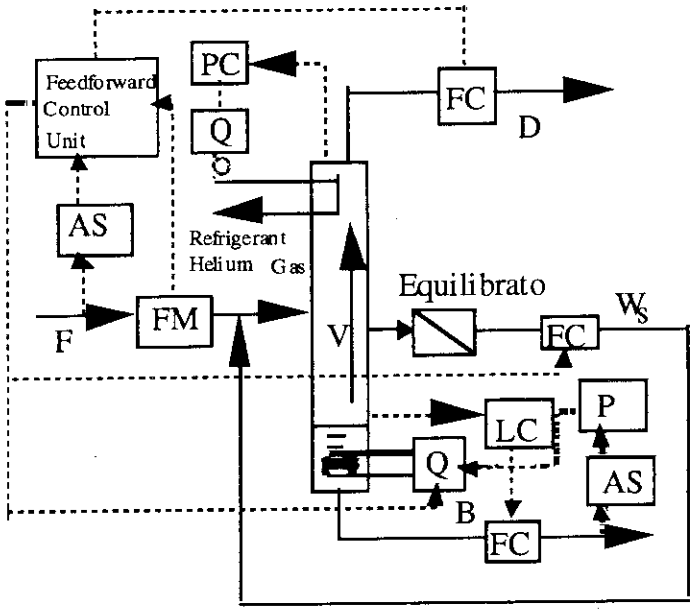

AS: Analysis System FM: Flow Meter
FC: Flow Controller
PC :Pressure Controller LC: Liquid Level
B: Flow rate of bottom stream (mol / h)
D: Flow rate of top stream (mol / h)
F: Flow rate of feed stream
V: Vapor flow rate of within column (mol / h)
Ws : Flow rate of feedback stream
PI: Proportional Integral controller

Fig. IV.5.2-3 Control systems of a cryogenic distillation column.

A study on Blanket Tritium Recovery consists of the study on the tritium inventory and the release behavior in solid breeder material, and the study on the optimum tritium recovery process for the blanket purge gas. With respect to the study on the tritium inventory and the release behavior in solid breeder material, lithium zirconate pellets were examined in experiments on water formation, water adsorption, and exchange reactions of hydrogen isotopes. This year, the study of isotope exchange reactions in H-D systems was conducted using a Li_2ZrO_3 packed bed. The exchange reaction between gaseous hydrogen and water was the rate controlling step. This reaction was expressed as a second-order reaction. Fig. IV.5.2-4 shows the temperature dependencies of the reaction rate constants. The temperature dependencies of rate constants for Li_2ZrO_3 dried at experimental temperatures (300～700°C) did not agree with that for Li_2ZrO_3 dried at 800°C. A further study, including a surface analysis of Li_2ZrO_3, is needed. The equilibrium constant of the isotope exchange reaction in the H-D system was 1.17. Experiments with the H-T system will be performed in the near future [5.2-3].

For the study on the optimum recovery process for the tritium blanket purge gas, a

Cryogenic Molecular Sieve Bed (CMSB) was studied as a promising process for recovery of tritium from the Solid Breeder Blanket purge gas. This year, experimental and theoretical work has been performed to optimize the regeneration method of the CMSB. Tests were performed using an 11 cm (diameter) × 8 cm (bed height) CMSB (MS5A, 500 g), with flow rates up to 60 l/min. (The H_2 and HT concentrations were 400 and 0.5 ppm, respectively.) Test results of regeneration experiments were evaluated by the modeling calculation previously derived by bench-scale experiments. The test results were consistent with the results from the bench-scale experiments. (See Fig. IV.5.2-5) The engineering data obtained are also applicable for the design of the CMSB process for ITER He GDC gas cleanup, where the flow rate of process gas (He) containing 1% H_2 and HT is 60 l/min [5.2-4].

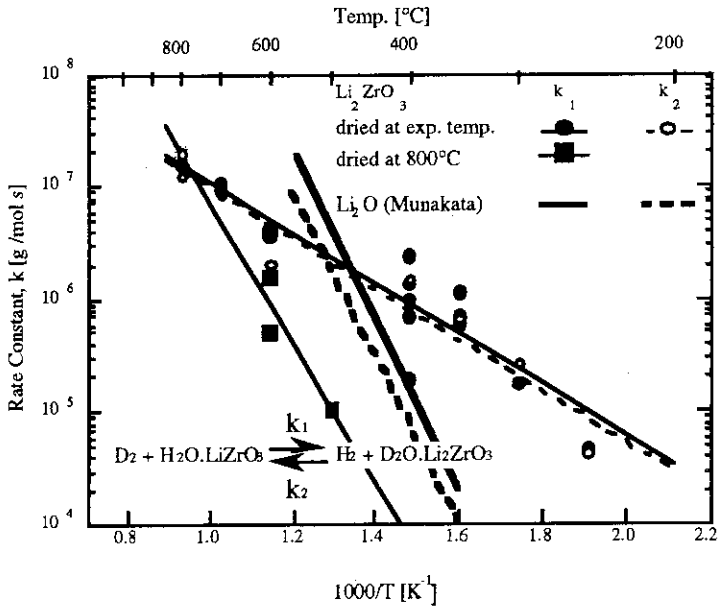

Fig. IV.5.2-4 Temperature dependence of reaction rate constant.

References

[5.2-1] Yamanishi T. and Okuno K., "Control Characteristics of Cryogenic Distillation Column with a Feedback Stream for Fusion Reactor", J. Nucl. Sci. and Technol., 34, 375 (1997).

[5.2-2] Iwai Y., Yamanishi T., Okuno K. et al., "Design Study of Feasible Water Detritiation Systems for Fusion Reactor of ITER Scale", J. Nucl. Sci. and Technol., 33, 981 (1996).

[5.2-3]Kawamura Y., Enoeda M., Okuno K., ISFNT4, April 6-11, 1997, Tokyo, Japan.

[5.2-4] Enoeda M., Kawamura Y., Okuno K., "Tritium Test of Cryogenic Molecular Sieve Bed for He GDS Gas Cleanup By 60 SLM Test Loop" Fusion Technol., 30,885-889 (1996).

5.3 Operation of Tritium Safety System in TPL

The tritium safety system at TPL has been in service since 1988 without an off-normal tritium release. During this fiscal year, the Glove Box Gas Purification System (GPS) was operated for about 8100 hr. The Effluent Tritium Removal System (ERS) processed 1860 m^3 of exhaust

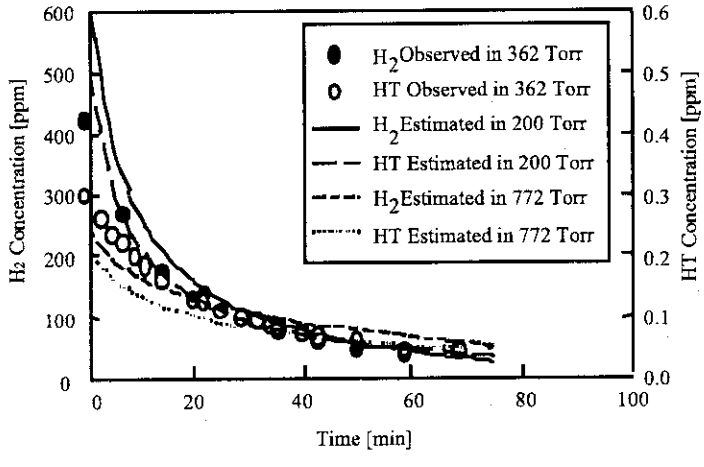

Fig. IV.5.2-5 Pressure effect in isothermal purge regeneration.

gas ($\sim 3.1\times10^{13}$ Bq of tritium). The Air Cleanup System (ACS) was operated for cleaning 63400 m^3 of air in the Glovebox and 57000 m^3 of exhaust gas during the maintenance and reassembly work on the Tritium Transportation Package. The Dryer Regeneration System (DRS) was operated for the recovery of 350 liters of tritiated water from the dryers of the GPS and ACS. Tritium gas in the capsule of the transportation package (20 g) that was shipped from Canada was transferred into the Tritium Storage System (TSS) successfully.

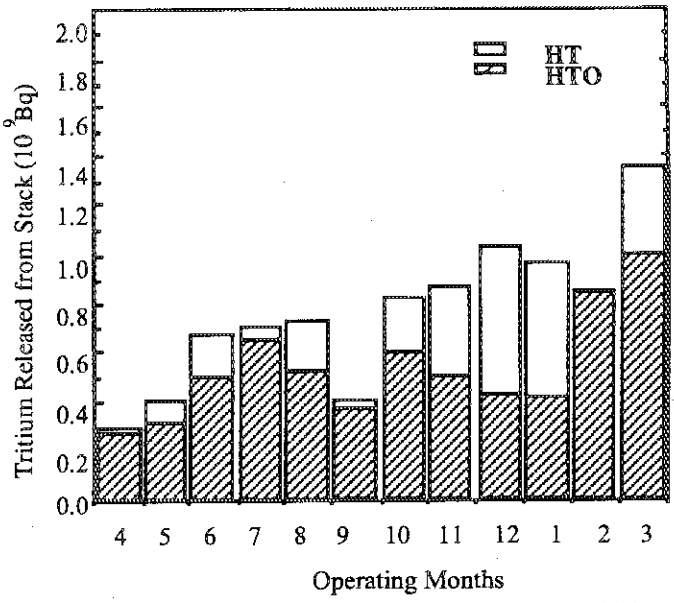

Fig. IV.5.3-1 Monthly release of tritium from TPL in FY 1996.

Fig. IV.5.3-1 shows the monthly environmental tritium release from the stack of TPL for this fiscal year. The total tritium release was less than 9.1×10^9 Bq, which is three orders of magnitude smaller than the target value of the Tokai Establishment of JAERI. Safe tritium handling operation at TPL has thus been demonstrated since 1988.

6. Development of Plasma Facing Components

Plasma facing components (PFCs) of the next fusion devices, such as ITER, are mainly composed of two high heat flux components. One is the first wall and the other is the divertor plate. The main role of these components is to protect in/ex-vessel components, such as blanket modules, vacuum vessel, and superconducting magnets from the high heat flux and neutron flux. Figure IV.6-1 shows the ITER divertor plate. The divertor plate consists of several high heat flux components such as a vertical target,

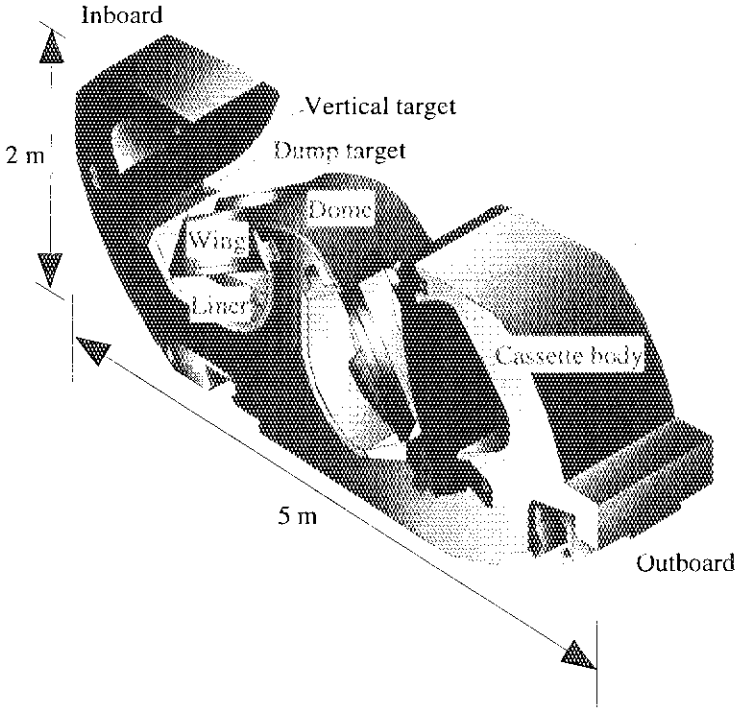

Fig. IV.6-1 ITER divertor plate (Cassette structure)

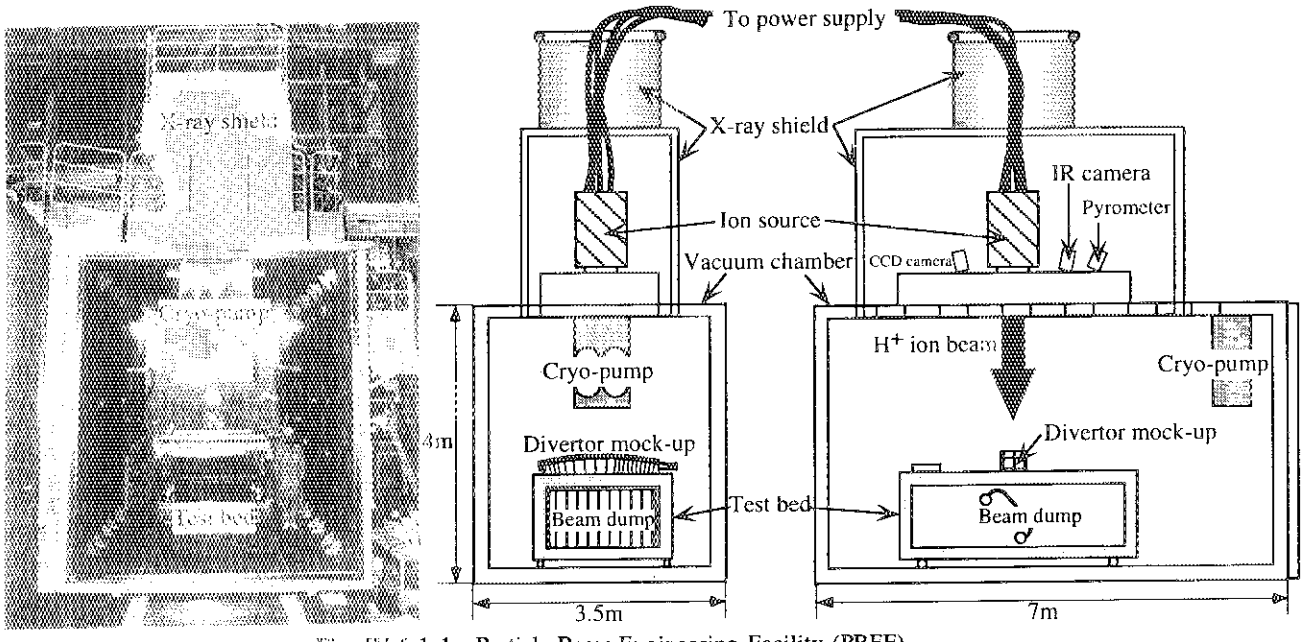

Fig. IV.6.1-1 Particle Beam Engineering Facility (PBEF)

a dump target, a wing, a dome, and a liner. These components are exposed to severe heat flux from the fusion plasma. In the ITER design, the estimated heat flux at the divertor plate is 5 - 20 MW/m^2 in normal operation. In addition, the incident energy to the divertor plate exceeds 1 MJ/m^2 for several milliseconds in plasma disruptions. Surface materials of the divertor plate suffer damage due to melting or sublimation. Therefore, we are developing cooling structures for the divertor plates so these plates can endure the heat flux in normal operation. We are also developing surface materials that have less degradation of performance from plasma disruptions.

6.1 Modification of Particle Beam Engineering Facility

As the ITER engineering design activity progresses, large test facilities are required to perform high heat flux experiments of large-scale/full-scale length divertor mock-ups. The Particle Beam Engineering Facility (PBEF) has been modified to improve its performance to meet ITER EDA requirements. Figure IV.6.1-1 shows an overall view and schematic views of PBEF. Major changes to the facility are summarized as follows;

(1) Large vacuum chamber (7 m (l) × 3.5 m (w) × 4 m (h)) was newly fabricated.

(2) Pulse duration of the ion beam was extended up to 1000 s.

(3) Removable test bed was newly installed.

(4) Vacuum pumping system was updated.

PBEF is now capable of performing high heat flux experiments of full length divertor plates with a cassette structure.

6.2 High Heat Flux Experiments of Divertor Mock-ups

6.2.1 Full Length Divertor Mock-Ups

Full length divertor mock-ups, vertical target mock-ups, and wing mock-ups, have successfully been developed and tested in PBEF. Figure IV.6.2-1 shows a schematic of the vertical target mock-up. The length of the mock-up is 1.3 m, which corresponds to the full-scale length of the vertical target. The armor material was made of a unidirectional carbon-fiber-reinforced carbon composite (UD-CFC) material. The armor was brazed directly onto the pure copper heat sink with Ti-Cu-Ag braze material. The heat sink was also directly brazed onto the stainless steel backplate. The cooling tube is known as a swirl tube; the tube has an Inconel twisted tape insert to promote heat transfer. The cooling tubes of these mock-ups were fabricated from pure copper except for one mock-up. This mock-up had a cooling tube constructed from dispersion-strengthened copper (DSCu). The DSCu cooling tube has the advantage of having an extended fatigue lifetime. The DSCu cooling tube has a duplex structure. It has a pure copper outer skin (1 mm thickness) to achieve good braze performance with the Ti-Cu-Ag braze material. The pure copper skin is clad on the DSCu tube.

In the thermal cycling experiment, a surface heat flux of 15 - 20 MW/m^2 was cyclically loaded on these mock-ups to evaluate the thermal fatigue behavior. At a heat flux of 15 MW/m^2 for 15 s, all mock-ups successfully withstood 1000 thermal cycles without failure. However, at 20 MW/m^2 for 15 s, a mock-up with a pure copper cooling tube developed water leakage from the cooling tube due to thermal fatigue cracking after 400 thermal cycles. On the other hand, the mock-up with the DSCu cooling tube showed no evidence of thermal fatigue damage for the 1000 thermal cycles. The DSCu cooling tube showed better performance than the pure copper cooling tube against the cyclic heat flux. Thus, DSCu cooling tube was found to be the most promising solution for the divertor plate cooling tubes. The optimization of braze technology, such as controlling the clearance between the armor material and the tube, for DSCu material is essential to obtain a reliable divertor structure.

6.2.2 Small-Scale Divertor Mock-Ups with Advanced Materials

From the viewpoint of mechanical strength, more strength is required for the armor material to resist thermal stress. Cracking of the UD-CFC armor material due to high thermal stress has occasionally been observed in high heat flux experiments of divertor mock-ups. To solve this problem, three-dimensional CFC (3D-CFC) material has been developed. The 3D-CFC material has higher strength than the UD-CFC and the 3D-CFC material has a thermal conductivity of 540 W/m/K at 25°C, which corresponds to 90% of that of the UD-CFC. A

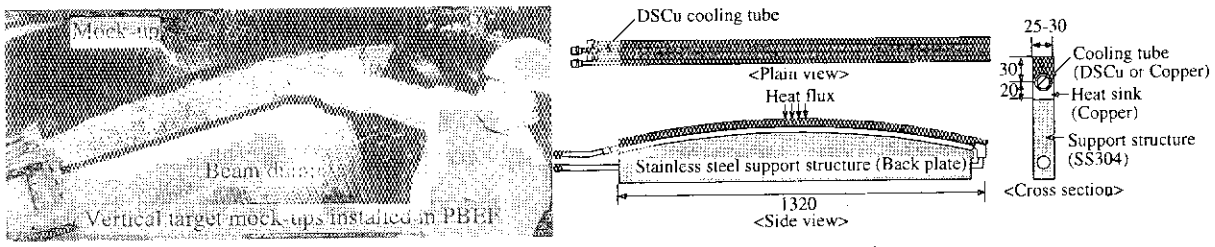

Fig. IV.6.2-1 Full-scale length vertical target mock-up.

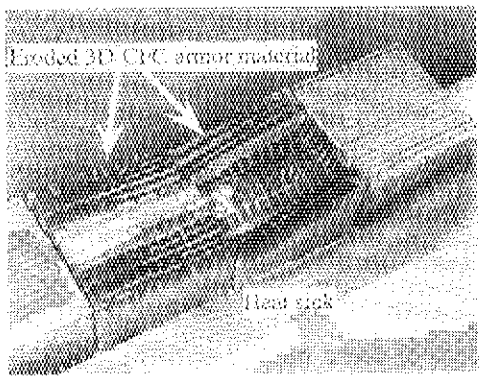

Fig. IV.6.2-2 Schematic of the mock-up

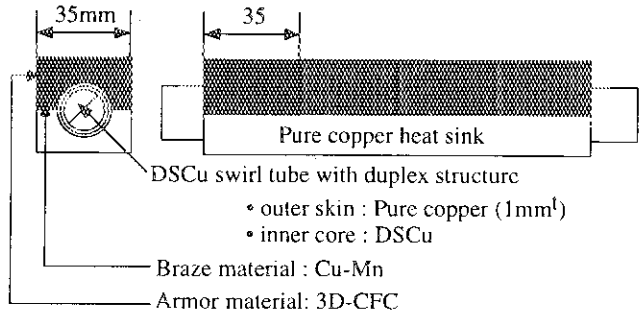

Fig. IV.6.2-3 Eroded 3D-CFC material

divertor mock-up with 3D-CFC armor material is shown in Fig. IV.6.2-2. The 3D-CFC armor material was brazed directly onto the pure copper heat sink with nonsilver braze material (Cu-Mn). In the ITER design, the use of nonsilver material for brazing is required because silver will degrade plasma performance due to the transmutation of silver resulting from neutron irradiation.

A thermal cycling experiment using the mock-up was carried out in PBEF. A maximum heat flux of 20 MW/m^2 for 15 s was cyclically applied to the mock-up. Figure IV.6.2-3 shows the heated surface of the mock-up after 1000 thermal cycles. The 3D-CFC armor material had significant erosion due to the extremely high surface temperature, over 2000°C, which was caused by initial braze defects. Further R&D for the nonsilver braze material is necessary to meet the ITER materials requirement.

6.3 Sputtering and Disruption Erosions of Plasma Facing Materials

A key task is to establish the database for the lifetime estimation of plasma-facing materials (PFMs). From this point of view, sputtering and disruption are the most dominant erosion processes of PFMs. JAERI has extensively carried out sputtering experiments and simulated disruption experiments. This year, the sputtering yield of UD, 2D, and 3D CFCs were measured in the SLEIS facility. Typical test conditions were as follows; a particle flux of 10^{20} ion/m^2/s, an incoming particle energy of 70 eV, and temperatures from 200 to 800°C. The measured sputtering yields were 0.08~0.11 at 200°C, 0.1~0.14 at 450°C, and 0.08~0.11 at 650°C. No major differences were found in the sputtering yield of these CFCs. In the simulated disruption experiments, the disruption erosion of various types of CFCs (UD, 2D, 3D, B_4C, and SiC doped CFCs) and tungsten were also measured with heat loads of 1000~2000 MW/m^2 for 2~4 ms in the JEBIS facility.

7. Reactor Structure Development

The ITER reactor core structure is basically composed of a vacuum vessel, shielding/breeding blankets, divertors, and a cryostat for the superconducting magnet system. These components are massive in both weight and size, and must be able to withstand the

combined severe loads of neutron irradiation, electromagnetic force, and heat. Also, each component must be compatible with full-remote maintenance/exchange. Therefore, the major factors driving development here are the manufacturing technology for large components and remote assembling/disassembling technology. This fiscal year, R&D efforts have focused on the development of a double-walled vacuum vessel, a full-scale manipulator for blanket handling, a divertor transportation system, a bore tool for nondestructive inspection, and radiation hardened components.

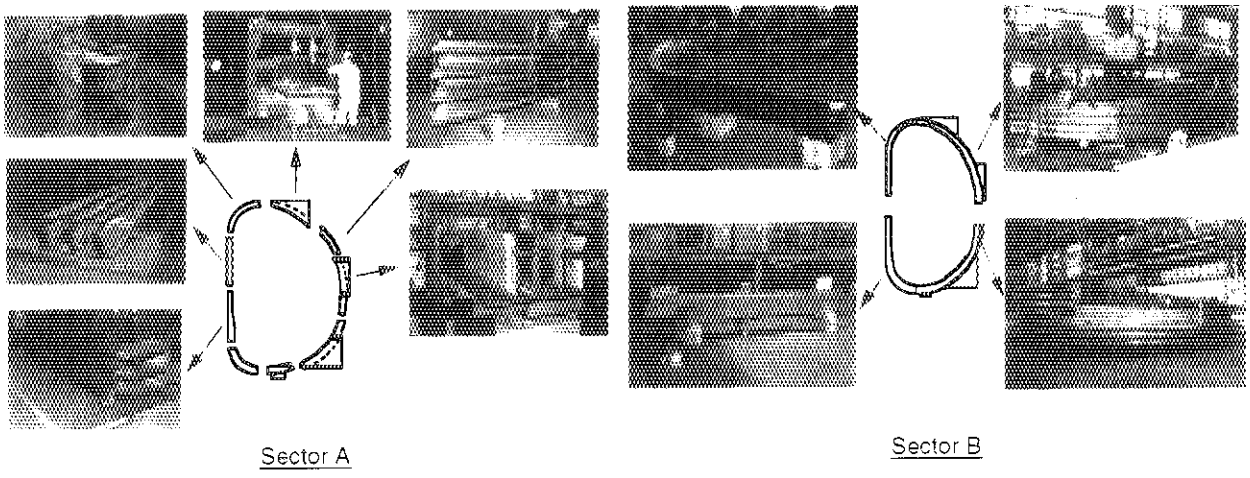

Fig. IV.7.1-1 Current status of the fabrication of half 9° sector A and B.

7.1 Reactor Structure Development

7.1.1 Fabrication of Double-Walled Vacuum Vessel Sector

In the current ITER EDA design, the vacuum vessel is a water-cooled, double-walled structure with a D-shaped cross section. It is approximately 9 m wide and 15 m high and is divided into 20 toroidal sectors. The major functions of the vacuum vessel are : 1) to maintain a high-quality vacuum for plasma, 2) to provide a one-turn electrical resistance over 4 μΩ together with in-vessel components, 3) to support gravity and disruption loads acting on in-vessel components, 4) to provide nuclear shielding to protect the superconducting magnets from irradiation damage, and 4) to provide a first safety barrier for tritium confinement. Its large size, tight manufacturing tolerances required for assembly, and large thermal and mechanical loads necessitate the fabrication and testing of a prototype vacuum vessel to demonstrate the fabrication technologies of the double-walled ITER vacuum vessel prior to ITER construction. For this purpose, the fabrication of a full-scale sector was initiated in 1995 as one of the Large Seven ITER R&D Projects. The full-scale sector model corresponds to an 18 deg. toroidal sector fabricated from 316L+N stainless steel. It is composed of two 9 deg. sectors, Sector-A and B, which are spliced at the port center based on the current ITER design. This year, the fabrication of both half sector-A and B was continued on schedule. As shown in Fig. IV.7.1-1, both sectors were 60% complete at the end of March 1997 and the feasibility of fabrication procedures with a

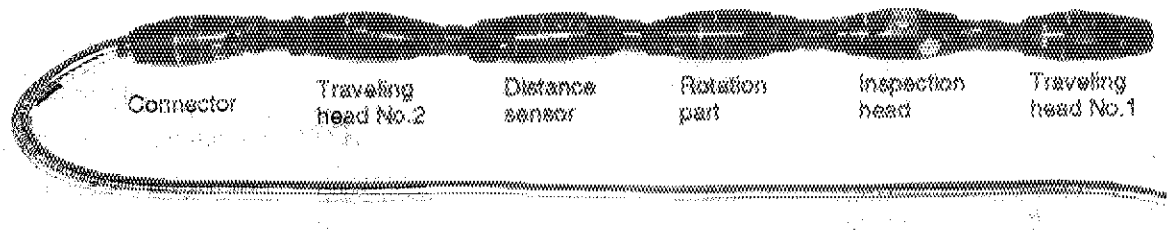

Fig. IV.7.1-2 Bore tool for nondestructive inspection

dimensional accuracy within ±3 mm to nominal values has been demonstrated. The fabrication of this full-scale sector model is continuing to complete a full-poloidal sector in FY 1997.

7.1.2 Welding/Cutting and Nondestructive Inspection Tools

In the design of the fusion experimental reactor, the function of the blanket/first wall module embodies the scheduled maintenance, which includes a complete change of shielding blanket with breeding blanket. In the current modular type blanket design, a branch cooling pipe connected to the cooling manifold has several bends. Therefore, the branch pipe has to be cut and re-welded when a module is replaced. Maintenance bore tools must be flexible to allow movement inside the manifold to reach the branch pipe for cutting, and welding, and inspection. For this purpose, a YAG laser type welding/cutting tool, based on optical fiber transmission, and a nondestructive inspection tool, based on an Electro-Magnetic Acoustic Transducer (EMAT), have been selected. The YAG laser type processing head was successfully fabricated and tested. This year, the fabrication of the inspection tool, shown in Fig. IV.7.1-2 was completed and its applicability to blanket branch pipe inspection has been demonstrated. In particular, this system can move inside a 100-A pipe with a minimum curvature of 400 mm. The inspection head with its telescopic mechanism can be extended into a branch pipe with a diameter of 54 mm for inspection. In addition, centering mechanisms and position sensors are also provided for positioning and restraining the inspection head during use. In parallel with these tool developments, nondestructive inspection experiments using an EMAT sensor have been performed to clarify the detectability using artificial defects on 3 mm-thick branch pipe welded by YAG laser. These tests examined the effects on measurement sensitivity of depth and all possible locations of defects of YAG laser pipe welds.

7.2 Remote Maintenance Development

7.2.1 Blanket Module Maintenance System

Blanket replacement requires advanced technologies that include heavy component handling and remote welding/cutting in restricted space under intense gamma radiation and high temperature conditions. The replacement of shield blankets with breeding blankets is an important milestone in the EDA for the transition from the Basic Performance Phase (BPP) to the Enhanced

Performance Phase (EPP). A rail-mounted vehicle maintenance system was developed for scheduled blanket maintenance. In this system, the rail is extended through the maintenance ports into the vacuum vessel sequentially while being supported by four arms from the respective 90 degree horizontal port to provide stable and reliable operation. This year, the full-scale rail-mounted vehicle system, which includes rail transporter, vehicle manipulator/end-effector, and rail supports, shown in Fig. IV.7.2-1, has been fabricated. Its design is based on the results of performance tests using the prototype models for blanket replacement. By June 1998, this system will be installed and tested to verify the feasibility of blanket module replacement.

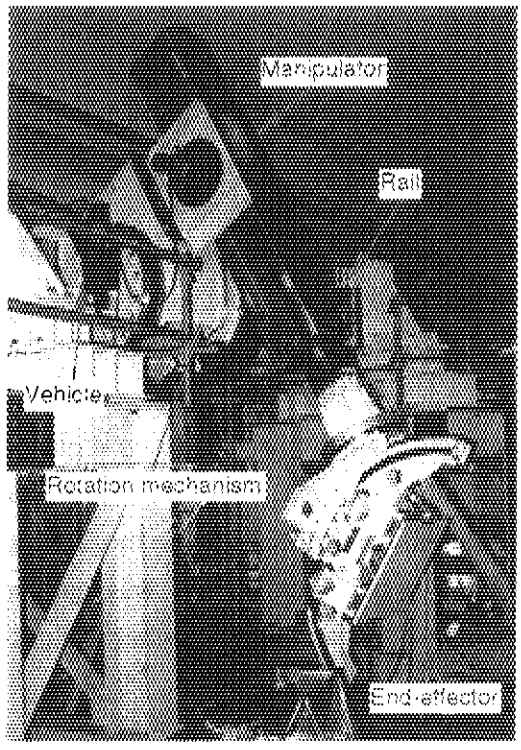

Fig. IV.7.2-1 Full-scale rail mounted-vehicle system

7.2.2 Divertor Cassette Remote Maintenance System

The divertor of ITER is classified into the scheduled maintenance component because of high temperature and particle flux exposure. It is divided into 60 cassettes for the sake of remote maintenance. Each cassette weights about 25 ton. Divertor remote maintenance equipment is

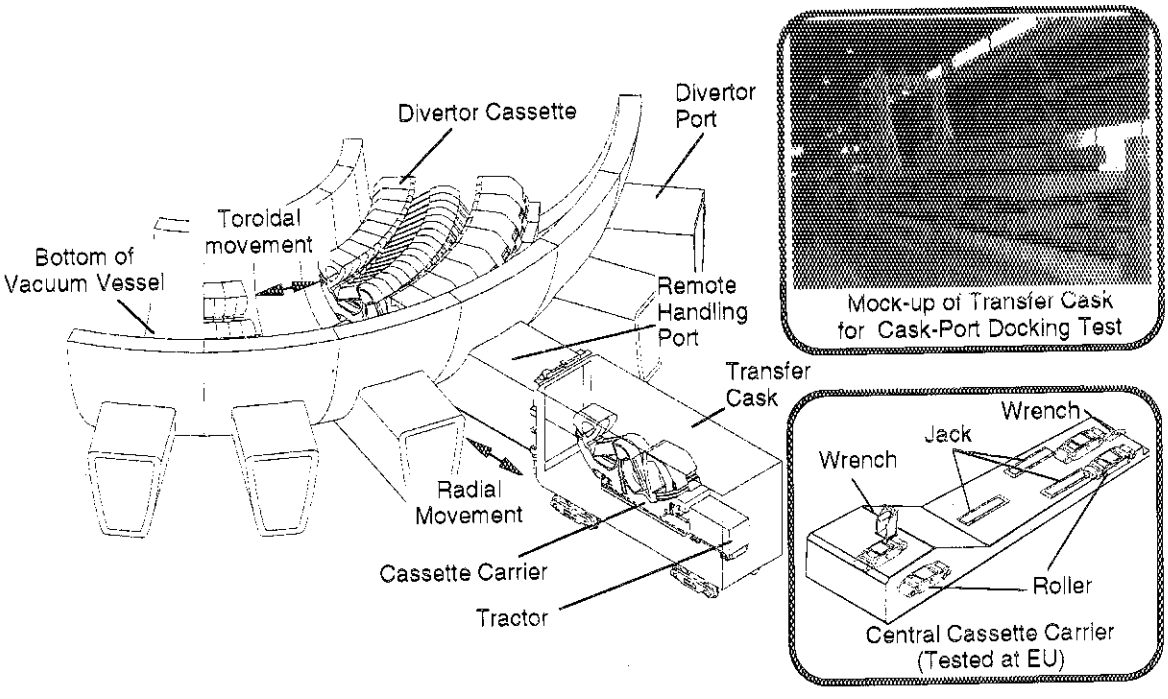

Fig. IV.7.2-2 Concept of remote maintenance for divertor cassette

required to install cassettes with a tolerance of ±2 mm. The equipment must be able to replace all cassettes in a six months period and replace one cassette in an eight weeks period. The skid-type maintenance system, shown in Fig. IV.7.2-2, was developed to meet the above conditions. The system transports a cassette in the toroidal direction using two rails laid on the bottom of the vacuum vessel. It removes the cassette from the vessel through a maintenance dedicated ports. The applicability of this system was confirmed at the beginning of this fiscal year by a partial mock-up test of the toroidal fork system and the cassette locking system. Based on this milestone, fabrication of full-scale prototype skids, which transport the cassette in the toroidal and radial directions, has been proceeded. The prototype skids will be completed by July 1997. An integrated cassette replacement test is planned at the Divertor Test Platform (DTP), which is under fabrication in Europe. For the transfer cask, which transports a removed cassette to the hot cell for refurbishment, the full-scale mock-up shown in Fig. IV.7.2-2 has been fabricated. Using the mock-up, a performance test was conducted on docking with the maintenance port and the transport of the cassette. The suitability of the transfer cask system was confirmed by this test.

7.2.3 Development of Radiation Hardened Components for the ITER Remote Handling System

Gamma irradiation tests on a number of critical components for the ITER remote handling system have been extensively conducted under ITER in-vessel radiation conditions. As a result, radiation-hardened-component development has been progressed. Critical components including an induction motor with polyimide insulation, reduction gears, proximity sensors, and some polymer type electric insulation materials have been demonstrated to be usable for an exposure of more than 10 MGy. This year, a radiation hardened CCD camera has been fabricated by adopting a radiation hardened lens as the objective lens and replacing the camera control unit (CCU) with new electric circuits able to correct the electric degradation of the camera head. The suitability of this camera under a gamma dose rate of 10 and 100 Gy/h in air was demonstrated. The radiation hardness of the radiation hardened CCD camera is estimated to be around 3 kGy. This value is three times better than that of a standard CCD camera.

V. INTERNATIONAL THERMONUCLEAR EXPERIMENTAL REACTOR (ITER)

1. Progress of ITER Engineering Design Activities (EDA)

The Detailed Design Report (DDR) was issued by the Director in November 1996, as the basis for the further work towards the Final Design Report (FDR). After the formal review by the Technical Advisory Committee (TAC), the DDR was officially accepted by the ITER Council at its 11th Meeting held in December 1996. The DDR is composed of various technical documents on the detailed design of plasma parameters, tokamak components, plant system and tokamak building. The major results of safety analyses described in the Non-site Specific Safety Report (NSSR) -1 was also included in the DDR. The technical review of the DDR is being conducted by the four Parties.

The Japanese Home Team contributes to the design progress in the various fields through the conduction of design tasks in close collaboration with the Joint Central Team (JCT). The JCT member built up to 155 including 45 Japanese members as of March 1997. The FDR will be prepared by the end of 1997 for presentation at the ITER Council.

The cut-away view and the machine parameters of the ITER Tokamak are shown in Fig. V.1-1 and Table V.1-1. The main features of the ITER Tokamak system (DDR) are also presented in Table V.1-2.

The major changes of the ITER design from the IDR are as follows;

1) The design of the Tokamak building and Tokamak pit have been reconfigured to give more efficient use of the space around and below the Tokamak.
2) A seismic design option which uses seismic isolator s for the Tokamak pit has been developed to accommodate a possible earthquake with a ground acceleration significantly greater than the site design assumption of 0.2g.
3) The shape of the cryostat vessel has been modified from the dome-type to the flat-type in order to improve use of space.
4) The design of vacuum vessel supporting structure has been altered to transmit vertical and horizontal loads of the vessel to the TF coils, for gravity, seismic events and vertical displacement events (VDEs)
5) Remote assembly and handling procedures and design of related equipments have been developed and optimized by considering maximum possible use of hands-on maintenance consistent with safety
6) Several changes have been made in the design of primary heat transfer systems in terms of number of cooling loops, routing of pipes, and reconfigurations to improve safety

The activities and current status of the ITER Technology R&D are summarized in Table V.1-3. Japan takes responsibilities in the construction of a CS model coil test facility, development of a outer module of CS model coil , manufacturing and testing of a full-scale 1/20 sector of the double-walled vacuum vessel, and the demonstration of a full-scale vehicle-type remote maintenance system for blanket module replacement. The details of the R&D progress in FY 1996 are described in Chapter IV.

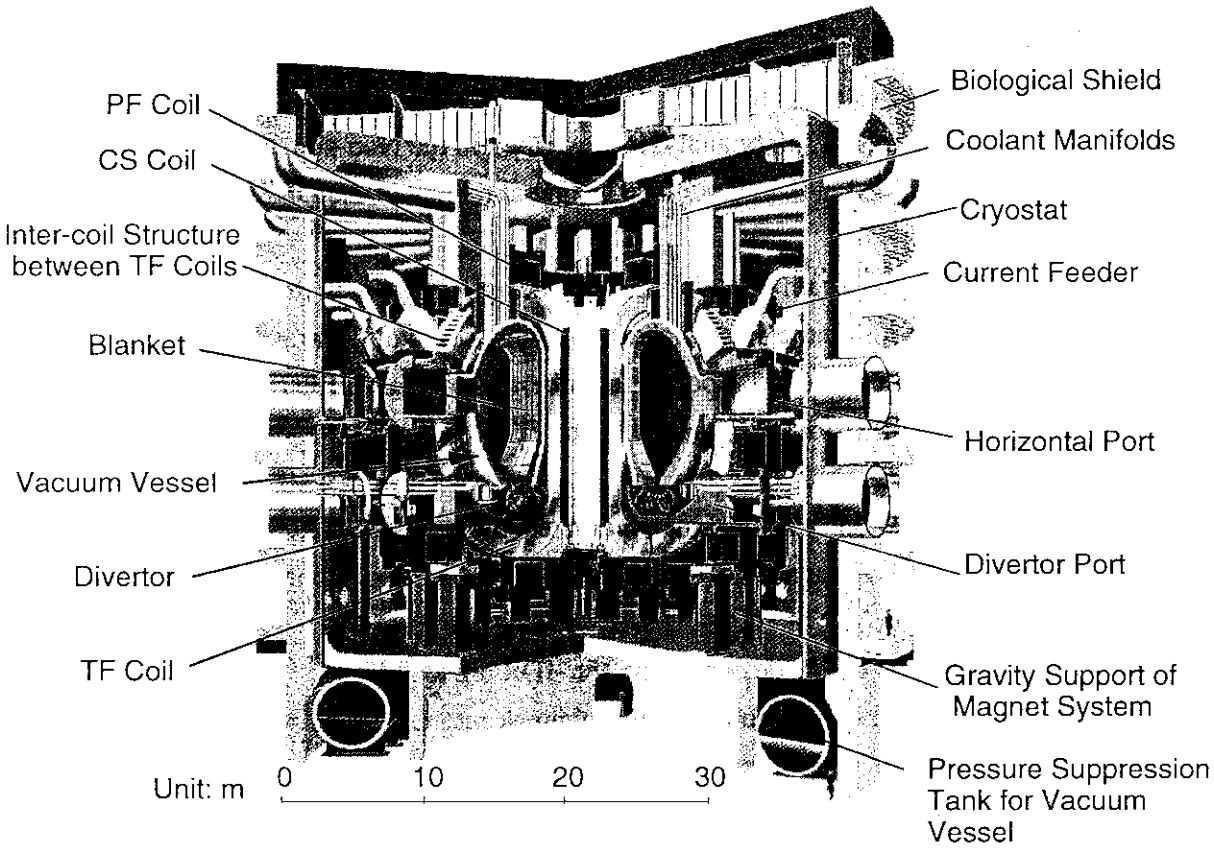

Fig. V.1-1 The cut-away view of ITER Tokamak Core (DDR)

Table V.1-1 Major Machine Parameters of ITER (DDR)

Major Radius	**8.14 m**
Minor Radius	**2.8 m**
Plasma Current	**21 MA**
Toroidal Magnetic Field at major radius at superconductor	**5.7 T**
Fusion Power	**1.5 GW**
Burn Time (Inductive)	**1000 s**
Neutron Wall Loading (Nominal)	**1.0 MW/m^2**
Total Neutron Fluence (BPP)	**0.3 MWa/m^2**
Plasma Heating Power	**100 MW**

Table V.1-2 Main features of the ITER Tokamak system (DDR)

Component	Features
Toroidal field coils (20 coils) - Superconductor - Structure	 Nb3Sn in circular Incoloy jacket in grooved radial plate Pancake wound , steel encased "wind, react and transfer" technology
Poloidal field coils (CS, PF2-PF8) - Superconductor - Structure	 CS, PF2&7 : Nb3Sn, PF3 - PF6, PF8 : NbTi Square Incoloy jacket, layer wound for CS, pancake wound for all others CS, PF 2&7 : "wind, react and transfer" technology
Vacuum Vessel - Structure - Material	 Double-wall welded ribbed shell structure Stainless Steel 316LN (0.06 ≤ N ≤ 0.08 wt%)
First Wall/Blanket (Basic Performance Phase) - Structure - Material	 Armor-faced modules on toroidal backplate Be armor Copper alloy heat sink Stainless Steel 316LN (0.06 ≤ N ≤0.08 wt%)
Divertor - Configuration - Structure	 Single-null 60 solid replaceable cassettes W alloy and C plasma facing components Copper alloy heat sink Stainless Steel 316LN (0.06 ≤ N ≤0.08 wt%)
Cryostat - Structure - Material	 Double-wall welded ribbed cylinder with flat end 36 m diameter, 30 m height Stainless Steel 304L
Heat Transfer System (water-cooled) - Heat released in the Tokamak during nominal pulsed operation	 2200 MW at ~4 MPa water pressure, 150°C
Cryoplant - Nominal average He refrigeration/liquefaction rate for magnets and Divertor cryopump (4.5K) - Nominal cooling capacity at 80 K	 100 kW/ 0.35 kg/s 225 kW
Additional Heating and Current Drive - Total injected power - Candidate Additional Heating and Current Drive (H&CD) systems	 100 MW Electron Cyclotron, Ion Cyclotron, Lower Hybrid, Neutral Beam from 1 MeV negative ions
Electrical Power Supply - Pulsed power supply from grid Total active/reactive power demand - Steady-state Power Supply from grid Total active/reactive power demand	 650 MW / 500 Mvar 230 MW / 160 Mvar

Table V.1-3 Activities and Current Status of Technology R&D

Field/Subjects	Activity and Current Status
Superconducting Coil	- All of 13.6 ton Nb3Sn strand production and all of 19 cables allocated to JA HT in the CS coil project have been completed - The winding of 4 layers within 8 layers for the JA CS model coil was completed. The heat treatment technique was established to SAGBO crack. - The developed turn insulation technique was confirmed by using 100 m length dummy conductor.
Test Facility for the Model Coil	- All test facilities were completed. - Supercritical helium circulation system will be reinforced according to the new requirement for the coil operation
Vacuum Vessel	- Fabrication of a full-scale 1/20 sector is in progress. Key fabrication technologies have been established. Feasibility to ITER construction has been demonstrated within the acceptable dimensional accuracy
Remote Handling System for Blanket	- The vehicle-type system was developed including a manipulator, transporter and an end-effector. The performance was demonstrated with load of 1 ton. - Fabrication of major components of full-scaled system for load of 5 tons, such as a full-scaled manipulator, rail transporter and rail deployment system was completed. Assembly of the components is continuing to demonstrate remote maintenance operation of a full-scale blanket module by 1998.
Remote Handling System for Divertor	- The design of full-scale cassette movers and bi-directional forks have been completed based on the results of partial mockup tests. - Fabrication of full-scale cassette movers and bi-directional forks is continuing.
Development of Remote Welding and Cutting Tools	- Development of welding/cutting tools of in-pipe access: Development of an in-pipe transporter and tools with YAG laser, Demonstration of welding, cutting and rewelding of pipes of 50 mm and 100 mm. - Development and demonstration of non-destructive inspection of welds and leak technology.
Development of Radiation-Resistant Components	- Development of motors, bearings, detectors, insulation wires, optical components and standard components that withstand radiation fluence of 10 - 100 MGy.
Components for Remote Maintenance	- Manufacturing of a full-scale periscope of 15 m in length with radiation-hard lens, optical performance was demonstrated at 250°C
Shield Blanket	- Optimization of HIP condition for joining Copper alloy and stainless steel - Obtain data on the mechanical properties of HIP joints - Manufacturing of a 1/2 scale blanket module integrated with first wall (0.5m wide, 0.8 m in height and 0.4 m thickness) with the dimensional accuracy of ± 1 mm to nominal values
Divertor	- Development of high heat flux components by combination of carbon plasma facing component and copper cooling tube - Development of high heat flux components by combination of tungsten plasma facing component and copper cooling tube
Neutron Beam Injector	- Development of MeV ion source test facility (1 MeV, 1A) - Development of multi-ampere negative ion source (13.5 A/D^- ion) - Development of high energy negative ion accelerator (805 keV, 0.15 A)
Electron Cyclotron Heating Facility	- Development of Gyrotron (170 GHz, 500 kW, 0.6 sec)
Diagnostic Equipment	- Neutron irradiation testing of ceramics, optical fibers, materials for mirror and window, and magnetic probes
Development of Tritium System	- Development of fuel purification system for ITER - Development of high performance air detritiation system using separation membrane - Development of tritium transportation container (25g)

VI. FUSION REACTOR DESIGN AND SAFETY RELATED RESEARCH

In FY 1996, the DREAM (drastically easy maintenance tokamak reactor) concept of a fusion power reactor progressed regarding the gross reactor configuration, the reactor internal structures, the plant design, and the building. In the area of safety research, safety evaluation code development, basic experiments of LOVA (loss of vacuum event) and ICE (ingress of coolant event), and the study of tokamak dust removal methods were also carried out.

1. Fusion Reactor Design

The DREAM fusion power reactor adopts silicon carbide (SiC/SiC) composites as the structural material for reactor internal structures such as the blanket and divertor. This enables early initiation of maintenance work, within several days after reactor shutdown, and therefore contributes to the enhancement of reactor availability. In addition, if the nitrogen impurity content is reduced below 1/300 of the current level, the SiC/SiC composites can be disposed as low-level radwaste. [1-1]

An overview of DREAM is shown in Fig. VI.1-1. The major design parameters are summarized in Table VI.1-1. The torus structure consisting of the blanket ring and movable shield is divided into 16 sectors in the toroidal direction. Each sector is removed horizontally in a single straight motion through a space between two toroidal coil structures. A compact blanket module was selected to enhance its fabricability. A neutronics calculation using the ANISN code was performed for this system. This calculation confirmed that the tritium breeding ratio is over 1.1. The plant system was reviewed and

Table VI.1-1 Major parameters of DREAM

major and minor radii	16 m/2 m
elongation	1.3
fusion power	5.5 GW
operation mode	steady state
plasma current	9.2 MA
bootstrap current ratio	0.87
current driver	NNBI (50 MW)
maximum toroidal field	20 T
number of TFCs	16
safety and Troyon factors	3/3
maximum ripple	1%
average neutron wall load	3 MW/m^2
peak heat flux	
divertor	5 MW/m^2
first wall	0.5 MW/m^2
breeder/neutron multiplier	Li_2O/Be
net TBR	1.1
structural material	SiC/SiC
maximum temperature	1100°C
coolant	helium gas
pressure	10 MPa
inlet/outlet temperature	600/900°C
power generation system	gas turbine
plant efficiency (net)	45%

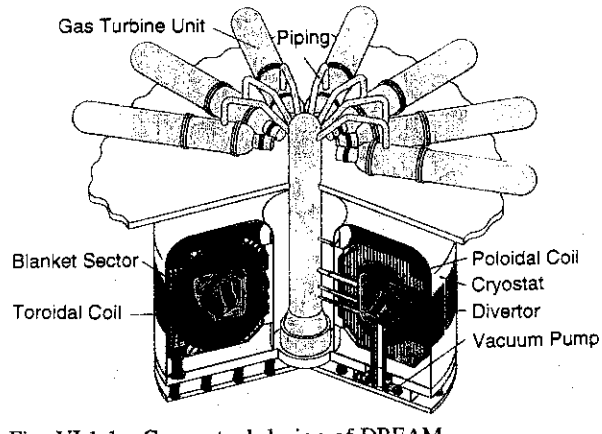

Fig. VI.1-1 Conceptual design of DREAM

redesigned. A gross thermal efficiency of 45% is attained by using a Brayton cycle helium gas turbine generator. The building in which the DREAM system will be installed was conceptualized. [1-2]

References

[1-1] Seki Y., Aoki I., Yamano N. et al., "Preliminary Evaluation of Radwaste in Fusion Power Reactors," Fusion Technol. 30(3) p.1624-1629 (1996).

[1-2] Kawaguchi I., Adachi J., Yamazaki S. et al., "Engineering Design of DREAM Components," Proceedings of the 19th SOFT, Lisbon (1996).

2. Fusion Safety

2.1 Study of In-Vessel Abnormal Events

The Fusion Reactor System Laboratory is focusing on studies of in-vessel abnormal events that may release tritium and radioactive materials to the environment. Experiments using a small-scale LOVA and ICE experimental apparatus, and the development of safety evaluation codes, TRAC-BF1 and SAFALY, have continued. In LOVA experiments, the relation between the exchange flow rate and breach parameters was measured. The ICE apparatus was completed and the pressure transient was measured by its first experiment. Figure VI.2.1-1 shows the ICE experimental apparatus.[2-1] This apparatus has a cylindrical stainless steel vacuum vessel with a diameter of 900 mm and a height of 600 mm. Required improvement of the TRAC-BF1 code was carried out for fusion application and used for sensitivity analysis on scale effects of ICE events. Figure VI.2.1-2 shows the calculation model of the ICE experiment. The ICE experimental apparatus is modeled by connecting BREAK, PIPE, VALVE, and VESSEL component models included in the TRAC-BF1 code. The comprehensive safety analysis code, SAFALY, had been developed to analyze events caused by a plasma transient. It was updated to include the plasma physical model in collaboration with the ITER Joint Central Team. In addition, the heat transfer

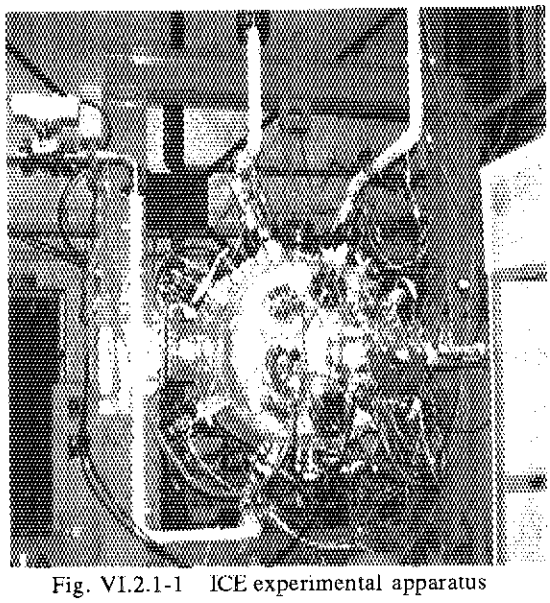

Fig. VI.2.1-1 ICE experimental apparatus

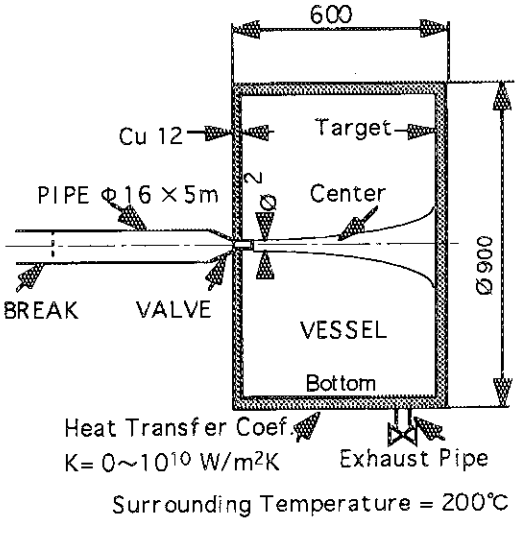

Fig. VI.2.1-2 Calculation model of ICE experiment

model of the internal structures inside the vessel was also improved. This code will be used to perform the ITER safety analysis.

2.2 Study of Tokamak Dust Removal Methods

A conceptual design of a dust removal system operating under ITER conditions was performed. The electrostatic dust transportation method was concluded to be the best to remove dust from the bottom of the vacuum vessel. Figure VI.2.2-1 shows a concept of the electrostatic conveyer belt dust removal system as applied to ITER.

Figure VI.2.2-2 shows the experimental apparatus for an electric curtain dust transportation test.[2-2] Laboratory-principle tests of the dust removal system were performed using aluminum and carbon particles simulating dust. Dust is polarized and floated by AC voltage imposed on the electrode. The dust is transported through an electric curtain formed by the an imposed array of AC excited electrodes. In examining dust transportation through an electric curtain, aluminum particles were found to be transportable in any direction with almost the same efficiency. Major progress in dust removal system study is as follows:

(1) The mobility of carbon dust in a vacuum by the electrostatic dust removal system was confirmed.

(2) Dust measuring methods under ITER conditions were investigated.

(3) The configuration of the present ITER design was examined and the possible application of the dust removal system was evaluated.

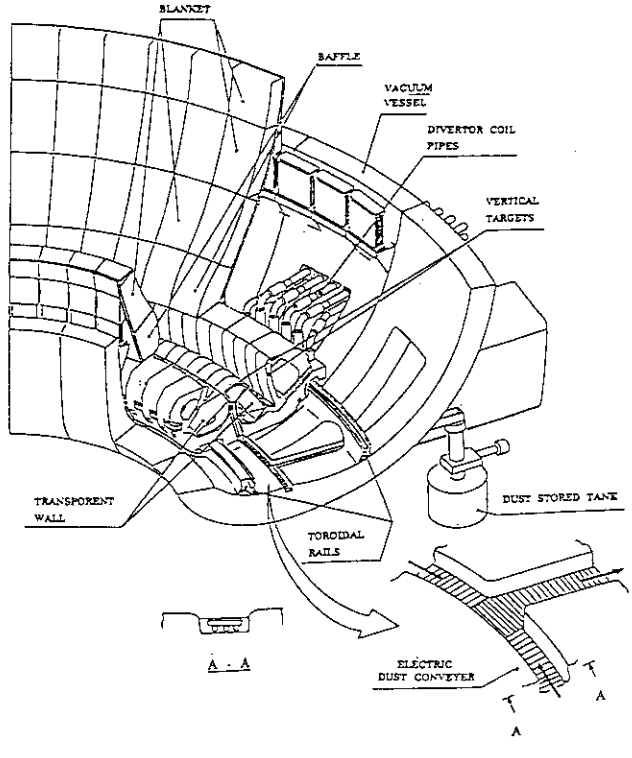

Fig. VI.2.2-1 Concept of conveyer belt dust removal system

References

[2-1] Takase K., Kunugi T., Seki Y. et al., "A Fundamental Study on a Water Jet Injected into a Vacuum Vessel," Fusion Technol. 30 p.1453-1458 (1996).

[2-2] Aoki I., Seki Y., Ueda S. et al., "In-Vessel Dust Removal System using Static Electricity," Proceedings of the 19th SOFT, Lisbon (1996).

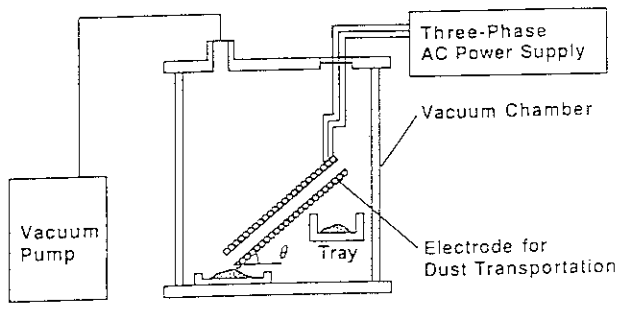

Fig. VI.2.2-2 Experimental apparatus for the electric curtain dust transportation test

VII. FUSION INTERNATIONAL COOPERATIONS

In the area of fusion research and development, Japan is recognized as one of the leading nations of the world together with Europe, USA and Russian Federation. Fusion reactor development is a long-term project which requires large resources both in man-power and development fund. It covers also broad area of science and technology. International cooperation has been recognized quite efficient in reducing risk as well as in avoiding unnecessary duplication, and in enhancing world's fusion program. JAERI is carrying out various international cooperation in fusion such as the ITER Engineering Design Activity (EDA) under IAEA, the three large tokamak cooperation under IEA, and broad activities under the US-Japan cooperation

International cooperations in terms of fusion research and development are implemented through multilateral cooperations under IEA in Organization for Economics Cooperation and Development (OECD) and IAEA and bilateral cooperations such as Japan-US cooperation. The multilateral and bilateral cooperations carried out in JAERI are summarized in Table VII. 1-1 and Table VII.2-1.

1. Multilateral Cooperations

1.1 IAEA

Under the coodination of International Fusion Research Council, International Atomic Energy Agency (IAEA) holds various conferences such as the International Fusion Energy Conference (so called IAEA international conference) and supports the ITER program. The IAEA international conference, which is held every other year, is one of the largest conferences in the area of fusion research. The 17th IAEA international conference is planned to take place in Yokohama, October 1998. IAEA also undertakes the EDA in the ITER program.

1.2 IEA Cooperation

Fusion Power Coordinating Committee (FPCC), which is organized under IEA, coordinates the research and development programs for member nations, selects the important areas and reviews the cooperation activities. Five cooperations are presently carried out in JAERI as shown in Table 1.

The IEA three large tokamak cooperation pursues personal exchange, holding expert meetings and information exchange among JT-60 in Japan, JET in EU and TFTR in USA. Currently six task proposals, namely "High-β_p plasma Research", "Disruption Studies", "Divertor Plate Technology", "Neutral Beam Current Drive Research", "Remote Participation in Experiments" and "Impurity Content of Radiative Discharges", have been successfully continued. Under these tasks, exchanges of personnel, data and discussions have been intensively carried out. For example, under "Remote Participation in Experiments" the effectiveness of remote participation was successfully demonstrated. By using Data Link System and a video conference

system, participants from both JAERI and PPPL jointly analyzed and discussed the JT-60U high performance reversed shear experiments data and achieved a high fusion performance (also described in 1.7.2).

In the Implementing Agreement on Plasma Wall Interaction in TEXTOR, a plasma-wall interaction research cooperation is carried out utilizing the facility of the TEXTOR tokamak built in Forschungszentrum Jülich, Germany.

The agreement for cooperation on fusion materials research is to investigate the irradiation damages by applying neutrons from a fission reactor to fusion materials. In order to develop fusion materials after a prototype reactor, a conceptual design of a 14 MeV intense neutron source (Fusion Materials and Irradiation Test Facility : IFMIF) is carried out by four parties of Japan, USA, EU and Russia.

The agreement for cooperation on environments, safety and economics is to carry out their evaluation researches which are ongoing with particular emphasis upon environments and safety.

The agreement for cooperation on fusion reactor engineering is to carry out research cooperation and information exchange in terms of neutron engineering, tritium breeding blanket, plasma-type volume production neutron source and so on.

Multilateral Cooperation	
IAEA	• ITER (International Thermonuclear Experimental Reactor) /EDA Project [Japan, USA, EC, Russia] • Information Exhange on Large Tokamaks • Information Exchange on Atomic and Molecular Data • International Conferences
IEA	• Three Large Tokamak Cooperation [JT-60(J), TFTR(US), JET(EU)] • Plasma Wall Surface Interaction Program [Japan, USA, EU. Canada] • Programme of Research and Development on Radiation Damage in Fusion Reactor Materials [Japan, EU, Canada, Switzerland, USA] • Joint Program for Environmental, Safety and Economic Performance of Nuclear Fusion Technology [Japan, USA, EU, Canada] • Cooperative Program on Nuclear Technology of Fusion Reactors [Japan, USA, EU, Canada]

Table VII.1-1. Multilateral cooperations in fusion international cooperations at JAERI

2. Bilateral Cooperation

On Japan-US cooperation, Coordinating Committee of Fusion Energy (CCFE) is formed to synthetically coordinate the cooperation activities under Agreement between the government of Japan and the government of the United States on cooperation in Research and Development in Energy and Related Fields. The Japan-US cooperation consists of four frameworks of exchange program, joint program, joint project and plasma physics. In particular, broad joint projects based on agreements and annexes have produced fruit results, playing a leading role in world's fusion research and development.

On Japan-EU cooperation, Agreement for Cooperation between the government of Japan and the European Atomic Energy Community in the field of controlled thermonuclear fusion was concluded February 1988. Based on this agreement, a joint experiment is carried out in which lower hybrid (LH) wave launcher module built at JAERI are installed into the LH test facility in Cadarache Institute.

With Canada, JAERI carries out expert meeting and information exchange on tritium technology and tokamak research through Atomic Energy Canada Ltd. (AECL). With Australia, information exchange and expert exchange are carried out by holding workshops mainly in the area of diagnostics, experiment and theory for toroidal plasmas. With Russia, information exchange and expert meeting on plasma and fusion are planned under Agreement between the government of Japan and the government of Russia in Research and Development in Science and Technology.

Bilateral Cooperation	
Japan - US	• Doublet III Project • HFIR Joint Irradiation Experiment Program • Fusion Fuel Processing Technology Development Program • Cooperation in Fusion Research and Development • Data Link Program • Joint Experiment Program on Negative Ions
Japan - EU	• Cooperative Activities Concerning a Lower Hybrid Antenna Module
Japan -Canada	• Cooperation in the Field of Controlled Nuclear Fusion • Cooperation on the Chronic Tritium Release Experiment
Japan - Australia	• Cooperation on Diagnostics, Experiments and Theory
Japan - Russia	• Cooperation in Fusion Research and Development

Table VII.2-1. Bilateral Cooperations in fusion international cooperations at JAERI

3. Cooperative Program on DIII-D (Doublet III) Experiment

The primary goal of the DIII-D tokamak research program is to provide data for development of a conceptual physics for a commercially attractive fusion power plant. Specific DIII-D objectives include the steady-state sustainment of plasma current as well as demonstrating techniques for microwave heating, divertor heat removal, ash exhaust and tokamak plasma control. The DIII-D program is addressing these objectives in an integration of high beta and good confinement.

3.1 Highlights of Research Results

3.1.1 Divertor and Boundary Research

The major goals of the Divertor and Boundary Physics studies are the control of impurities, efficient heat removal and understanding a role of the edge plasma that plays in the global energy confinement of the plasma. Partially detached plasmas, which is produced by deuterium puffing, make a long (50 cm), radiating divertor leg with only a 2:1 variation of the emission along the leg, exceeding ITER requirement as shown in Fig.VII.3-1. The aim of the ITER divertor solution is to reduce the peak heat flux at the divertor plate by spreading the heat flux along the divertor channel, but ITER only requires a 6:1 uniform spreading. Preliminary analysis indicates that the length of the radiating zone in Fig.VII.3-1 exceeds substantially the predictions of the standard model, requiring investigation of the role of non-coronal and convective effects. The core plasma confinement in the case of Fig.VII.3-1 was progressively reduced to the L-mode level by the high neutral pressures (reaching 1 mTorr) near the core plasma that resulted from the strong gas flow through to the divertor pump and the inadequate divertor baffling in DIII-D. The full installation of the double null, triangular plasma, Radiative Divertor in DIII-D will provide the baffling need to allow simultaneous high performance core plasmas with low impurity and neutral

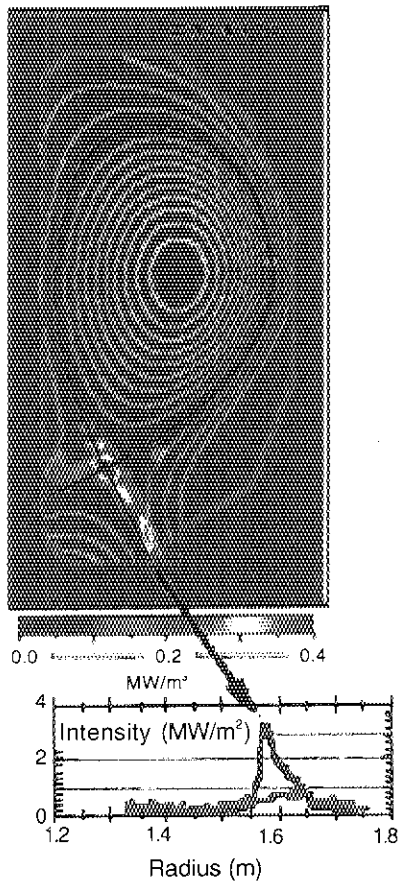

Fig.VII.3-1 Long radiation divertor leg demonstrating effective radiation exceeding ITER requirements

pressure with high plasma and neutral densities in the detached divertor.

3.1.2 Advanced Tokamak Research

The goal of the Advanced Tokamak program is to optimize both energy confinement time and beta in a non inductively driven discharge relevant to steady state operation. To discuss the normalization constants which permit comparisons with certain standard condition to be made, we use H-factor and β_N. Here, H-factor is a ratio of the energy confinement time with the baseline set by ITER-89P L-mode scaling and $\beta_N=\beta_T/(I/aB)$ (%, MA, m, T). The approach of DIII-D to the advanced tokamak is to increase the stability limit of these high confinement regimes without degrading the confinement. The feasibility of an advanced physics approach to tokamak reactors was demonstrated by discharges with negative central magnetic shear (NCS).

NCS discharges are characterized by a non-monotonic safety factor (q) profile and the existence of internal transport barriers supporting steep gradients in T i , n e ,V f . L–mode and H–mode NCS discharges with inside limiter, single-null divertor (SND), and double-null divertor (DND) configurations have been produced in DIII–D. A way of combining the favorable feature of enhanced fusion yield in an NCS L–mode with the higher β limit of NCS H–mode was successfully implemented in DIII–D. This is estimated by the ideal MHD calculation (Fig. VII.3-2). An NCS L–mode is produced initially and its β and core pressure are allowed to increase with further heating up to the point when the β limit is approached. Plasma shape control is then deployed to induce a transition to H–mode. The density profile flattens quickly resulting in a broadened pressure profile which in turn raises the β limit. This technique allows a steeper core pressure profile than standard H–mode and a higher β than NCS L–mode. Since the fusion production rate depends on optimizing the pressure profile, this path led to the highest neutron rate on DIII–D to date (Q_{DT}^{eq} =0.32).

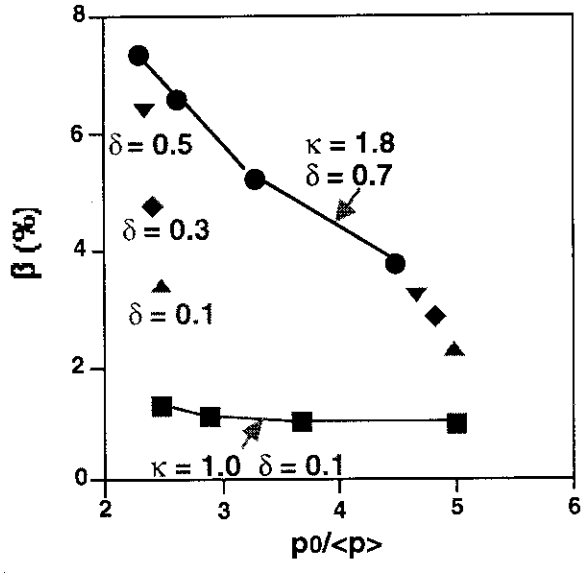

Fig.VII.3-2 Maximum b stable to the ideal n=1 kink mode vs. pressure peaking factor.Results are shown for a circular cross section (k=1) and an elongatied cross section (k=1.8) with various triangularity (d=0.1-0.7).

3.1.3 Tokamak Physics Studies

The Tokamak Physics Program in DIII-D contributes to the fundamental understanding of key physics issues in toroidal confinement system. Understanding what determines the input power threshold for transport barrier formation is important for projection to future tokamaks. Theory has suggested that the threshold is given by the balance between the microinstability growth rate and the ExB shear damping rate, and the internal transport barrier should first form in the plasma core where the magnetic shear stabilization has the biggest impact. This is corroborated by DIII-D measurements which show the core transport barrier first formed in the interior and expanded with increased beam power and contracted with decreased power. The threshold power varies over a wide range in present experiments. DIII–D requires only a few MW to produce the transition to high confinement with internal transport barriers while other tokamaks such as TFTR and JT-60U typically require much higher power. This could perhaps be explained by two possible reasons. The first may be related to the different mechanisms which drive the ExB shear flow. The ExB shear damping rate in toroidal geometry is given by

$$\omega_{ExB} = (B_\theta R/B)\, d(Er/RB_\theta)/dr, \quad 1/(RB_\theta)d/dr = d/d\psi,$$

and assuming neoclassical ion poloidal velocity,

$$Er/(RB_\theta) \cong V_\phi/R + (1\text{-}K1)/(Z_i e)\, dT_i/d\psi \quad + T_i/(Z_i e n_i)\, dn_i/d\psi.$$

Since K1 ~ 1 in the plasma core, only toroidal flow and density gradient contribute significantly to producing the ExB flow. DIII–D with tangential NBI can induce turbulence suppression effectively with toroidal flow shear from the toroidal momentum input. This is absent for balanced beam injection in which case the flow is purely diamagnetic and the flow drive depends largely on the density gradient. High beam power may thus be required to provide a steep density gradient to drive the flow. The second speculation is that the turbulence growth rate and thus the threshold depends strongly on shape in addition to magnetic shear. This is supported by the H–mode power threshold observed in the DIII–D elongation-ramp experiment and is also consistent with a recent experiment to study bean and peapod configurations on DIII–D. Preliminary results from this experiment indicate that these configurations produce transitions to higher confinement modes readily at low input power. The power threshold to enter an enhanced confinement regime is clearly a subject which needs further study if these enhanced confinement modes are to be applied to next step experiments.

4. Collaborative Activities Concerning Fusion Technologies

4.1 Collaborative Activities on Technology for Fusion-fuel Processing between US-DOE and JAERI

Research and development of technology for Fusion Safety has been carried out at the Tritium Systems Test Assembly (LANL) and the Tritium Process Laboratory (JAERI) since 1995. Current activities are related to studies on tritium behavior in confinements, decommissioning of tritium contaminated components, accountancy and analysis of tritium, and the tritium plasma experiment for prediction of tritium inventory in plasma facing components. Last year an experiment with intentional tritium release inside the main cell of TSTA was carried out for investigation of the behavior of tritium in a room. Tritium (T_2 , 1 Ci) was released into the main cell, and data related to phenomena being considered for the safety evaluation such as diffusion and mixing in the room atmosphere (Fig. VII.4.1-1), the conversion rate to water (HTO), the removal of residual tritium by operation of the ventilation system, the absorption on the several wall surface materials existing in the main cell, etc., were obtained. Also a simulation by a code developed for this experiment was compared with the experimental results. This code will be validated.

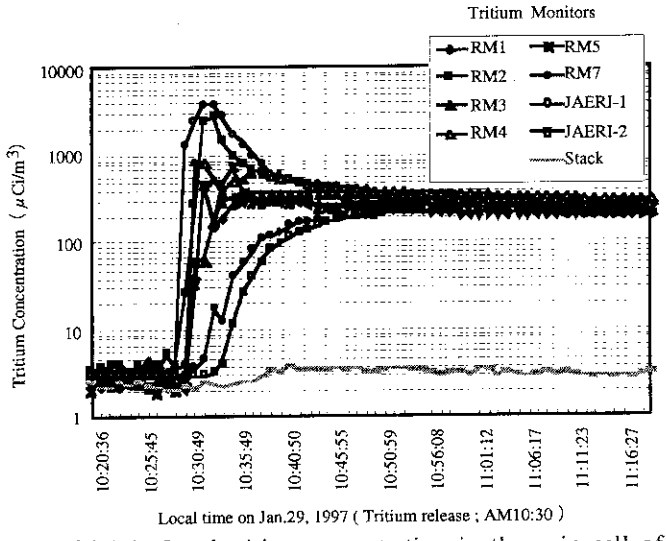

Fig. VII.4.1-1 Local tritium concentration in the main cell of TSTA after 1 Ci of tritium release.

Radio-chemical reactions induced by tritium beta decay were investigated with a system containing a tritium-air mixture. An example of reaction rates and reaction products obtained is shown in Fig. VII.4.1-2. The amounts of tritium retained in tungsten and Inconel samples after irradiation by a high current D/T ion beam that simulated plasma facing conditions were measured. The effect of sintering a tungsten sample, which resulted in the reduction of tritium retained in defects, was investigated.

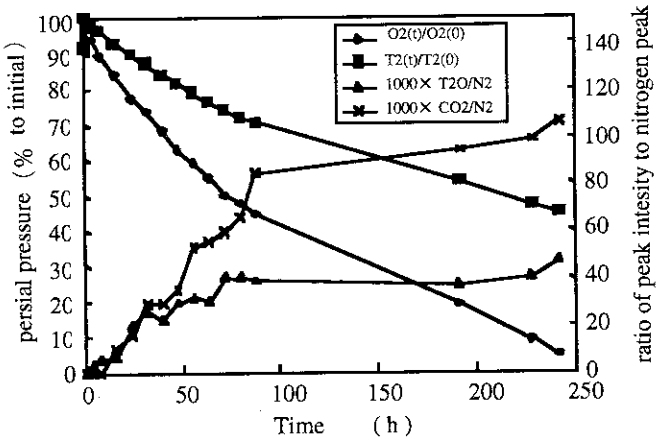

Fig. VII.4.1-2 Time dependence of partial pressures of components in the air (66.5 kPa) and T2 (26.6 kPa) mixed gas. (Nitrogen peak intensity had little change. Production of carbon dioxide was supposed to be due to a surface reaction of tritiated water condensed and contained in stainless steel.)

4.2 Collaboration between JAERI and CEA- Cadarache for a Lower Hybrid Antenna Module

Cooperative activities have begun to obtain a detail outgassing database during high- power, long-pulse RF operation of a launcher designed for a future LHCD system. An RF test was performed at the CEA-Cadarache RF Test Facility that allowed high power injection up to 500 kW, under quasi-continuous operation at a frequency of 3.7 GHz. In the first step, from 1993 to 1995, outgassing experiments were carried out with a 4-waveguide and a 3x6 waveguide multi-junction module constructed from Dispersion Strengthened Copper. The outgassing rate during RF injection was almost the same as that for a stainless steel module. In the second phase of this collaboration, from 1995 to 1998, outgassing experiments with mouth modules made of Carbon Fiber Composite are being conducted to develop a heat resistant LH antenna front.

4.3 Collaborative Activities between CEA and JAERI on Testing of Negative Ion Sources and Accelerators for Neutral Beam Injectors

The JAERI-CEA joint experiment on a negative ion source has been carried out under the framework of ITER-EDA. The purpose of the experiment is to demonstrate high current density D^- ion beam production, 20mA/cm^2, at a low source pressure, 0.3 Pa, which is required for the ITER ion source. A negative ion source designated a KAMABOKO ion source has been developed at JAERI and tested at the Cadarache Laboratory in France. The KAMABOKO source is a Cs-seeded volume source with a semicylindrical shape to confine a plasma efficiently. A 20mA/cm^2 D^- ion beam has been successfully produced at 0.3 Pa. In addition, the extracted electron current has been decreased to half the D^- ion beam current while the D^- ion beam current has been maintained at 1.4 A by increasing the magnetic filter filed from 800 to 1800 Gauss・cm. The current density, source pressure, and electron ratio now satisfy ITER requirements.

4.4 Collaborative Activities of Research and Development on Plasma Wall Interaction in TEXTOR

An IEA implementing agreement for a program of research and development on plasma wall interaction in TEXTOR has been extended for five years, up to December 2002. TEXTOR management is under KFA Julich, ERM/KMS Brussels, and FOM Nieuwegein under the Trilateral Euregio Cluster (TEC). Japan is a member of the executive committee and NIFS (Cooperation Center of Japan) leads Japanese programs. JAERI as a Japan technical committee member joins the program. However, recent activity has been comparatively low; only three staff members recently visited TEXTOR to exchange information and discuss experimental results.

4.5 Collaborative Activities on Environmental, Safety, and Economic Aspects of Fusion Power

Designated by the Government of Japan, JAERI has been participating in the IEA Implementing Agreement on a Cooperative Program on the Environmental, Safety, and Economic (ESE) Aspects of Fusion Power. This collaborative activity has been carried out by Canada, EURATOM, JAERI, MINATOM, and the USA since 1992. JAERI is coordinating the tasks on the Transient Thermofluid Modeling and Validation Tests, and the Safety System Study Methodology. Recent contributions on this task included a dose calculation for activation products[4.5-1].

[4.5-1] T. Homma and O. Togawa, "Estimates of External Dose-Rate Conversion Factors and Internal Dose Conversion Factors for Selected Radionuclides Released from Fusion Facilities," JAERI-Data/Code 96-034 (1996).

4.6 Collaborative Activities on Technology for Tritium Transfer between AECL and JAERI

The objectives of cooperation in the field of controlled nuclear fusion between JAERI and the National Fusion Program, Atomic Energy of Canada Limited (AECL) are to conduct information and personnel exchanges to develop fusion technologies on tritium handling, the breeding branket, and plasma physics. In 1996 several information exchanges were held for the importation procedure of tritium and the tritium transportation container, and on the effect of BeO on tritium release characteristics from beryllium, etc.

Tritium will be shipped from the AECL Chalk River Laboratory to the Tritium Process Laboratory (JAERI) based on a contract for purchasing tritium for research and development of tritium handling technology. Meetings were held to discuss the technical items for loading and shipping of tritium. Procedures for accountancy and calibration were discussed and general information was exchanged for mutual understanding of this program.

5. Other Activities

The mutual inforamtion and personal exchanges between JAERI and fusion research institutes in Asian area are rapidly increasing during this several years under significant development on fusion research in this area, especially in China and Korea. These exchanges are performed under STA scientist exchange program (in 1998, four scientists from China for one year and two JAERI scientists to China for two weeks), the scientist invitation program (in 1998, one senior scientis from China for one month), STA and JAERI fellowships and so on. A new framework to make more fruitful cooperation between JAERI and these countries on fusion research filed should be prepared under Science and Technology Cooperation Agreement between Japan and these countries.

APPENDICES

A. 1. Publication List (April 1996 - March 1997)

A. 1. 1. List of JAERI reports

1) Aoyagi T., Nagashima K., Kitai T., et al., "The Design Study of the JT-60SU Device -The Power Supply for Coils of JT-60SU-" JAERI-Research 97-010 (1997) (In Japanese).
2) Arai T., Koike T., Shimizu M., JAERI-Tech, 97-003, "Development of Fiber Scope for JT-60 Toroidal Field Coil Cooling Pipe" (1997).
3) Hatano T., Sato K., Fukaya K. et al., "High Heat Flux Testing of HIP Bonded DS-Cu/316SS First Wall Panel for Fusion Experimental Reactors," JAERI-Research 97-017 (1997).
4) Hayashi N., Takizuka T., Hatayama A., et al., "Analysis of Divertor Asymmetry Using a Simple Five-point Model", JAERI-Research 97-018 (1997).
5) Hayashi T., Miya N., Kikuchi M., et al., "The Design Study of the JT-60SU Device (No.9) -Fuel Handling, Confinement and Clean up Systems for JT-60SU-" JAERI-Research 97-007 (1997) (In Japanese).
6) Ishida S., "Review of JT-60U Experimental Results from February to November, 1996" JAERI-Research 97-047 (1997) (in Japanese).
7) Ishii Y., Ozeki T., Tokuda S., et al., "Review of JT-60U Experimental Results from February to November 1996", JAERI-Research 97-047, Section 2.5.
8) Iwai Y., Yamanishi T., Okuno K., "Study of Column Construction and Tritium Inventory of Cryogenic Distillation Columns for Tritium Plant of a Fusion Reactor," JAERI-Tech 96-043 (1996).
9) Kanamori N., Nakahira M., Ohkawa Y. et al. "Assembly Tool Design," JAERI-Tech 96-023 (June 1996).
10) Kasugai A., Sakamoto K., Takahashi K. et al., "High Power Millimeter Wave Transmission Through CVD Diamond" JAERI-Research 97-020 (1997).
11) Kawai M.,etc,"Development of the Negative-ion Based NBI Computer System for the JT-60", JAERI-Tech 97-012,P.69.
12) Kikuchi M., Nagami M., Kurita G., et al., "The Design Study of The JT-60SU Device (vol.1) -Objectives and Outline of JT-60SU Program-" JAERI-Research 97-026 (1997) (in Japanese).
13) Kikuchi M., "An Economical Consideration of Fusion Reactor Advanced SSTR (A-SSTR)" JAERI-Research 97-004 (1997) (In Japanese).
14) Kitamura K., Koizumi K., Shimane H. et al., "Structural Analysis of Vacuum Vessel and Blanket Support System for International Thermonuclear Experimental Reactor(ITER)," JAERI-Tech 96-049 (1996).
15) Kitamura K., Komatsuzaki M., Nishio S. et al., "Assessment of F/W Electrical Cutting for Reduction of Electromagnetic force on the Blanket Module," JAERI-Tech 96-031 (1996).
16) Koizumi K., Nakahira M., Oka K., et al., "Development of radiation-hard ultrasonic probes for ITER vacuum vessel", JAERI-Tech 96-041 (1996)
17) Koizumi K., Nakahira M., Shibui M. et al., "Conceptual design of separated first wall and testing of small-size mock-ups", JAERI-Tech 96-048 (1996)
18) Kurita G., Nagashima K., Tobita K., et al., "The Design Study of The JT-60SU Device -The Physical Design and Diagnostic System of JT-60SU-" JAERI-Research 97-023 (1997) (in Japanese).
19) Kuriyama M., Ushigusa K., Ito T., et al., "The Design Study of the JT-60SU Device-The Neutral Beam Injection System of JT-60SU-" JAERI-Research 97-005 (1997) (In Japanese).
20) Liu C.G., Yamagiwa M., Qian S.J., "Production of sheared flow by means of ICRF heating in tokamak plasmas", JAERI-Research 96-068 (1997).
21) Maebara S., Seki M., Suganuma K. et al., "Development of a new lower hybrid antenna module using a poloidal power divider" JAERI-Research 96-036 (1996).
22) Maki K., Sato S. and Kawasaki H., "Development of Displacement Cross Section Set for Evaluating Radiation Damage by Neutron Irradiation in Materials Used for Fusion Reactors," JAERI-Data/Code 97-002 (1997).
23) Nakamura Y., Yoshino R., Pomphrey N., et al., "Extremely Fast Vertical Displacement Event Induced by a Plasma βp Collapse in High βp Tokamak Disruptions," JAERI-Research 96-023 (1996).

24) Neyatani Y., Mori K., Oguri S., et al.,"Magnetic Sensor for Steady State Tokamak" JAERI-Research 96-026 (1997) (in Japanese).
25) Neyatani Y., Ushigusa K., Tobita K., et al., "The Design Study of The JT-60SU Device -The vacuum vessel and cryostat of JT-60SU" JAERI-Research 97-024 (1997) (in Japanese).
26) Nishitani T., Iguchi T., Ebisawa K., et al, "Design of Radial Neutron Spectrometer for ITER", JAERI-Tech 96-038(1996)
27) Nishitani T., Iida T., Ikeda Y., et al., "Irradiation Tests on Diagnostics Components for ITER in 1995", JAERI-Tech 96-040(1996)
28) Obara K., Kakudate K., Oka K., "Irradiation Tests of Critical Components for Remote Handling System in Gamma Radiation Environment," JAERI-Tech 96-011 (1996).
29) Oda M., Kurasawa T., Kuroda T. et al., "Development of HIP Bonding Procedure and Mechanical Properties of HIP Bonded Joints for Reduced Activation Ferritic Steel F-82H," JAERI-Tech 97-013 (1997).
30) Oka K., Nakahira M., Kakudate S. et al. "Development of Remote Bore Tools for Pipe Welding/Cutting by YAG Laser," JAERI-Tech 96-035 (July 1996).
31) Sato M., Isei N., Isayama A., et al., "Determination of Radial Position in the Measurement of Electron Temperature Profiles from Electron Cyclotron Emission", JAERI-Research 97-011 (1997).
32) Sato S., Takatsu H., Sasaki T. et al., "Topics of ITER Nuclear Design," JAERI-Conf 96-005 (1996).
33) Seki M., Obara K., Maebara S. et al., "Performance test of lower hybrid waveguide under long/high-RF power transmission" JAERI-Research 96-025 (1996).
34) Tokamak Program Division (Compiled by Toyosima N.), "Material Characteristic of Ti Alloy (Ti-6Al-4V)" JAERI-Research 97-012 (1997) (in Japanese).
35) Tokami I., Nakahira M., Kuroda T. et al., "Investigation on Welding and Cutting Methods for Blanket Support Legs of Fusion Experimental Reactors," JAERI-Tech 96-032 (1996).
36) Tokuda S., Watanabe T., "Finite Difference Method for Inner-layer Equations in the Resistive Magnetohydrodynamic Stability Analysis," JAERI-Research 96-004 (1996).
37) Tokuda S., Watanabe T., "Theory of Asymptotic Matching for Resistive Magnetohydrodynamic Stability in a Negative Magnetic Shear Configuration," JAERI-Research 96-057 (1996).
38) Toyoshima N., Masaki K., Kaminaga A., et al., "The Design Study of the JT-60SU Device -Auxiliary System, Plan of Displacement, and Dismantlement Construction-" JAERI - Research, 97-008, 148 (1997) (In Japanese).
39) Ushigusa K., Mori K., Nakagawa S., et al., "The Design Study of The JT-60SU Device -The Superconductor-Coils of JT-60SU-" JAERI-Research 97-027 (1997) (in Japanese).
40) Yamamoto T., Ushigusa K., Sakamoto K., et al., "The Design Study of the JT-60SU Device -The ECRF System of JT-60SU-" JAERI-Research 97-006(1997) (In Japanese).
41) Yoshida H., Naito O., Hatae T., et al., "Solution for a window coating problem developed in the JT-60U Thomson scattering system", JAERI -Research 96-062(1996)
42) Yoshida H., Naito O., Yamashita O., et al., "JT-60U Thomson scattering system with multiple ruby lasers and high spatial resolution for high electron temperature plasma measurement", JAERI-Research 96-061(1996)

A. 1. 2. List of papers published in journals

1) Aoyagi T., "Examples of Data Processing Systems / Data Processing System for JT-60", J. Plasma and Fusion Research 72 (1996) 1370-1375.
2) Araki M., Ogawa M., Kunugi T. et al., "Experiments on heat transfer of smooth and swirl tubes under one-sided heating conditions," Int. Heat Mass Transfer, 39, 3045-3055 (1996).
3) Araki M., Sato K., Suzuki S. et al., "Critical-Heat-Flux Experiment on the Screw Tube Under One-Sided-Heating Conditions," Fusion Technology, 29, 519-528 (1996).
4) Araki M., Suzuki S., Sato K. et al., "Analytical study of electromagnetic forces induced by eddy current in ITER divertor," Fusion Technology, 30, 674-679 (1996).
5) Araki M., Youchison D. L., Akiba M. et al., "Manufacturing and testing of a Be/OFHC-Cu divertor module," J. Nucl. Materials, 233-237, 632-637 (1996).

6) Arita T. Yamanishi T., Iwai Y. et al., "A tritium recovery system from waste water of fusion reactor using CECE and Cryogenic-wall thermal diffusion column" Fusion Technol., 30,864-868 (1996).
7) Asakura N., Hosogane N., Iio S., et al., "Field Reversal Effects on Divertor Plasmas under Radiative and Detached Conditions in JT-60U", Nucl. Fusion, 36, 795 (1996).
8) Barabash V., Akiba M., Mazul I. et al., "Selection, development and characterization of plasma facing materials for ITER," J. Nucl. Materials, 233-237, 718-723 (1996).
9) Bolt H., Araki M., Linke J. et al., "Heat flux experiments on first wall mock-ups coated by plasma sprayed B_4C," J. Nucl. Materials, 233-237, 809-813 (1996).
10) Carlson R.V., Okuno K., "Twelve years of Tritium Operation Experience at the Tritium Systems Test Assembly" Fusion Technol., 30,900-904 (1996).
11) Carlson R.V., Willms R., Okuno K., "Studies of Tritiated Water Absorbed on Molecular Sieve" Fusion Technol., 30,895-899 (1996).
12) Cordey J.G., Takizuka T., Miura Y., et al., "ITER Forecasts", Science 275 (1997) 290-291.
13) Enoeda M., Kawamura Y., Okuno K., "Tritium Test of Cryogenic Molecular Sieve Bed for He GDS Gas Cleanup By 60 SLM Test Loop" Fusion Technol., 30,885-889 (1996).
14) Falter H. D., Ciric D., Araki M. et al., "Vapotron as Heat Sink for Flat High-Conductivity Unidirectional Carbon-Fiber-Composite Tiles," Fusion Technology, 29, 571-583 (1996).
15) Fujita T., Ide S., Shirai H., et al., "Internal Transport Barrier foe Electrons in JT-60U Reversed Shear Discharges", Phys. Rev. Lett. 78, 2377 (1997).
16) Hatano T., Sato S., Sato K. et al., "High Heat Flux Testing of HIP Bonded DS-Cu/316SS First Wall Panel for Fusion Experimental Reactors," Fusion Technol., 30, 752-756 (1996).
17) Hayashi M., Shibata K., Matsumoto R., "X-ray flares and mass outflows driven by magnetic interaction between a protostar and surrounding disk", Astrophys. J. 468, 37 (1996).
18) Hayashi T., Suzuki T., Yamada M. et al., "Tritium Inventory Measurements by "INBED" Gas Flowing Calorimetry" Fusion Technol., 30,931-935 (1996).
19) Hiroki S., Abe T. and Murakami Y., "Sensitive Helium Leak Detection in a Deuterium Atmosphere using a high Resolution Quadrupole Mass Spectrometer," Vacuum, 47, 767-769 (1996).
20) Hoek M., Nishitani T., Carlson M., et al., "Triton burnup measurements by neutron activation at JT-60U ", Nucl. Instrum. Methods A368(1996) 804-814
21) Honda T., Okazaki K., Maki K. et al., "Comprehensive Safety Analysis Code System for Nuclear Fusion Reactors III: Ex-Vessel LOCA Analyses Considering Passive Safety," Fusion Technol. 29 p.116-125 (1996).
22) Honda T., Okazaki K., Seki Y. et al., "Comprehensive Safety Analysis Code System for Nuclear Fusion Reactors IV: Preliminary Estimation of Dust Production due to Plasma Disruptions," Fusion Technol. 30 p.95-103 (1996).
23) Horton W., Tajima T., Kishimoto Y., et al., "Ion transport analysis of a high-beta poloidal JT-60U discharge", Plasma Phys. Control. Fusion 38 (1996) 1323-1326.
24) Horton W., Tajima T., Kishimoto Y., et al., "Thermal Transport Barriers in Tokamaks from Bifurcations in the Sheared Mass Flows", Comments Plasma Phys. Controlled Fusion 17 (1996) 205-219.
25) Hudson S.R. and Dewa R.L., "Almost invariant surface for magnetic field-line flows," Journal of Plasma Physics, 56(2):361, 1996.
26) Hudson S.R. and Dewa R.L., "Manipulation of islands in a heliac vacuum field," Physics Letters A, 226:85,1997.
27) Ide S., Fujita T., Naito O., et al., "Sustainment and Modification of Reversed Magnetic Shear by LHCD on JT-60U", Plasma Physics and Controlled Fusion, 38 1645 (1996).
28) Ide S., Naito O., Kondoh T., et al., "Response of Lower Hybrid Wave Driver Current profile on Wave Launching Position", Nucl. Fusion, 36, 1057 (1996).
29) Ikeda Y. Tobita K. Hamamatsu K., et al , "Ripple Enhanced Banana Drift Loss at the Outboard Wall during ICRF/NBI Heating in JT-60U ", Nuclear Fusion 36 759-767 (1996).
30) Ishida T., Hayashi T., Yamada M. et al., "R&D of a Compact Detritiation System Using a Gas Separation Membrane Module" Fusion Technol., 30,926-930 (1996).

31) Ishiyama S., Akiba M., Eto M. et al., "Irradiation damage analysis on the flat plate type target plate of the divertor for fusion experimental reactors," J. Nucl. Materials, 228, 275-283 (1996).
32) Itami K., Yoshino R., Asakura N.,et al., "Isolation of the improved core confinement from high recycling and radiative boundary in reversed magnetic shear plasmas of JT-60U", Phys. Rev. Lett. 78, 1267 (1997).
33) Itoh Y., Ogiwara N., Saidoh M., et al., "Simulation of RBS spectra for a surface with a periodic roughness", Nucl. Instrum. Methods, B117, 161-169, (1996).
34) Iwai Y., Yamanishi T., Okuno K. et al., "Design Study of Feasible Water Detritiation Systems for Fusion Reactor of ITER Scale" J. Nucl. Sci. Technol., 33, 981-992 (1996).
35) Jimbou R., Saidoh M., Nakamura K. et al., "New composite composed of boron carbide and carbon fiber with high thermal conductivity for first wall," J. Nucl. Materials, 233-237, 781-786 (1996).
36) Kawano Y., Nagashima A., Hatae T., et al., "Dual CO_2 Laser interferometer with a wavelength combination of 10.6 and 9.27 μm for electron density measurement on large tokamaks", Rev.Sci.Instrum. 67(1996) 1520
37) Kikuchi. M. and JT-60 team., "Recent Results of JT-60U"(invited), Fusion Technology, 30, No.3, Part2A 660 (1996).
38) Kikuchi. M., "An Economically Competitive Fusion Reactor" (invited), Fusion Technology, 30, No.3, Part2B 1631 (1996).
39) Kimura H. and JT-60 Team, "Recent results from high performance and steady state researches in the Japan Atomic Energy Research Institute Tokamak 60 Upgrade", Physics of Plasmas, 3, 1943 (1996).
40) Kishimoto Y., "3-Dimensional Simulation Model of Raman Regime Free-Electron Laser", J. Phys. Soc. Jpn. 65 (1996) 3877-3889.
41) Kishimoto Y., Tajima T., Horton W., et al., "Theory of Self-organized Critical Transport in Tokamak Plasmas", Phys. Plasmas 3 (1996) 1289-1307.
42) Konishi S., Hara M., Okuno K., "Plasma Exhaust Processing by Palladium Permeation and Electrolytic Oxidation and Reduction "Fusion Technol., 30,890-894 (1996).
43) Kurasawa T., Takatsu H., Sato S. et al., "Diffusion Bonding of Reduced Activation Ferritic Steel F82H for DEMO Blanket Application," J. Nucl. Mater., 233-237, 313-318 (1996).
44) Kurihara R., Ueda S., Tada E., "Fracture Mechanics of a Postulated Crack in ITER Vacuum Vessel," Fusion Technol. 30(3) p.1465-1469 (1996).
45) Kuriyama M., et al, "Development of Negative-Ion Based NBI System for JT-60(in Japanese)", Journal of the Atomic Energy Society of Japan (8.11.30) VOL.38 NO.11 P.912.
46) Kuriyama M., et al, "Trend of High Power Negative-Ion Based NBI Development (in Japanese)", Journal of Plasma and Fusion Research VOL.72 NO.11 P.1162
47) Masaki K., Kodama K., Ando T., et al., "Tritium retention in graphite inner wall of JT-60U", Fusion Engineering & Design 31, 181-187 (1996).
48) Matsuda T., "Data Utilization", J. Plasma and Fusion Research 72 (1996) 1235-1242.
49) Miura Y. and JFT-2M Group, "Change of neutral energy distribution at L/H, H/L transitions and ELMs in the JFT-2M tokamak", Nucl. Fusion, 37, 175 (1997).
50) Miura Y., Okano F., Suzuki N., et al., "Ion Heat Pulse after Sawtooth Crash in the JFT-2M Tokamak", Phys. Plasmas 3, 3696-3700 (1996).
51) Miya K., Muto Y., Takatsu H. et al., "Present Activity for the Preparation of a Japanese Draft of Structural Design Guidelines for the Experimental Fusion Reactor," Fusion Eng. Des., 31, 145-165 (1996).
52) Nagashima K., Ide S., Naito O., "Particle Transport Analysis in Lower Hybrid Current Drive Discharges of JT-60U", Plasma Physics and Controlled Fusion, 38, 1975-1984 (1996).
53) Nagatsu M., Takada N., Akiba M. et al., "Effect of electron and ion beam irradiation on power reflectivity of C/C first wall materials," J. Nucl. Materials, 233-237, 1284-1288 (1996).
54) Naito O., Yoshida H., Hatae K., et al., "A formula for reconstructing fully relativistic electron distribution from in coherent Thomson scattering data", Physics of Plasmas, 4, 1171-1172 (1997).
55) Naitou H., Kitagawa H., Tokuda S., "Linear and Nonlinear Simulation of Kinetic Internal Kink Modes", J. Plasma and Fusion Research 73, 174 (1997)

56) Nakamura K., Akiba M., Araki M. et al., "Erosion of newly developed CFCs and Be under disruption heat loads," J. Nucl. Materials, 233-237, 730-735 (1996).
57) Nakamura Y., Nishio S., Yoshino R., et al., "VDE Characteristics during Disruption Process and its Underlying Acceleration Mechanism in the ITER-EDA Tokamak", J. Plasma and Fusion Research 72 (1996) 1387-1396.
58) Nakamura Y., Yoshino R., Neyatani Y., et al., "Mechanism of Vertical Displacement Events in JT-60U Disruptive Discharges," Nucl. Fusion 36 (1996) 643.
59) Nakamura Y., Yoshino R., Pomphrey N., et al., "Acceleration Mechanism of Vertical Displacement Event and its Amelioration in Tokamak Disruptions", J. Nucl. Science & Technol. 33 (1996) 609.
60) Neudatchin S.V., Takizuka T., Shirai H., et al., "Time Behavior of Heat Diffusivity during L-H-L Transition in JT-60U", Jpn. J. Appl. Phys. 35 (1996) 3595-3602.
61) Nishitani T., Hoek M., Harano H., et al., "Triton burnup study in JT-60U ", Plasma Phys. Control. Fusion, 38(1996) 355-364
62) Ogiwara N., Miyo Y., Ueda Y., "Application of the time-of-flight measurements in XHV by a quadrupole mass spectrometer", Vacuum, 47, 575 (1996).
63) Ohira S., Okuno K., "Development of Realtime and Remote Fuel Process Gas Analysis System Using Laser Raman Spectroscopy" Fusion Technol., 30,869-873 (1996).
64) Ohta M., "Status of Japanese Fusion Technology, " Fusion Technology, Vol.30, No.3, Part2A, p404-410 (1996).
65) Onozuka M., Tsujimura T., Toyoda M. et al., "Electrical Insulation and Conduction Coating for Fusion Experimental Devices," Fusion Technol., 29, 73-82 (1996).
66) Ozeki T., Azumi M., Ishii Y., et al., "Physics issues of high bootstrap current tokamaks", Plasma Phys. Control. Fusion 39 A371 (1997).
67) Qiang Ji, Singer C., Hirayama T., "Simulation of JT-60 Discharges with an Experimentally Calibrated Theoretical Transport Model", Jpn. J. Appl. Phys. 35 (1996) 2797-2802.
68) Ryter F. and H-mode Database Working Group, "Results from the ITER H-mode threshold database", Plasma Phys. Control. Fusion, 38, 1279 (1997).
69) Ryter F., H-mode Database Working Group(Takizuka T., Miura Y., et al.), "H Mode Power Threshold Database for ITER", Nucl. Fusion 36 (1996) 1217-1264.
70) Saigusa M., Moriyama S., Kimura H. et al., "Effect of Non-Linear Wave Absorption on the Radiation Loss Fraction during second Harmonic Minority Heating Experiments in JT-60U," Jpn. J. Appl. Phys., 36, 345-349(1997).
71) Sakamoto K., Kasugai A., Takahashi K. et al., "Stable, Single-Mode Oscillation with High-Order Volume Mode at 1MW, 170GHz Gyrotron," J. Phys. Soc. Japan, 65, 1888-1890(1996).
72) Sato K., Nakamura K., Suzuki S. et al., "High heat flux test of CVD-tungsten coated Cu heat sink divertor mock-up," Fusion Technology, 30, 769-773 (1996).
73) Sato M., Fukuda T., Takizuka T., et al., "Threshold power for the H-mode transition in JT-60", Plasma Phys. Control. Fusion, 38, 1283 (1996).
74) Sato S., Maki K., Takatsu H. et al., "Shielding Analysis for Toroidal Field Coils around Exhaust Duct in Fusion Experimental Reactors," Fusion Technol., 30, 1076-1080 (1996).
75) Sato S., Ohsaki T., Koga S. et al., "Welding and Cutting Characteristics of Blanket Module and Backplate for Fusion experimental reactors," FAPIG, 144, 39-45 (1996).
76) Sato S., Takatsu H., Seki Y. et al., "Streaming Analysis of Gap between Blanket Modules for Fusion Experimental Reactors," Fusion Technol., 30, 1129-1133 (1996).
77) Seki Y., Aoki I., Yamano N. et al., "Preliminary Evaluation of Radwaste in Fusion Power Reactors," Fusion Technol. 30(3) p.1624-1629 (1996).
78) Shimakawa S., Sakamoto N., Sato K. et al., "New electron beam facility for irradiated plasma facing materials testing in hot cell," J. Nucl. Materials, 233-237, 1582-1585 (1996).
79) Shimizu K., Takizuka T., "Simulation of Divertor Plasma", J. Plasma and Fusion Research 72 (1996) 909-915.

80) Suzuki S., Sato K., Araki M. et al., "High heat flux experiments on divertor mock-ups with a thermal bond layer for fusion experimental reactors," Fusion Technology, 30, 788-792 (1996).
81) Suzuki S., Sato K., Araki M. et al., "Thermal cycling experiments on a 1 meter long divertor mock-up with a rigid support structure," Fusion Technology, 30, 793-797 (1996).
82) Tada E., Obara K., Kakudate S. et al. "Development of Remote Maintenance Technology for Fusion Reactor," Journal of Plasma and Fusion Research Vol.73 No.1, 19-82 (1997).
83) Takada N., Nagatsu M., Akiba M. et al., "Reflectivity characteristics of carbon materials irradiated with hydrogen ion-beam," J. Plasma and Fusion Research, 72, 776-782, (1996).
84) Takahashi K., Kasugai A., Sakamoto K. et al., "Measurement of Temperature Dependence of Dielectric Permittivity of Sapphire Window for High Power Gyrotron," Jpn. J. Appl. Phys., 35, 4413-4416 (1996).
85) Takase K., Kunugi T., Seki Y. et al., "A Fundamental Study on a Water Jet Injected into a Vacuum Vessel," Fusion Technol. 30 p.1453-1458 (1996).
86) Takiyama K., Katsuta T., Watanabe M., et al., "Spectroscopic method to directly measure electric field distribution in tokamak plasma edge", Rev. Sci. Instrum. 68, 1028 (1997).
87) Takizuka T., Ogawa Y., Toi K., et al. , "Confinement and Transport / Database and Modelling Related to ITER", J. Plasma and Fusion Research 72 (1996) 498-504.
88) Toda S., Itoh S-I., Yagi M., et al., "A theoretical model of H-mode transition triggered by condensed neutral near X-point", Plasma Phys. Control. Fusion, 39, 301 (1997).
89) Tokami I., Nakahara M., Sato S. et al., "Welding and Cutting Methods for Blanket Support Legs of Fusion Experimental Reactor," Fusion Technol., 30, 574-578 (1996).
90) Tsuneoka M., Fujita H., Imai T. et al., "Development of DC100kV, 10A, 360A IGBT switch" IEE Japan D116, 497-498 (1996).
91) Ushigusa K., "Simple Modeling to Explain Temperature Dependence of the Lower Hybrid Current Drive Efficiency", Plasma Physics and Controlled Fusion, 38, 1825-1830 (1996)
92) Watanabe H., Muroga T., Akiba M. et al., "Microstructure of neutron irradiated graphite/Cu joint," Fusion Technology, 30, 774-777 (1996).
93) Yamagiwa M., "Positron-emitting radionuclide yield in deuterium beam-injected 3He plasma", Nuclear Science and Engineering 125 218-222 (1997).
94) Yamagiwa M., Hirose A., and Elia M., "Kinetic shooting code study of ballooning modes in a tokamak", Plasma Phys. Control. Fusion 39 531 (1997).
95) Yamanishi T., Enoeda M., Okuno K. et al., "A control method for the cryogenic distillation column with a feedback stream" Fusion Technol., 29,232-243 (1996).
96) Yamauchi T., Grek B., Hoshino K., et al., "Detailed profile of m=2 island with TVTS on JFT-2M", Physics Letters A, 223, 179 (1996).
97) Yamauchi T., Ishige Y., Shiina T., et al., "Development of high-spatial resolution TV Thomson scattering system for JFT-2M", Journal of Plasma and Fusion Research, 72, 692 (1996) (in Japanese).
98) Yoshida H., Naito O., Hatae T., et al., " Approach to a window coating problem by in situ transmission monitoring and laser blow-off cleaning developed in the JT-60U Thomson scattering system", Rev. Sci. Instrum. 68(1) 256-257
99) Yoshida H., Naito O., Matoba T., et al., "Quantitative method for precise, quick, and reliable alignment of collection object fields in the JT-60U Thomson scattering diagnostic", Rev. Sci. Instrum. 68(2) 1152-1161
100) Yoshino R., Koga J.K., Takeda T., "Sensor Algorithms of the Plasma Vertical Position to Avoid a Vertical Displacement Event dusting Plasma-Current Quench on JT-60U", Fusion technology, 30, 237 (1996).
101) Yoshino R., Kondoh T., Neyatani Y., et al., "Fast plasma shutdown by killer pellet injection in JT-60U wit reduced heat flux on the divertor plate and avoiding runaway electron generation", Plasma Phys. Control. Fusion, 39, 313 (1997).
102) Yoshino R., Nakamura Y., Neyatani Y., "Avoidance of VDEs during Plasma Current Quench in JT-60U", Nucl. Fusion, 36, 295 (1996).
103) Yoshino R., Ohsawa M., "Fluctuations in Plasma Equilibrium Control on JT-60U", Fusion Technology, 30, 159 (1996).

104) Yoshino R., Seki M., "Low electric field (0.08Vm-1) plasma-current start-up in JT-60U", Plasma Phys. Control. Fusion, 39, 205 (1997).

A. 1. 3. List of papers published in conference proceedings

1) Aoki I., Seki Y., Ueda S. et al., "In-Vessel Dust Removal System using Static Electricity," Proceedings of the 19th SOFT, Lisbon (1996).
2) Arai T., Honda M., Koike T., et al., "Inspection techniques for JT-60 toroidal field coil cooling pipes", 19th SOFT, Lisbon, Portugal, (1996).
3) Araki M., Nakamura K., Sato K., et al., "Development of 3D based CFC with High thermal conductivity for fusion application", Proc. of 19th Symp. on Fusion Technology, Sept.16-20, 1996, Lisbon, Portugal
4) Arita M., Hayashi T., Okuno K., "Permeation behavior of deuterium implanted into Ti-6A1-4V alloy" International Workshop on Interfacial Effects in Quantum Engineering Systems (IEQES-96),Aug. 21-23, Mito, Japan (1996).
5) Asakura N., Koide Y., Itami K., "SOL Plasma Profiles under Radiative and Detached Divertor conditions in JT-60U", 12th Int. Conf. on Plasma Surface Interactions in Controlled Fusion Devices (St. Raphael) (1996).
6) Baba A., Nishikawa M., Kawamura Y. et al., "Isotope exchange capacity of solid breeder materials" International Workshop on Interfacial Effects in Quantum Engineering Systems (IEQES-96),Aug. 21-23, Mito, Japan (1996).
7) Chiocchio S., Williamson D., Araki M., et al., "Loads on the ITER in-vessel components from electromagnetic transients", Proc. of 19th Symp. on Fusion Technology, Sept.16-20, 1996, Lisbon, Portugal
8) Dacosta O., Kimura H., Moriyama S., et al., "Ion Cyclotron Emission (ICE) New Experimental Results in JT-60U, Theory of Direct Emission", Proc. of Int. Conf. on Plasma Physics, 1, 246 (1996).
9) Daenner W., Cardella A., Ioki K. et al., "The ITER L-4 Blanket Project," Proc. Of 19th SOFT, Lisbon, Portugal (1996).
10) Fujiwara Y, Inoue T, Miyamoto K et al., "Design and R&D for ITER NBI system at JAERI," Proc. of the 12th Topical Meeting on the Technology of Fusion Energy, Reno, Nevada(1996).
11) Fukatsu S., Takeda N., Kakudate S. et al. "Development of Locking and Mover System for ITER Divertor Maintenance," 19th Symposium on Fusion Technology, Lisbon, Portugal (1996).
12) Fukaya K., Sato S., Kuroda T. et al., "Fabrication of Small-Scaled Shielding Blanket Module and First Wall Panel for International Thermonuclear Experimental Reactor," Proc. Of 19th SOFT, Lisbon, Portugal (1996).
13) Gohar Y., Billone M., Cardella A. et al., "Design and Analysis of the ITER Breeding Blanket," Proc. Of 19th SOFT, Lisbon, Portugal (1996).
14) Hamamatsu K., Nishitani T., Tani K., et al., "Transport and Losses of Energetic Tritons and Beam Ions in JT-60U", IEA Tripartite Workshop on TAE and Energetic Particle Physics, Naka Fusion Research Establishment, JAERI, February 25-27, 1997.
15) Hatano T., Fukaya K., Dairaku M. et al., "Post-Mortem Analysis of HIP Bonded First Wall Panel Made from SS316 and DS-Cu after High Heat Flux Testing," Proc. Of 19th SOFT, Lisbon, Portugal (1996).
16) Hemsworth RS, Feist HD, Hanada M, et al., "Neutral Beams for ITER," Rev. Sci. Instrum. vol67, No3, 1120-1125 (1996).
17) Higashijima S., Kubo H., Sugie T., et al., "Study of Carbon Impurity Generation by Chemical Sputtering in JT-60U", 12th Int. Conf. on Plasma Surface Interactions in Controlled Fusion Devices (St. Raphael) (1996).
18) Hino T., Akiba M., "Summary of Japan-US workshop on high heat flux components and plasma surface interactions for next fusion devices," Fusion Eng. Design, 31, 83-87, (1996).
19) Hiratsuka H., Sasajima T., Kodama K., et al., "Effect of plasma behavior on in-vessel components in JT-60 operation, 19th SOFT, Lisbon, Portugal, (1996).
20) Inoue T, Okumura Y, Fujiwara Y, "Design and R&D of High Power Negative Ion Source/Accelerator for ITER NBI," Proc. of the 19th Symp. on Fusion Tech., Lisbon, 16-21 (1996).
21) Jacquot C, Riz D, Trainham T et al., "Negative D- Ion Source Relevant for Application to ITER Neutral Beam Injectors," Proc. of the 19th Symp. on Fusion Tech., Lisbon (1996).

22) Jimbou R., Kodama K., Saidoh M., et al., "Thermal conductivity and retention characteristics of composites made of boron carbide and carbon fibers with extremely high thermal conductivity for first wall", 12th Inter. Conf. on Plasma Surface Interactions in Controlled Fusion Devices (1997).
23) Kakudate S., Oka K., Nakahira M. et al. "Blanket Maintenance Development for ITER," 6th International Symposium on Robotics and Manufacturing (ISRAM'96) France (1996).
24) Kamada Y., "Characteristics of and issues regarding combined H-mode", Plasma Physics and Controlled Fusion Vol.38, No.8(1996) P.P.1173-1188
25) Kamada Y., Yoshino R., Neyatani Y., et al., "Onset Condition of ELMs in JT-60U", Plasma Phys. Control. Fusion 38 (1996) 1387-1391.
26) Kasugai A., Sakamoto K., Tsuneoka M., "Development of 170GHz long pulse Gyrotron with Depressed Collector," Proc. of 19th Symp. on Fusion Tech. Portugal (1996).
27) Kawaguchi I., Adachi J., Yamazaki S. et al., "Engineering Design of DREAM Components," Proceedings of the 19th SOFT, Lisbon (1996).
28) Kishimoto Y., Kim J.Y., Azumi M., et al., "Theory and simulation of self-organized critical transport by toroidal ITG turbulence in tokamak plasmas", Theory of Fusion Plasma, Joint Varenna-Lausanne International Workshop, Villa Monastero, Varenna, Italy, August 26-30, 1996.
29) Kitamura K., Koizumi K., Takatsu H., et al., "Structural analysis of blanket system and vacuum vessel for international thermonuclear experimental reactor (ITER)", Proc. of 19th Symp. on Fusion Technology, Sept.16-20, 1996, Lisbon, Portugal.
30) Koide Y. and the JT-60 Team, "Progress in the JT-60U Experiments with Negative-ion Based Neutral Beams", 38th Annual Meeting of American Physical Society, Division of Plasma Physics, Denver, 3IA 2 (1996).
31) Koizumi K., Nakahira M., Itou Y. et al. "Development of Full-scale Sector Model for ITER Vacuum Vessel," 19th Symposium on Fusion Technology, Lisbon, Portugal (1996).
32) Koizumi N. et al., "Cool-down Simulation of 46 kA and 13 T Nb_3Al Insert ," ICEC16/ICMC Proc., p.791 (1997).
33) Konishi S., Enoeda M., Yamanishi T. et al., "Development of a fusion Fuel Processing System at the Japan Atomic Energy Research Institute" 19th SOFT Aug.16-21,1996, Lisbon, Portugal (1996).
34) Krylov A, Di Pietro E, Hanada M et al., "General Design of the Neutral Beam Injection System and Integration with ITER," Proc. of the 19th Symp. on Fusion Tech., Lisbon (1996).
35) Kurihara K. and Kawamata Y., "Development of a Precise Long-time Digital Integrator for Magnetic Measurements in a Tokamak," in Proceedings of 19th Symposium on Fusion Technology, Lisbon, Portugal (1996).
36) Kurihara R., Seki Y., Ueda S. et al., "Integrated Facility for the In-Vessel Thermofluid Test of the Fusion Reactor Safety," IAEA-TCM on Development in Fusion Safety (Naka), (1996).
37) Kuriyama M, Akino N, Aoyagi T, et al., "Initial Beam Operation of 500keV Negative-Ion-Based NBI system for JT-60U," Proc. of the 19th Symp. on Fusion Tech., Lisbon (1996).
38) Linke J., Akiba M., Bolt H. et al., "Performance of beryllium, carbon and tungsten under intense thermal fluxes," Proc. 12th Int. Conf. on Plasma Surface Interactions in Controlled Fusion Devices, pp.210, St.Raphael, France, May 20-24 (1996).
39) Maebara S., Seki M., Suganuma K., "Development of a new lower hybrid antenna module using a poloidal power divider," Proc. of 19th Symp. on Fusion Tech. Portugal (1996).
40) Miura H., Kitamura K., Takatsu H., et al., " Design development of breeding blanket based on pebble bed concept for fusion experimental reactor", Proc. of 19th Symp. on Fusion Technology, Sept.16-20, 1996, Lisbon, Portugal
41) Miyamoto K, Akino N, Ebisawa N et al., "Production of Multi-MW Deuterium Negative Ion Beams for Neutral Beam Injectors," Proc. of the 16th IAEA Fusion Energy Conf, Montreal, F1-CN-64/G2-5 (1996).
42) Mori M., "Active Control of H-mode", Plasma Physics and Controlled Fusion Vol.38,No.8(1996) P.P.1189-1200
43) Nakahira M., Koizumi K., Itou Y. et al. "Feasibility Study of ITER Vacuum Vessel and Blanket," 12th Topical Meeting on the Technology of Fusion Energy (ANS) (1996).

44) Nakahira M., Oka K., Kakudate S. et al. "Development of an End-Effector for ITER Blanket Module Handling," 19th Symposium on Fusion Technology, Lisbon, Portugal (1996).
45) Nakajima H. et al.," 4K mechanical properties of pure titanium for the jacket of Nb_3Sn superconductors," Proceedings of ICEC16/ICMC, Kitakyusyu, Japan, May (1996).
46) Nakamura K., Dairaku M., Akiba M. et al., "Sputtering experiments on B4C doped CFC under high particle flux with low energy," Proc. 12th Int. Conf. on Plasma Surface Interactions in Controlled Fusion Devices, pp.139, St. Raphael, France, May 20-24 (1996).
47) Nakamura Y., Yoshino R., Pomphrey N., et al., "VDE Dynamics and Acceleration / Deceleration Mechanisms in Tokamak Disruptions", American Physical Society, Program of the Thirty-Eighth Annual Meeting of the Division of Plasma Physics, Denver Colorado (1996).
48) Nakamura Y., Yoshino R., Pomphrey N., et al., "βp Collapse-Induced Vertical Displacement Event in High βp Tokamak Disruptions", Plasma Phys. Contr. Fusion 38 (1996)1791-1804.
49) Nishitani T., Iguchi T., Takada E., et al., "Neutron Spectrometers for ITER", Diagnostics for Experimental Thermonuclear Fusion Rector Plenum Press New York(1996)
50) Nunoya Y. et al., "Experimental Results of 13 T- 46 kA Nb_3Al Conductor in Sultan," ICEC16/ICMC Proc., p.1665 (1997).
51) Ogawa H., Kawashima H., Miura Y. and JFT-2M Group, "Closed divertor experiments on JFT-2M", Proceedings of 16th Int. Conf. on Plasma Physics, Nagoya, 1996, 2, 1250 (1997).
52) Oguri H, Miyamoto N, Okumura Y et al., "Development of a Negative Ion Source for a High Intensity LINAC," Proc. of the 18th Int. LINAC Conf., Geneva (1996).
53) Oguri H. Okumura Y, Miyamoto N et al., "Development of the high brightness negative ion source," Rev. Sci. Instrum. vol67, No3, 1051-1053 (1996).
54) Ohara Y, "Recent NBI technology," Journal of plasma and fusion research Vol72, No5, 493-402 (1996).
55) Ohira S., Hayashi T., Okuno K., "Tritium safety related studies at TPL of JAERI" IAEA 6th TCM on Developments in Fusion Safety Oct. 25. 1996, Naka, Japan.
56) Ohsawa M., Yoshino R., "Vertical displacement caused by giant ELM in JT-60U", Proc. of Int. Conf. on Plasma Physics, 1, 638 (1996).
57) Oka K., Kakudate S., Nakahira M. et al. "Blanket Cooling Pipe Maintenance System for Fusion Experimental Reactor," 19th Symposium on Fusion Technology, Lisbon, Portugal (1996).
58) Okumura Y, Fujiwara Y, Honda A et al., "Development of a 500 keV, 22A D- ion source for the neutral beam injector for JT-60U," Rev. Sci. Instrum. vol67, No3, 1018-1021 (1996).
59) Okumura Y, Fujiwara Y, Inoue T et al., "High power negative ion sources for fusion at JAERI," Rev. Sci. Instrum. vol67, No3, 1092-1097 (1996).
60) Okuno K., Konishi S., Yamanishi T. et al., "Tritium technology research and development at the tritium process laboratory of JAERI" 19th SOFT Aug.16-21,1996, Lisbon, Portugal (1996).
61) Portone A., Gribov Y., Senda I., et al., "Control of the magnetic configuration in ITER", Proc. of 19th Symp. on Fusion Technology, Sept.16-20, 1996, Lisbon, Portugal
62) Ryter F., H-mode Database Working Group(Miura Y., Takizuka T., et al.), "Results from the ITER H-mode Threshold Database", Plasma Phys. Control. Fusion 38 (1996) 1279-1282.
63) Sakamoto K., Kasugai A., Takahashi K. et al., "Development of 170GHz High Power Long Pulse Gyrotron for ITER," Digest of 21th Int. Conf. on Infrared and Millimeter Waves, AT1, 14-19 (1996).
64) Sakurai S., Asakura N., Itami K., "Effect of Particle and Heat Fluxes and Carbon Generation during ELMy Phase in JT-60U", Proc. of Int. Conf. on Plasma Physics, 1, 646 (1996).
65) Sakurai S., Hosogane N., Kodama K., et al., "Design of a Compact W-Shaped Pumped Divertor in JT-60U", 19th. Symp. on Fusion Technology (Lisbon) (1996).
66) Sato M., Fukuda T., Takizuka T., et al., "Threshold Power for the H-mode Transition in JT-60U", Plasma Phys. Control. Fusion 38 (1996) 1283-1288.
67) Sato M., Ishida S., Isei N., et al., "Determination of radial position in the measurement of electron temperature profiles from electron cyclotron emission", Proceedings of 16 th Int. Conf. on Plasma Physics, Nagoya, 1996, 2, 1438 (1997).

68) Sato S., Kuroda T., Kurasawa T. et al., "Mechanical Properties of HIP Bonded Joints of Austenitic Stainless Steel and Cu-alloy for Fusion Experimental Reactor Blanket," J. Nucl. Mater., 233-237, 940-944 (1996).
69) Sato S., Takatsu H., Maki K. et al., "2-D Overall Shielding Analysis of ITER Tokamak Machine," Proc. Of 19th SOFT, Lisbon, Portugal (1996).
70) Sato S., Takatsu H., Maki K. et al., "Evaluation of the Environmental Gamma-Ray Dose Rate by Skyshine Analysis during the Maintenance of an Activated TFC in ITER," Proc. Of IAEA 6th Tech. Committee Meeting on Developments in Fusion Safety, Naka (1996).
71) Seki Y., Aoki I., Yamano N. et al., "Preliminary Evaluation of Radwaste in Fusion Power Reactors," Proc. of IAEA-TCM on Development in Fusion Safety (Naka), (1996).
72) Sengoku S. and JFT-2M Group, "Coexistent regime of H-mode with a dense & cold divertor plasma in JFT-2M closed divertor", Bull. Am. Phys. Soc. 41, 1487 (1996).
73) Shimizu K., Takizuka T., Sakasai S., "A Review on Impurity Transport in Divertors", 12th Int. Conf. on Plasma Surface Interactions in Controlled Fusion Devices, Saint-Raphael, France, May 20-24, 1996.
74) Shimizu K., Takizuka T., Tokuda S., et al., "Monte Carlo Modeling of Impurity Transport in Divertor Plasma", IAEA Technical Committee Meeting on Advances in Computer Modeling of Fusion Plasmas, Los Angels, 2-4 October, 1996.
75) Shirai H., Takizuka T., Koide Y., et al., "Time Evolution of Transport Properties in JT-60U H-mode Plasmas with Improved Core Confinement", Plasma Phys. Control. Fusion 38 (1996) 1455-1460.
76) Shirai H., Takizuka T., Sato M., et al., "Analyses of Electron and Ion Transport Properties in JT-60U H-mode Plasmas with Improved Core Confinement" Proc. 23rd Eur. Phys. Soc. Conf. on Control. Fusion and Plasma Phys. (1996, Kiev), Vol. 1, page 339
77) Steiner A., Ohira S., Hayashi T. et al., "Desorption behavior of different plasma facing materials after bombardment with deuterium ion beam" International Workshop on Interfacial Effects in Quantum Engineering Systems (IEQES-96),Aug. 21-23, Mito (1996).
78) Takenaga H., Asakura N., Shimizu K., et al., "Effects of Edge and Central Fueling and particle Confinement in JT-60U", 12th Int. Conf. on Plasma Surface Interactions in Controlled Fusion Devices (St. Raphael) (1996).
79) Takenaga H., Kubo H., Sugie T., et al., "Neutral Deuterium and Helium Behavior in JT-60U Divertor Plasmas", Proc. of Int. Conf. on Plasma Physics, 1, 642 (1996).
80) Takizuka T., "Particle Simulation of Divertor Plasma", Proc. Australia-Japan Workshop on Plasma Theory and Computation, Robertson, Australia, 15-17 November, 1995 (Research School of Physical Science and Engineering, Australian National University, Canberra, 1996) ANU-PRL-TR-96/01, 67-69.
81) Takizuka T., "Scaling Study and Modeling of Improved Confinement", US-Japan JIFT Workshop on Plasma Turbulence and Transport in Toroidal Systems, Kyoto University, 29-31 October, 1996.
82) Tanabe T., Philipps V., Nakamura K. et al., "Examination of material performance of W exposed to high heat load," Proc. 12th Int. Conf. on Plasma Surface Interactions in Controlled Fusion Devices, pp.198, St. Raphael, France, May 20-24 (1996).
83) Tokuda S., Takizuka T., Kishimoto Y., et al., "Massively Parallel Computing with Plasma Simulation Codes in Tokamak Research", Proc. Australia-Japan Workshop on Plasma Theory and Computation, Robertson, Australia, 15-17 November, 1995 (Research School of Physical Science and Engineering, Australian National University, Canberra, 1996) ANU-PRL-TR-96/01, 70-72.
84) Tsuchiya K., Takenaga H., Fukuda T., et al., "Effect of Edge Neutrals on the Condition of the H-mode Transition in JT-60U", Plasma Phys. Control. Fusion 38 (1996) 1295-1299.
85) Watanabe K., Akino N., Aoyagi T. et al., "Recent progress of high power negative ion beam development for fusion plasma heating" The 7th International Symp. on Advanced Nuclear Energy Research, Takasaki, March 18 - 20 (1996).
86) Watanabe K., et al.,"Recent progress of High-Power Negative on Beam Development for Fusion Plasma Heating", 7th Int. Symp. on Advanced Nuclear Energy Research (8.3.22 Takasaki)

87) Yagyu J., Ogiwara N., Saidoh M., et al., "Properties of thin boron coatings formed during deuterated-boronization in JT-60", 12th Inter. Conf. on Plasma Surface Interactions in Controlled Fusion Devices, Saint Raphael, France, (1996).
88) Yamagiwa M., Hirose A., Elia M., "Kinetic analyses of ballooning modes in tokamaks", Proc. 1996 International Conference on Plasma Physics (ICPP, Nagoya, 1996), Vol. 1, 366 (1997).
89) Yamaki T., Gotoh Y., Jimbou R., et al., "Erosion and thermal desorption characteristics of 1D-CF/B4C composite", 12th Inter. Conf. on Plasma Surface Interactions in Controlled Fusion Devices, Saint Raphael, France, (1996).

A. 1. 4. List of other papers

1) Araki M. and Tsunematsu T., "ITER-EDA in JAERI", 4th Japan-China Symp. on Materials for Advanced Energy Systems and Fission and Fusion Engineering, Aug. 27, 1996 (Hokkaido Univ.)
2) Araki M., "Electromagnetic analysis of the divertor cassette (ITER Design Task D308)", ITER Divertor Task Meeting (ST. Louis, June 12-16, 1996)
3) Asakura N., Takizuka T., Itami K., "High Density H-mode in JT-60U", 4th Meeting of ITER Confinement Database and Modelling Expert Group, Moscow, 15-17 April, 1996.
4) Fukuyama A., Takizuka T., "Present Status of CDBM Transport Modelling", 4th Meeting of ITER Confinement Database and Modelling Expert Group, Moscow, 15-17 April, 1996.
5) Hada K., Koizumi K., "Pressure test requirements in home team's technical standards", ISDC & MPH meeting, March 4-7, 1997 (ANL, USA)
6) Hada K., Koizumi K., "Review of ISDC drafts as its applicability to ITER in-vessel components", ISDC & MPH meeting, March 4-7, 1997 (ANL, USA)
7) Hashimoto M., Ohkawa Y., Interim report on maintainability of the JCT design layout, ITER/EDA Design Task Report, (D313)
8) Hatano T., "High Heat Flux Tests of Small-Scaled First Wall Panel," Japan-US Workshop on High Heat Flux Components and Plasma Surface Interactions for Next Fusion Devices, Naka.
9) Hayashi T., Nakamura H., Okuno K., "Permeation of Tritium in PFMs" Japan-US Workshop p279 on High Heat Flux Components and Plasma Surface Interactions for Next Fusion Devices.
10) Ishiyama S., Fukaya K., Akiba M. et al., "The characterization of copper alloys for the application of fusion reactors," Fitness-For-Service and Decisions for Petroleum and Chemical Equipment, PVP-vol.315, 545-550 (1996).
11) Itou Y., "Review on assembly of ITER VV and in-vessel components", Progress meeting on ITER tokamak assembly at San Diego JWS, June 25, 1996
12) Itou Y., "The approach of task for assembly plan", Progress meeting on ITER tokamak assembly at San Diego JWS, June 25, 1996
13) Kamada Y., Takizuka T., JT-60 Team, "Status of JT-60U Experiments and Future Plan", 4th Meeting of ITER Confinement Database and Modelling Expert Group, Moscow, 15-17 April, 1996.
14) Kimura H., "ICRF Heating Results on JT-60U", Meeting of the European Coordinating Committee on Fast Wave Heating and Current Drive (Garching), (1996).
15) Kitamura K., Takatsu H., "Electromagnetic analysis of modular type blanket structures", Blanket T.M. at Garching (April 24-28)
16) Kitamura K., Takatsu H., "Mechanical assessment on blanket module under EM forces and thermal loads", Technical meeting on Blanket at Garching JWS, Feb. 24 1996
17) Koizumi K., Hada K., "Domestic activity on structural design code development --Fusion Structural Design Committee--", ISDC & MPH meeting, March 4-7, 1997 (ANL, USA)
18) Kondoh T., Kimura H., Kusama Y., et al., "Confinement and Loss of MeV-protons in JT-60U ICRF Experiments", IEA Tripartite Workshop on TAE Modes and Energetic particle Physics ,W36 (Naka) (1996).
19) Kunugi T., Takase K., Shibata M. et al., "Present Status of the Preliminary ICE Apparatus," ITER LOVA/ICE/DUST Task Meeting (Naka), (1996).

20) Kuroda T., "1-D Thermal Analysis of Shielding Blanket Design," Blanket Task Meeting, Garching Germany, (1996).
21) Kuroda T., "Fabrication of Breeding Blanket," Blanket Task Meeting, Garching Germany, (1996).
22) Kuroda T., Sato S., Hatano T. et al., "Development of HIPed Cu-Alloy/SS First Wall for Fusion Experimental Reactor," 4 th Japan-China Symp. On Materials for Advanced Energy Systems and Fusion Engineering, Hokkaido Univ., Aug. 26-28 1996.
23) Nagashima A., "Experiment Status of JT-60U/JFT-2M", 4th Japan Australia Diagnostic Workshop (Canberra) (1996).
24) Nagashima A., "Recent Progress of Dual CO_2 Interferometer", 4th Japan Australia Diagnostic Workshop (Canberra) (1996).
25) Nakamura Y., Yoshino R., Pomphrey N., et al., "TSC Analyses on VDE Dynamics and Acceleration Mechanism during Disruptions", 4th ITER Physics R&D Expert Group Meeting on Disruption, Plasma Control and MHD, JAERI-Naka, April 15-18, 1996.
26) Neyatani Y., "Hallow Current", Journal of Plasma and Fusion Research Vol.72 No.5 (1996) P.P.403-414
27) Nishio S. and DREAM design team, "Design Guideline and Physics Design of the DREAM Reactor," Japan-US Workshop on Fusion Power Plant (UCSD U.S.A.), (1996).
28) Oda Y., Seki Y., Aoki I. et al., "Dust Removal Experimental Status-Experimental Results," ITER LOVA/ICE/DUST Task Meeting (Naka), (1996).
29) Ogawa Y., Hiwatari R., Takizuka T., "Transport Simulation of JT-60U Discharges", 5th Workshop of ITER Confinement Database and Modelling Expert Group, Montreal, 13-16 October, 1996.
30) Ohira S., Steiner A., Okuno K., "Retention of Tritium in PFMs" Japan-US Workshop p279 on High Heat Flux Components and Plasma Surface Interactions for Next Fusion Devices.
31) Ohkawa Y., Hashimoto M., "Interim report on seismic pipe design", ITER/EDA Design Task Report (S62TD14F1)
32) Ohkawa Y., "Final report on Building cost estimate and construction plan", ITER/EDA Design Task Report (D231) 1996
33) Ohkawa Y., "Final report on Building design", ITER/EDA Design Task Report (D230) 1996
34) Ohkawa Y., "Final report on Dynamic analysis of tokamak building", ITER/EDA Design Task Report (D325/JA-B2), 1996
35) Ozawa Y., "Comments on ITER water chemistry from the existing experience of Japanese fission reactor", ITER task related meeting on corrosion and water chemistry, Sep. 3, 1996, (Studsvik)
36) Saidoh M., "Effect of plasma behavior on tokamak components under JT-60 operation",Tripartite Exchange Agreement Workshop, JET, England, Sept. 10-12, (1996).
37) Sakamoto K., "High Efficiency Operation of High Power Gyrotron," J. Plasma and Fusion Research, 73 294-297 (1996).
38) Sakasai S., "Divertor of JT-60U", Japan US Workshop on High Flux Components and Plasma Surface Interactions for Next Fusion Devices (Naka) (1996).
39) Sato S., Furuya K., Hatano T. et al., "Development of HIP bonded ITER First Wall/Blanket Structure made of Stainless Steel and DS-Copper," Japan-US Workshop on High Heat Flux Components and Plasma Surface Interactions for Next Fusion Devices, Naka.
40) Seki Y., Aoki I., "Comparison of Radioactive Waste Disposal of a Fission and Fusion Reactor," Japan-US Workshop on Fusion Power Plant (UCSD U.S.A.), (1996).
41) Senda I., Shoji T., Fujieda H., et al., " Field control in ITER DDR/FDR", D-324 Task Review meeting at Garching, Mar, 10-14 1996
42) Senda I., Shoji T., Nishio T., Fujieda H., Tsunematsu H., "ITER plasma shape-position control in disturbance", D-324 Task Review meeting at Naka (June 17-21)
43) Senda I., Shoji T., Nishio T., Fujieda H., Tsunematsu H., "The progress in the analysis on 3D eddy currents and plasma shape-position-current control system", D-255/324 Task Review meeting at Naka (April 24-25)
44) Shoji T., Senda I., Fujieda H., Nishio T., Tsunematsu H., "Design task D324 Plasma and control",D-255/324 Task Review meeting at Naka (April 24-25)

45) Shoji T., Senda I., Fujieda H., Nishio T., Tsunematsu H., "Design task D324 - Configurations and Scenario -", ", D-324 Task Review meeting at Naka (June 17-21)
46) Shoji T., Senda I., Fujieda H., et al., "PF configuration study for FDR", D-324 Task Review meeting at Garching, Mar, 10-14 1996
47) Shoji T., Senda I., Fujieda H., et al., "Phase-1 Final Report on Design Task D324-2 on Poloidal Field Scenario and Control", ITER/EDA Design Task Report
48) Shoji T., Senda I., Tsunematsu T., et al., "Phase-1 Final Report on Design Task D318 on Power Supply System Design Support, ITER/EDA Design Task Report
49) Shoji T., Senda I., Tsunematsu T., "Final Report on Alternative power supply design with local energy storage", ITER/EDA Design Task Report (N41TD08FJ), 1996
50) Tado S., "Conceptual procedure for critical assembly steps", ITER tokamak assembly progress meeting on Task D310, Sept. 25, 1996, at San Diego JWS
51) Takase K., Kunugi T., Shibata M. et al., "Experimental Results of the Preliminary LOVA Apparatus," ITER LOVA/ICE/DUST Task Meeting (Naka), (1996).
52) Takatsu H., "Comments and Summary for Shielding Blanket Design," Blanket Task Meeting, Garching Germany, (1996).
53) Takatsu H., "Task Status Report on Shielding Blanket Design: D307A," Blanket Task Meeting, Garching Germany, (1996).
54) Takatsu H., "Task Status report on Shielding Blanket R&D:L-4," Blanket Task Meeting, Garching Germany, (1996).
55) Takizuka T., "Activity Plan for the Task 4.5", 5th Workshop of ITER Confinement Database and Modelling Expert Group, Montreal, 13-16 October, 1996.
56) Tobita K., Fukuyama J., "Physics of a-particles (ITER Physics R&D)", Journal of Plasma and Fusion Research Vol.72 No.6 (1996) P.495
57) Tsuneoka M, "ECH and CD System Design, final Report(G52TD07FJ)," ITER JCT Report, No.D321-J
58) Tsuneoka M., Imai T., Yoshida T. et al., "The Third Progress Report of RF Additional Heating Power Supply for ITER," ITER JCT Report No. D319-J1 (1996).
59) Ueda S., Nishio S., Seki. Y. et al., "Engineering Design and Materials Consideration of the DREAM Reactor" (UCSD U.S.A.), (1996).
60) Ueda S., Nishio S., Seki. Y., "DREAM-3 Design using LAMs" US-Japan WS on Low Activation Structural Materials for Fusion Application (Oarai), (1996).
61) Ushigusa K., Fukuyama J., "Heating and Current Drive on ITER", Journal of Plasma and Fusion Research, 72, 517 (1996).
62) Yamagiwa M., Hirose A., Elia M., "Kinetic shooting code study of ballooning modes in tokamak", University of Saskatchewan, Plasma Physics Laboratory Report, PPL-163 (1997).

A.2 Personnel and Financial Data

A.2.1 Change in number of personnel and annual budget (FY 1988-1996)

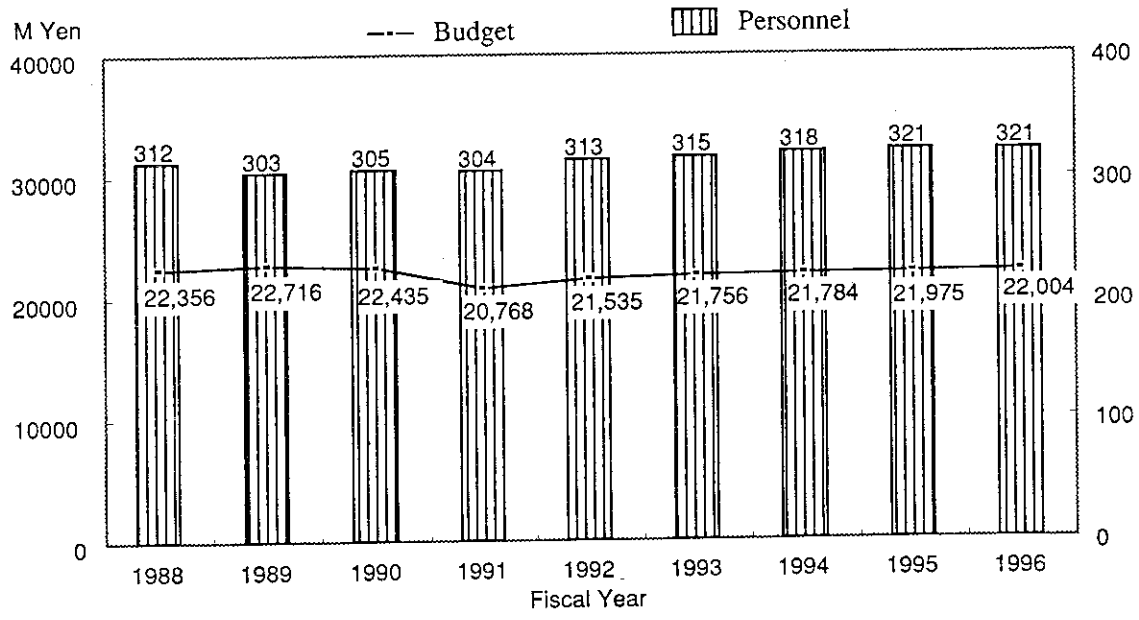

A.2.2 Organization Chart(Mar. 31, 1997)

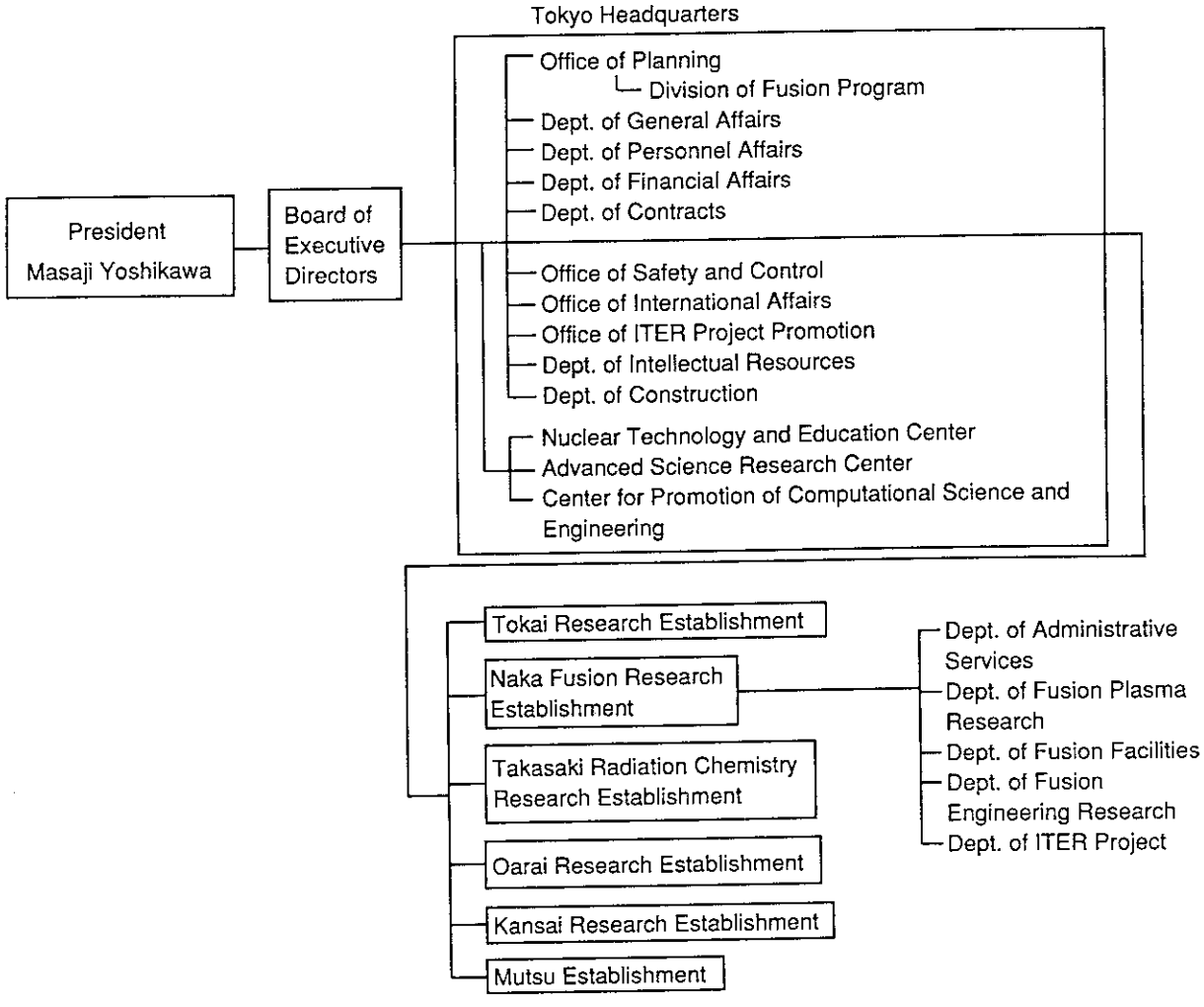

A.2.3 Scientific Staffs in the Naka Fusion Research Establishment (April,1996 - March, 1997)

Naka Fusion Research Establishment
SHIMAMOTO Susumu (Director General)
OHKAWA Tihiro (Scientific Consultant)
SEKIGUCHI Tadashi (Scientific Consultant)
TANAKA Yuji (Scientific Consultant)
MIYAMOTO Kenro (Invited Researcher)
TANAKA Masatoshi (Invited Researcher)
TOMABECHI Ken (Invited Researcher)

Department of Administrative Services
KOMAKI Akira (Director)
KUNIEDA Shunsuke (Deputy Director)

Department of Fusion Plasma Research
KISHIMOTO Hiroshi (Director)
AZUMI Masafumi (Deputy Director)
TAKAHASHI Ichiro (Administrative Manager)

Tokamak Program Division
NAGAMI Masayuki (General Manager)

KIKUCHI Mitsuru	KITAI Tatsuya(*15)	KOIDE Yoshihiko
KURITA Genichi	MORI Katsuharu(*15)	MIYA Naoyuki
NAGASHIMA Keisuke	NAITO Osamu	NAKAGAWA Shouji(*15)
OGURI Shigeru(*15)	TAMAI Hiroshi	TOYOSHIMA Noboru
USHIGUSA Kenkichi		

Plasma Analysis Division
HIRAYAMA Toshio (General Manager)

HAGINOYA Hirofumi (*32)	HAMAMATSU Kiyotaka	KIM Jin Yong (*38)
KISHIMOTO Yasuaki	NAKAMURA Yukiharu	
NEUDATCHIN SergeiV.(*22)	OHSHIMA Takayuki	POLEVOI Alexei(*11)
SAITO Naoyuki	SAKATA Shinya	SATO Minoru
SHIRAI Hiroshi	TAKIZUKA Tomonori	TSUGITA Tomonori
TSURUOKA Takuya (*30)	WATANABE Kazuhiko (*32)	

Large Tokamak Experiment Division I
MORI Masahiro (General Manager)

CAO Jianyong(*37)	CHIBA Shinichi	FUKUDA Takeshi
GAO Xiang(*8)	GUNJI Souichi	HARANO Hideki(*45)
ISAYAMA Akihiko	ISEI Nobuyuki	ISHIDA Shinichi
KAMADA Yutaka	KASHIWABARA Tsuneo	KAWANO Yasunori
KAZAMA Daisuke	KITAMURA Shigeru	KOKUSEN Shigeharu
KRAMER Gerrit Jakob(*38)	KUSAMA Yoshinori	MORIOKA Atsuhiko
NAGAYA Susumu	NEMOTO Masahiro	NEYATANI Yuzuru
NISHITANI Takeo	OIKAWA Toshihiro	ONOSE Yoshiaki
SHITOMI Morimasa	SUNAOSHI Hidenori	TAKEJI Satoru
TCHERNYCHEV Fedor Vsevodovich (*9)		TOBITA Kenji
TSUCHIYA Katsuhiko	TSUKAHARA Yoshimitsu	URAMOTO Yasuyuki
YAMASHITA Osamu	YAN Longwen(*37)	YOSHIDA Hidetoshi

Large Tokamak Experiment Division II
YOSHINO Ryuji (General Manager)

ASAKURA Nobuyuki	DaCOSTA Olivier (*2)	
FUJITA Takaaki	HATAE Takaki	HIGASHIJIMA Satoru
HOSOGANE Nobuyuki	IDE Shunsuke	ITAMI Kiyoshi
KIMURA Haruyuki	KONDOH Takashi	KONOSHIMA Shigeru
KUBO Hirotaka	NAGASHIMA Akira	OHSAWA Masaya(*23)
SAKASAI Akira	SAKURAI Shinji	SHIMIZU Katsuhiro
SUGIE Tatsuo	TAKENAGA Hidenobu	

Plasma Theory Laboratory
HIRAYAMA Toshio(Head)

HUDSON Stuart(*38)	ISHII Yasutomo	
KAWANOBE Mitsuru (*30)	MATSUMOTO Taro	OZEKI Takahisa
TOKUDA Shinji	TUDA Takashi	YAMAGIWA Mitsuru

Experimental Plasma Physics Laboratory
SUZUKI Norio (Head)

HOSHINO Katsumichi	KAWAKAMI Tomohide	KAWASHIMA Hisato
LIU Wandong(*45)	MAEDA Mitsuru(*14)	MAENO Masaki
MIURA Yukitoshi	OGAWA Hiroaki	OGAWA Toshihide
OASA Kazumi	SATO Masayasu	SENGOKU Seio
SHIINA Tomio	UEHARA Kazuya	
YAMAUCHI Toshihiko		

Department of Fusion Facilities
FUNAHASHI Akimasa (Director)
SHIMIZU Masatsugu (Deputy Director)

Fusion Facility Administration Division
TAKAHASHI Ichiro (General Manager)

JT-60 Facility Division I
KIMURA Toyoaki (General Manager)

ADACHI Hironori(*24)	AKASAKA Hiromi	ARAKAWA Kiyotsugu
FUKUDA Hiroyuki(*15)	FURUKAWA Hiroshi(*31)	KAWAMATA Youichi
KURIHARA Kenichi	MATSUKAWA Makoto	MIURA Yushi
NOBUSKA Hiromichi(*15)	OKANO Jun	OMORI Shunzo
OMORI Yoshikazu	OOBA Toshio(*31)	SEIMIYA Munetaka
SHIMONO Mitugu	TAKANO Shoji(*32)	TERAKADO Tsunehisa
TOTSUKA Toshiyuki		

JT-60 Facility Division II
SAIDOH Masahiro (General Manager)

ARAI Takashi	HIRATSUKA Hajime	HONDA Masao
ICHIGE Hisashi	KAMINAGA Atsushi	KODAMA Kozo
KOMURO Ken-ichi(*27)	MASAKI Kei	MIYATA Hiroshi(*6)
MIYO Yasuhiko	MORIMOTO Masaaki(*26)	OGIWARA Norio
OKABE Tomokazu	SANO Jyunya(*12)	SANTO Masahide(*6)
SASAJIMA Tadashi	SASAKI Noboru(*6)	TAKAHASHI Shoryu(*6)
YAGYU Jun-ichi		

RF Facility Division
YAMAMOTO Takumi (General Manager)

ANNOU Katsuto	ISAKA Masayoshi	FUKUDA Hiromi (*39)
HIRANAI Shinichi	KIYONO Kimihiro	MORIYAMA Shinichi
SATO Tomio (*31)	SEKI Masami	SHIBAYAMA Minoru(*27)
SUGANUMA Kazuaki	TERAKADO Masayuki	YOKOKURA Kenji

NBI Facility Division
KURIYAMA Masaaki (General Manager)

AKINO Noboru	EBISAWA Noboru	HONDA Atsushi
ISOZAKI Nobumitsu	ITOH Takao	KAWAI Mikito
KAZAWA Minoru	MOGAKI Kazuhiko	OHGA Tokumichi
OHSHIMA Katsumi(*27)	OOHARA Hiroshi	SEKI Hiroshi(*31)
TAKAHASHI Shunji	TAKENOUCHI Tadashi(*43)	TOTUKAWA Ryoji(*27)
USUI Katsutomi	YAMAMOTO Masahiro	ZHOU Capin(*37)

JFT-2M Facility Division
TAKEUCHI Hiroshi (General Manager)(April, 1996-June, 1996)
SHIMIZU Masatsugu(General Manager)(Aug., 1996-March, 1997)
KOIKE Tsuneyuki (Deputy General Manager)

HASEGAWA Koichi	KASHIWA Yoshitoshi	KIKUCHI Kazuo
KOMATA Masao	OKANO Fuminori	OHUCHI Yutaka
SAWAHATA Masayuki	SHIBATA Takatoshi	SUZUKI Sadaaki
TANI Takashi	UMINO Kazumi(*31)	

Department of Fusion Engineering Research
OHTA Mitsuru (Director) NAGASHIMA Takashi (Deputy Director)
MURASAWA Michihiko (Administrative Manager)

Plasma Engineering Laboratory
TAKATSU Hideyuki (Head)

ABE Tetsuya	FURUYA Kazuyuki	HARA Shigemitu (*6)
HATANO Toshihisa	HIROKI Seiji	KASAI Satoshi
KURASAWA Toshimasa	KURODA Toshimasa(*18)	NAKAMURA Jyun-ichi(*34)
ODA Masahiro	SATO Satoshi	TOKAMI Ikuhide(*21)
UEHARA Toshiaki(*31)		

Superconducting Magnet Laboratory
TSUJI Hiroshi (Head)

ANDO Toshinari	AZUMA Katsunori (*6)	HAMADA Kazuya
HANAWA Hiromi (*31)	HIYAMA Tadao	ISONO Takaaki
ISHIO Koutarou (*13)	ITO Toshinobu (*44)	KATO Takashi
KAWANO Katsumi	KOIZUMI Norikiyo	MATSUI Kunihiro
NAKAJIMA Hideo	NOZAWA Masanobu (*3)	NUNOYA Yoshihiko
OSHIKIRI Masayuki (*31)	SEKI Syuichi (*31)	SUGIMOTO Makoto
TAKAHASHI Yoshikazu	TAKANO Katsutoshi (*31)	TANEDA Masanobu (*19)
WAKABAYASHI Hiroshi(*31)	WATANABE Ikuo (*44)	

NBI Heating Laboratory
OHARA Yoshihiro (head)

AKIBA Masato	BANDOURKO Vassili (*11)	BOSCARY Jean (*38)

DAIRAKU masayuki
INOUE Takashi
MIYAMOTO Kenji
SAWAHATA Osamu
WATANABE Kazuhiro
FUJIWARA Yukio
JIMBOU Ryutaro (*6)
NAKAMURA Kazuyuki
SUZUKI Satoshi
YOKOYAMA Kenji
HANADA Masaya
MIYAMOTO Naoki (*29)
OKUMURA Yoshikazu
SUZUKI Takayuki (*6)

RF Heating Laboratory
IMAI Tsuyoshi (Head)
IKEDA Yukiharu
KOARAI Tohru (*31)
SAIGUSA Mikio
TAKAHASHI Kouji
KASUGAI Atsushi
MAEBARA Sunao
SAKAMOTO Keishi
TSUNEOKA Masaki
KATO Yasushi (*31)
NUMATA Hiroyuki (*28)
SHIHO Makoto
WATANABE Akihiko (*28)

Tritium Engineering Laboratory
OKUNO Kenji (Head)
ARITA Tadaaki(*39)
HONMA Takashi
ITO Takeshi (*17)
KOBAYASHI Kazuhiro
NAKAMURA Hideki (*44)
STEINER Andre (*38)
YAMADA Masayuki
ENOEDA Mikio
ISHIDA Toshikatsu (*18)
IWAI Yasunori
KONISHI Satoshi
NAKAMURA Hirofumi
SUZUKI Takumi
YAMANISHI Toshihiko
HAYASHI Takumi
ISOBE Kanetsugu (*23)
KAWAMURA Yoshinori
MARUYAMA Tomoyoshi(*26)
OHIRA Shigeru
TADOKORO Takahiro (*6)

Fusion Reactor System Laboratory
SEKI Yasushi(Head)
AOKI Isao
NISHIO Satoshi
AJIMA Toshio (*6)
UEDA Shuzo
KURIHARA Ryoichi

Reactor Structure Laboratory
TADA Eisuke(Head)
AKOU Kentaro (*18)
KAKUDATE Satoshi
OKA Kiyoshi
TAKEDA Nobukazu
FUKATSU Seiichi (*44)
NAKAHIRA Masataka
TAGUCHI Kou (*31)
ITOU Akira (*10)
OBARA Kenjiro
TAKAHASHI Hiroyuki (*6)

Department of ITER Project
MATSUDA Shinzaburo (Director)
SEKI Masahiro (Prime Scientist)
SHIMOMURA Yasuo (Prime Scientist)
FUJISAWA Noboru

Administration Group
SHOJI Kuniaki (Leader)

Project Management Group
SEKI Shogo (Leader)

Joint Central Team Group
SEKI Shogo (Leader)
ANDO Toshiro
HATTRORI Yukiya (*6)
HOSOI Yuichi (*10)
IIZUKA Takayuki
ISHIMOTO Kazuyuki (*35)
KATAOKA Yoshiyuki (*6)
KODAMA Tetsuhiko (*26)
MATSUMOTO Hiroshi
EBISAWA Katsuyuki (*44)
HIROKI Seiji
IIDA Fumio (*6)
IOKI Kimihiro (*26)
ITOH Kazuyoshi (*39)
KAWAI Shigetaka (*25)
MARUYAMA So
MIZOGUCHI Tadanori (*6)
HANADA Masaya
HORIKIRI Hitoshi (*36)
IIDA Hiromasa
INOUE Takashi
ITOH Mitsuyoshi (*10)
KOBAYASHI Noriyuki (*44)
MATSUHIRA Nobuto (*44)
MORI Seiji (*18)

MOHRI Kensuke (*18)
MIKI Nobuharu (*44)
OIKAWA Akira
OSANO Katsuharu (*5)
SHIBANUMA Kiyoshi
SUGIHARA Masayoshi
TAKIGAMI Hiroyuki (*44)
YAMADA Masao (*26)
YOSHIDA Hiroshi
MORIYAMA Kenichi (*40)
NAKASHIMA Yoshitane (*10)
OKUNO Kiyoshi
SAJI Gen
SHIMADA Mamoru (*44)
TACHIKAWA Nobuo (*44)
TANAKA Eiichi (*16)
YAMAMOTO Shin
YOSHIDA Kiyoshi
MITA Yoshiyuki (*33)
NAKAMURA Hiroo
ONOZUKA Masanori(*26)
SATO Kouichi (*1)
SHIMIZU Katsusuke (*26)
TAKAHASHI Kenji (*26)
TANAKA Shigeru
YONEKAWA Izuru
YOSHIMURA Kunihiro(*44)

Home Team Design Group
TSUNEMATSU Toshihide (Leader)
ARAKI Masanori
KITAMURA Kazunori
MIYAMOTO Masanori (Kandenko Corp.)
ODAJIMA Kazuo
OZAWA Yoshihiro (*6)
TAKAI Hidehiro (*4)
HASHIMOTO Masayoshi (*10)
KOIZUMI Koichi
OHNO Isamu (*10)
SENDA Ikuo (*44)
TADO Shigeru (*25)
ITOH Yutaka (*6)
MIURA Hidenori (*18)
OOKAWA Yoshinao
SHOJI Teruaki
YAGENJI Aira (*4)

Safety Evaluation Group
INABE Teruo (Leader)
MARUO Takeshi
MITSUI Jin (*39)

*1 Atomic Data Service Corp.
*2 Ecole Polytechnique
*3 Fuji Electric Co., Ltd.
*4 Hazama-gumi Ltd.
*5 Hitachi Information Systems, Ltd.
*6 Hitachi Ltd.
*7 Hitachi Nuclear Engineering Co., Ltd
*8 Institute of Plasma Physics Academia Sinica(China)
*9 Ioffe Physical-Technical Institute
*10 Ishikawajima-Harima Heavy Industries, Ltd.
*11 JAERI Fellowship
*12 Japan Expert Clone Corp.
*13 Japan Steel Works Ltd.
*14 JST Fellowship
*15 Kaihatsu Denki Co.
*16 Kajima Corporation
*17 Kaken Co.
*18 Kawasaki Heavy Industries, Ltd.
*19 Kobe Steel Ltd.
*20 Korea Atomic Energy Research Institute
*21 Kumagai-gumi Ltd.
*22 Kurchatov Institute
*23 Kyushu University
*24 Mito Software Engineering Co.
*25 Mitsubishi Electric Co., Ltd.
*26 Mitsubishi Heavy Industries, Ltd.
*27 Nippon Advanced Technology Co., Ltd.
*28 Nissei Sangyo Co., Ltd.
*29 Nissin Electric Co., Ltd.

*30 Nuclear Energy Data Center Co.
*31 Nuclear Engineering Co., Ltd.
*32 Nuclear Information Service Co.
*33 Obayashi Corp.
*34 Osaka Vacuum Ltd.
*35 Shimizu Corparation
*36 Shinryo Corporation
*37 Southwestern Institute of Physics(China)
*38 STA Fellowship
*39 Sumitomo Heavy Industries, Ltd.
*40 Taisei Corp.
*41 The Graduate University for Advanced Studies
*42 Troitsk Institute
*43 Tomoe Shokai
*44 Toshiba Corp.
*45 University of Science and Technology of China